Design of C-RAN Fronthaul for Existing LTE Networks

Hugo Miguel Inácio Rodrigues da Silva

Thesis to obtain the Master of Science Degree in

Electrical and Computer Engineering

Supervisor: Prof. Luís Manuel de Jesus Sousa Correia

Examination Committee

Chairperson: Prof. José Eduardo Charters Ribeiro da Cunha Sanguino

Supervisor: Prof. Luís Manuel de Jesus Sousa Correia

Members of Committee: Prof. António José Castelo Branco Rodrigues

Eng. Pompeu Costa

November 2016

"A saudade é a única luz que o vento nunca apaga"

(Anónimo, 2014)

Acknowledgements

Abstract

C-RAN is a mobile network architecture that enables the share of network resources in a centralised data centre, being cost-effective to operators. The objective of this thesis was to design and analyse a C-RAN architecture implemented in an existing LTE network. This work consists of a study of the impact of C-RAN and virtualisation in an operator's network, namely the fronthaul connections and the capacity needed per data centre, taking latency and capacity constraints into account. One also analysed the costs associated with the implementation of C-RAN, comparing it with the corresponding decentralised network. A model was implemented, taking the positioning of RRHs and possible available BBU Pools as input, as well as the costs associated with each component. The model presents five types of connection algorithms, based on technical issues, in order to test different aspects of the network. Finally, an analysis of Minho and Portugal is made, using typical values for the various delay and capacity contributions. An approach to the different areas of the scenario is made, classified as dense urban, urban and rural. Results show that Minho and Portugal require respectively 9 and 44 BBU Pools. In what concerns to fronthaul connections, the outcomes illustrate that a microwave link is not cost effective comparing with fibre. It is also shown that the cost savings, comparing a decentralised architecture with a C-RAN one, is around 13%. Due to the scenarios' dimensions, fronthaul costs reveal to be the most expensive component.

Keywords

Resumo

C-RAN é uma arquitetura de rede móvel que permite a partilha de recursos de rede em centros de dados centralizados, reduzindo os custos para os operadores. O objetivo desta tese foi projetar e analisar uma arquitetura C-RAN numa rede LTE. Este trabalho estuda o impacto de C-RAN e virtualização na rede de um operador, nomeadamente as ligações fronthaul e a capacidade necessária por centro de dados, tendo em conta as limitações de latência e capacidade. São também analisados os custos associados à implementação de C-RAN, comparando-a com a rede descentralizada correspondente. O modelo implementado tem como parâmetros de entrada o posicionamento de RRHs e possíveis pontos de agregação de BBUs disponíveis, bem como os respetivos custos. O modelo apresenta cinco algoritmos com base em questões técnicas, a fim de testar diferentes parâmetros da rede. Para finalizar, uma análise do Minho e de Portugal é feita usando os valores típicos para as várias contribuições de atraso e de capacidade. É feita uma abordagem sobre as diferentes áreas do cenário, classificadas como densa urbana, urbana e rural. Os resultados mostram que Minho e Portugal exigem respetivamente 9 e 44 pontos de agregação de BBUs. No que diz respeito às ligações fronthaul, os resultados mostram que as transmissões por microondas não são rentáveis comparativamente à fibra. É também elaborada uma análise de redução de custos comparando uma rede descentralizada com uma arquitetura de C-RAN, sendo cerca de 13%. Devido à dimensão dos cenários, os custos fronthaul revelam ser a componente mais caro.

Palavras-chave

LTE, C-RAN, Fronthaul, OPEX, CAPEX.

Table of Contents

List of Figures

List of Tables

List of Acronyms

3GPP	3rd Generation Partnership Project
4G	Fourth Generation
5G	Fifth Generation
A/D	Analogue/Digital
API	Application Programming Interfaces
ARPU	Average Revenue Per User
AS	Autonomous Systems
BBU	Baseband Unit
BER	Bit Error Rate
BS	Base Station
C-RAN	Cloud Radio Access Network
CAPEX	Capital Expenditures
CN	Core Network
CoMP	Coordinated Multipoint
CP	Control Plane
CPRI	Common Public Radio Interface
CPRI2Eth	CPRI2Ethernet
D-QPSK	Differential Quadrature Phase Shift Keying
D/A	Digital/Analogue
DAS	Distributed Antenna Systems
DL	Downlink
E-UTRAN	Evolved Universal Terrestrial Radio Access Network
eNodeB	Evolved Nodes B
EPC	Evolved Packet Core
EPS	Evolved Packet System
FDD	Frequency Division Duplex
FEC	Forward Error Correction
FFR	Fractional Frequency Reuse
GOPS	Giga Operations Per Second
GPS	Global Positioning System
HetNet	Heterogeneous Networks
HSS	Home Subscription Service
IEEE	Institute of Electrical and Electronics Engineers

IMS	IP Multimedia Sub-System
IP	Internet Protocol
LTE	Long Term Evolution
LTE-A	LTE-Advanced
MAC	Media Access Control
MIMO	Multiple Input Multiple Output
MM	Mobility Management
MME	Mobility Management Entity
MMW	MilliMetre-Wave
MPLS	Multi-Protocol Label Switching
NFV	Network Functions Virtualisation
NV	Network Virtualisation
OBSAI	Open Base Station Architecture Initiative
OFDMA	Orthogonal Frequency Division Multiple Access
ONF	Open Networking Foundation
OPEX	Operating Expenditures
OTN	Optical Transport Network
OWD	One-Way Delay
P-GW	Packet Data Network Gateway
PAPR	Peak to Average Power Ratio
PCC	Policy and Charging Control
PCEF	Policy Control Enforcement Function
PCRF	Policy and Charging Rules Function
PDN	Packet Data Network
PS	Packet-Switched
QAM	Quadrature Amplitude Modulation
QoE	Quality of Experience
QoS	Quality of Service
QPSK	Quadrature Phase Shift Keying
RAN	Radio Access Network
RANaaS	RAN as a Service
RB	Resource Blocks
RE	Resource Element
RF	Radio Frequency
RoF	Radio over Fibre
RRH	Remote Radio Head
RRH++	Future RRH
RRM	Radio Resource Management
RTT	Round Trip Time

S-GW	Serving Gateway
SAE	System Architecture Evolution
SC-FDMA	Single Carrier - Frequency Division Multiple Access
SDF	Software Defined Fronthaul
SDN	Software Defined Networks
TCO	Total Cost of Ownership
TDD	Time Division Duplex
UE	User Equipment
UL	Uplink
VBS	Virtual Base Station
VNF	Virtualised Network Functions
VoIP	Voice over IP
WAN	Wide Area Network
WDM	Wavelength Division Multiplexing
WDM-PON	WDM - Passive Optical Network

List of Symbols

$\delta_{BBU,DL}$	BBU DL delay
$\delta_{BBU,UL}$	BBU UL delay
$\delta_{fronthaul}$	Fronthaul OWD
δ_{OWD}	One-Way Delay
$\delta_{RRH,DL}$	RRH DL delay
$\delta_{RRH,UL}$	RRH UL delay
$\delta_{RTT,BBU-RRH}$	Fronthaul RTT delay
δ_{RTT}	Round Trip Time
δ_{SW}	Switch delay
ϕ_{XPCI}	XPCI factor
A	Area occupied by a RRH
B	Bandwidth
C_{BB10}	Cost of construction of a 10MHz cell
C_{BB20}	Cost of construction of a 20MHz cell
$C_{Cabinet,C-RAN}$	Cost of a C-RAN cabinet
$C_{Cabinet,local}$	Cost of a local cabinet
$C_{CAPEX,C-RAN}$	Cost of CAPEX for a C-RAN architecture
$C_{CAPEX,computer}$	Cost of computer investment
$C_{CAPEX,deplyment}$	Cost of deployment investment
$C_{CAPEX,hardware}$	Cost of hardware investment
$C_{CAPEX,local}$	Cost of CAPEX for a local architecture
C_{CAPEX}	Total cost of CAPEX
C_{DU}	Cost of rent a squared metre per month in a dense urban area
C_{energy}	Cost of the energy consumption
C_{fee}	Energy fee
C_{fiber}	Cost of dark fibre per kilometre
$C_{fibfronthaul}$	Cost of maintenance of fibre fronthaul
C_l	Line coding factor
$C_{maintnence}$	Cost of a maintenance of infrastructures
$C_{microwave}$	Cost of microwave equipment
$C_{mwlicences}$	Cost of microwave fronthaul licences
C_{OPEX}	Total cost of OPEX per year

C_R	Cost of rent a squared metre per month in a rural area
$C_{renting}$	Cost of renting
$C_{site,C-RAN}$	Cost of a C-RAN site
$C_{site,local}$	Cost of a local site
C_{Total}	Total cost of the architecture
C_U	Cost of rent a squared metre per month in an urban area
C_w	Factor of CPRI control word
$d_{fronthaul}$	Fronthaul distance
E_{BBU}	Energy consumed per hour for a BBU
F_{index}	Fairness index
G_{mux}	Multiplexing gain
I	Multiplication factor for in-phase data
k_1	Factor related to the bandwidth
L_i	Load of the RRH i
N_{ant}	Number of antennas per sector
N_{BB10}	Number of 10MHz cells
N_{BB20}	Number of 20MHz cells
N_{BBU}	Number of BBUs
$N_{cab,c}$	Number of aggregation points in a C-RAN architecture
$N_{cab,l}$	Number of aggregation points in a local architecture
N_{DU}	Number of RRHs in a dense urban area
N_{fl}	Number of kilometres of fibre link
N_{ml}	Number of microwave link
N_R	Number of RRHs in a rural area
$N_{RRH,con}$	Number of RRH connected
N_{site}	Number of sites
N_U	Number of RRHs in an urban area
N_{years}	Number of years considered for OPEX
$P_{BBU,i}$	Required processing power per BBU
P_{BS}	Total processing power of a BS
P_{Fixed}	Fixed processing power
$P_{i,ref}$	Complexity associated with each function
P_{pool}	Total processing power
Q	Multiplication factor for quadrature-phase data
R_b	Data rate of a CPRI link
$s_{i,x}$	Scaling exponent for sub-component
S_r	Sampling rate used for digitisation
S_w	Sample width

T_{peak}	Peak of traffic during the day
v	Transmission speed in the link
V	Virtualisation factor
x_{act}	Actual value for input parameter
x_{ref}	Reference value for input parameter

List of Software

Microsoft Word 2016	Text editor software
Microsoft Excel 2016	Calculation and graphical software
Matlab	Computing environment
Google Maps	Geographical plotting tool

Chapter 1

Introduction

This chapter presents an overview of the context in which this thesis was developed, taking the current mobile communications scenario into account. It also presents the motivations behind the present work, followed by a presentation of its structure.

1.1 Overview

The way that people communicate with each other has changed due to the mobile communications. In the last years, the impact mobile communications have is justified by the increasing number of subscriptions compared to the population growth worldwide. According to [Eric15], the rise of mobile data subscriptions, along with a continued increase in average data volume per subscription, is generating a large growth in data traffic. Figure 1.1 shows the present data traffic dominance compared with voice, being possible to observe the contrasting increasing trend of data traffic growth with the roughly constant voice traffic evolution. Between 2019 and 2020, it is expected that the increase in data traffic will be greater than the total sum of all mobile data traffic up to the end of 2013.
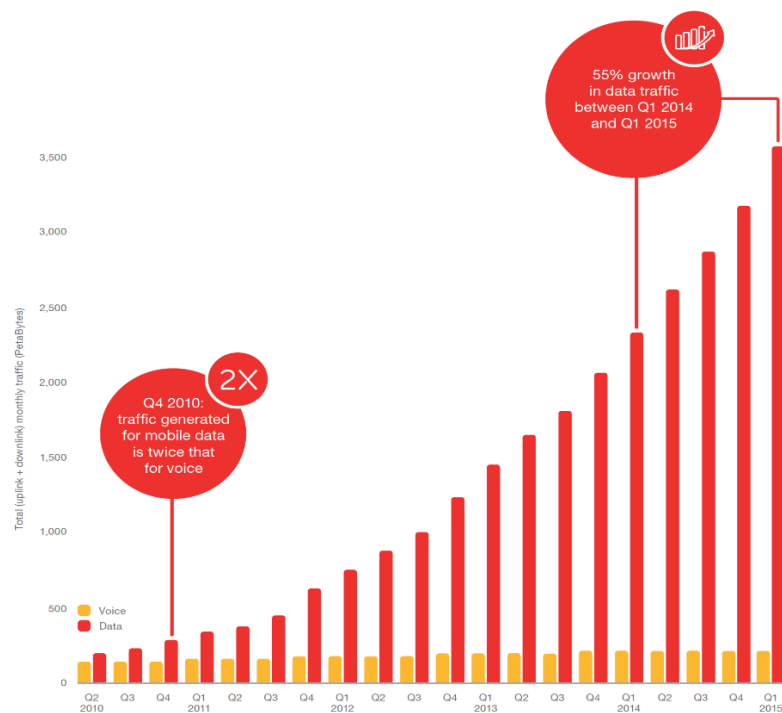
Figure 1.1. Global total traffic in mobile networks, 2010-2015 (extracted from [Eric15]).

In 2004, the first targets of the 3rd Generation Partnership Project (3GPP) Long Term Evolution (LTE) were defined. A need for more wireless capacity, higher efficiency, and competition from other wireless technologies generated the development of the Fourth Generation (4G). The first LTE release, Release 8, provided a high-data rate, low-latency and packet-optimised system, supporting theoretical peak data rates up to 300 Mbit/s in Downlink (DL) and 75 Mbit/s in Uplink (UL). LTE-Advanced (LTE-A) is standardised in Release 10, which specifies data rates up to 3 Gbit/s in DL and 1 Gbit/s in UL.

Mobile operators have been increasing their network capacity in order to satisfy consumer usage growth. Operators had to deal with the implementation or improvements of Base Stations (BS), caused by the fast technological changes and declining voice revenue, where investment is high and return is not high enough. For this reason, the Average Revenue Per User (ARPU) is affecting mobile operators' profit;

Figure 1.2 illustrates this behaviour. Although the typical user is more "data-hungry", he/she expects to pay less for data usage, which makes ARPU almost flat over time. Thus, it is harder for mobile network operators to cover the expenses for network construction, operation, maintenance and upgrade.
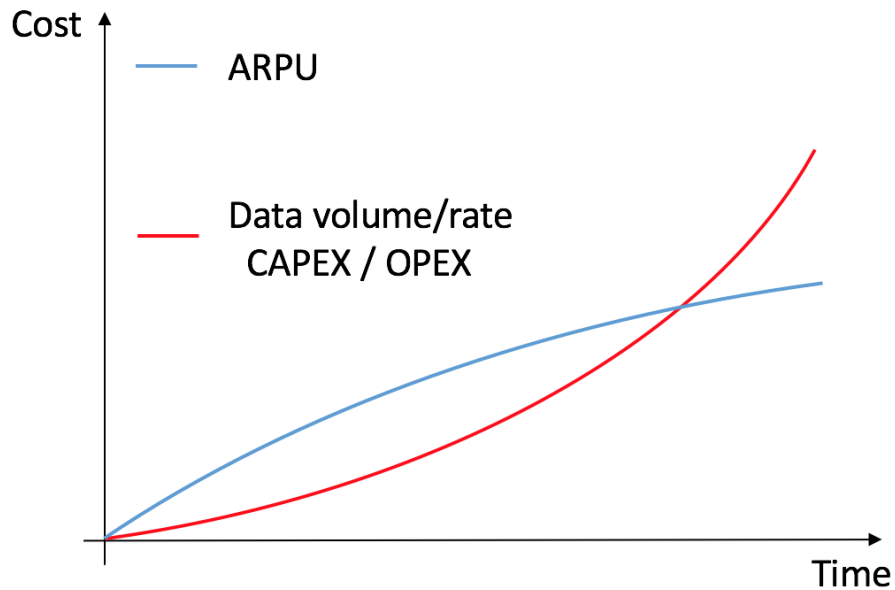
Figure 1.2. Comparison between the ARPU and CAPEX/OPEX.

Network operators must find solutions to overcome the critical challenges imposed by the mobile data traffic growth trend. The success of cloud technologies provides one of the possible solutions. In order to take advantage of the cloud to obtain benefits, the vision of the telecommunication industry is to develop economies of scale, cost effectiveness, scalability, lower Capital Expenditure (CAPEX) and Operational Expenditure (OPEX). CAPEX is mainly associated with building network infrastructure, while OPEX is with network operation and management. Figures 1.3 illustrate an example of CAPEX and OPEX per year of a cell site, respectively.

(a) CAPEX

(b) OPEX per year
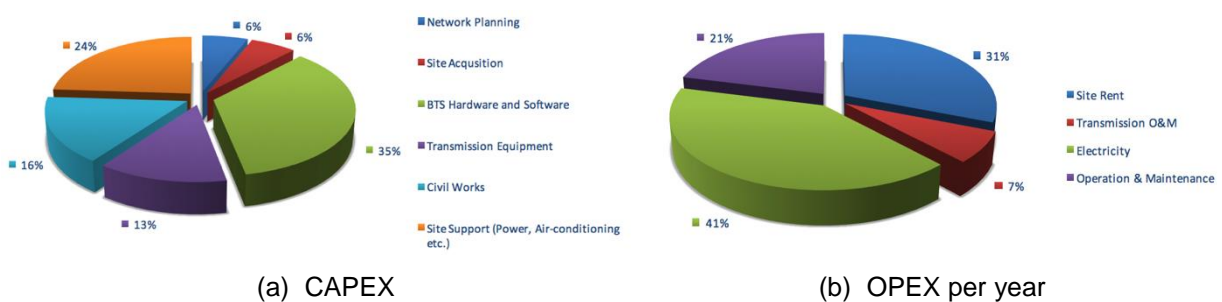
Figure 1.3. CAPEX and OPEX analysis of cell site (extracted from [HDDM13]).

Since mobile network virtualisation enables abstraction and sharing of infrastructure, as well as radio spectrum resources, the overall expenses of deployment and operation can be significantly reduced. Virtualisation provides also opportunities for new flexible software design. Nowadays, the existing networking services are supported by diverse network functions that are connected in a static way. The introduction of Network Functions Virtualisation (NFV) enables additional dynamic schemes to create and manage network functions. In this way, the network can be further optimised.

The architectures of mobile networks are typically split into two segments: Core Network (CN) and Radio Access Network (RAN). The latter provides higher data rates, Quality of Service (QoS) and guarantees service parameters, consequently, it is where most upgrades have been made.

The introduction of the new Cloud-RAN (C-RAN) approach is an alternative to the available RAN solutions. Architecture changes created a new connectivity segment between the multiple distributed Remote Radio Head (RRH) and the centralised Baseband Unit (BBU), called "fronthaul". This new transport segment is one of the main interests of network operators in what concerns capacity, latency, jitter and synchronisation. For this reason, the design of this section may be either implemented in wired or wireless links. This brings a lot of benefits from the economic perspective as well as from the performance and flexibility ones. Figure 1.4 shows that, with centralisation, instead of having peaks of traffic in each cell, C-RAN can produce a constant traffic generated by the aggregation of each cells'.

(a) RAN with RRH.   (b) C-RAN.
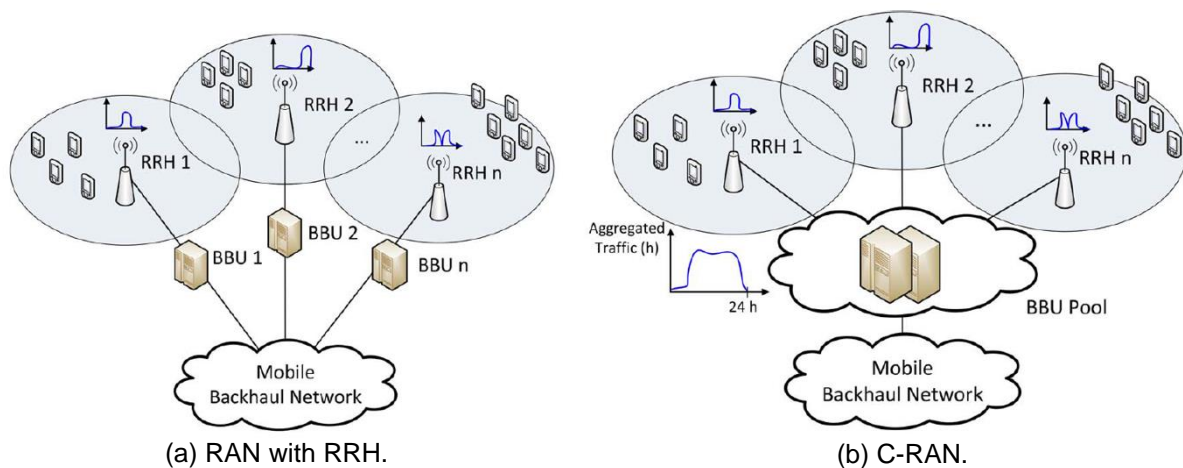
Figure 1.4. Statistical multiplexing gain in C-RAN architecture (extracted from [CCYS14]).

Mobile clouds can also provide RAN as a Service (RANaaS). For this reason, operators can easily share the available infrastructures, each one being responsible for the appropriate processing at the data centres. Consequently, new operators could join the market without huge investments, by simply paying for the rental of RANaaS, and use the already deployed network.

Currently, the mobile communication industry is developing the Fifth Generation (5G) system, which aims to provide universal always-on, always-connected broadband packet services. Compared to 4G, 5G may achieve a system capacity increase by a factor of 1 000, as well as data rate and spectral/energy efficiency growth by a factor of 10, [PWLP15]. To achieve these objectives, new technologies need to be developed. The C-RAN has been proposed as a combination of emerging technologies from both wireless and information technology industries, by including cloud computing into RANs.

1.2   Motivation and Contents

With smartphones and tablets driving mobile data transmission volume, mobile network operators have

to increase network capacity to satisfy growing user demands. The capacity of a mobile network is linked to the provided coverage, being challenging to provide both in an efficient way. It is important to consider that traffic loads change over time during the day, so operators deploy BSs to accommodate peak hour traffic. Future network deployments are expected to be much denser than today's, in order to provide significantly higher data rates to a larger number of users. It is possible, with additional transmission requirements, to influence the overall RAN performance within the context of a centralised baseband architecture. This centralisation can provide benefits in resource management, less power consumption especially for cooling, simplified network operation, and thus lower costs.

The main goal of this master thesis was to investigate the pros and cons of solutions for the fronthaul link, such as fibre or radio. The aim was also to develop a model that evaluates the Total Cost of Ownership (TCO) of different solutions for different scenarios.

This thesis consists of 5 chapters, including the present one, and a group of appendixes. Chapter 2 starts by introducing the LTE network architecture and radio interface, followed by a similar approach on Software Defined Networks (SDN). An introduction on Virtualisation and Cloud is also given in this chapter, which concludes with the state of the art, presenting the latest work developments on the subject of the thesis.

Chapter 3 starts by presenting an overview regarding the developed model and the model parameters to be analysed. It is followed by a deeper explanation of the model, represented by its layers and algorithms developed. It ends with the results assessment in order to check the validity of the model.

Chapter 4 consists of the analysis of the obtained results. It begins with the description of the scenarios considered, followed by an analysis of the reference scenario. To conclude an analysis where some key parameters are changed in order to see the impact on the network.

Chapter 5 is a summary of this thesis, displaying the most important conclusions and results, also addressing some suggestions for future work on this topic.

At the end, a group of annexes are presented in order to give auxiliary information. Annex A contains the user manual, explaining how to perform the simulations done in this thesis. Annex B suggests some complexity indexes adopted to calculate the processing power for the BBU Pools. Annex C offers the reference values to compute the microwave licencing costs. The Annex D presents some confidential information related with this thesis, namely the location of the RRHs

Chapter 2

Fundamental Concepts

This chapter provides firstly a background on the fundamental concepts of LTE, SDN and Virtualisation. It includes LTE's network architecture and radio interface, and a synopsis of SDN and OpenFlow. An introduction to NFV, C-RAN and an overview of the "fronthaul" link is also given. Then, a brief discussion of QoS in LTE follows. The last section is dedicated to an analysis of the state of the art.

2.1 LTE aspects

2.1.1 Network architecture

In this subsection, an overview of LTE's network architecture is given, based on [SeTB11] and [HoTo11].

In order to provide transparent Internet Protocol (IP) connectivity between User Equipment (UE) and Packet Data Network (PDN), without any anomaly to end users' applications during mobility, LTE was designed to support only Packet-Switched (PS) services. For this reason, in parallel to the work on LTE's radio-access technology in 3GPP, the overall system architecture of both CN and RAN was revisited, including the split of functionalities in between them.

LTE's architecture is divided into four main high-level domains, as presented in Figure 2.1:

- External Networks: Services.
- CN: Evolved Packet Core (EPC).
- RAN: Evolved Universal Terrestrial Radio Access Network (E-UTRAN).
- User Equipment.
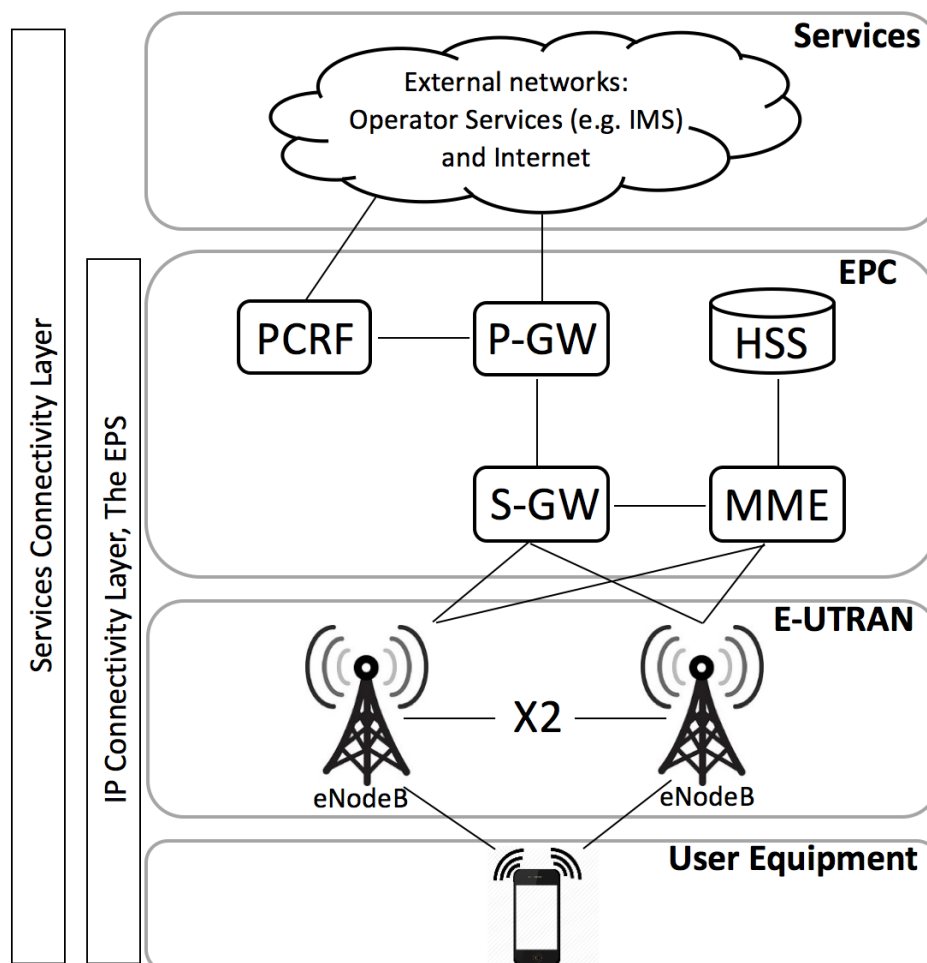
Figure 2.1. Network architecture of LTE (adapted from [HoTo11]).

The Evolved Packet System (EPS) is characterised by the UE, E-UTRAN and EPC representing the IP

Connectivity Layer.

The term 'System Architecture Evolution' (SAE) represents the evolution of the non-radio aspect of the complete system, in which LTE is inserted. E-UTRAN and EPC are the only layers with new architectural developments. Nevertheless, although the UE and Services domains remain architecturally intact, the functional evolution has also continued.

In what concerns the Services Connectivity Layer, the IP Multimedia Sub-System (IMS) is a good example that can be used to provide services on top of the IP connectivity provided by the lower layers, which is the case of voice services, like Voice over IP (VoIP).

EPC is responsible for the overall control of the UE and the establishment of the bearers (an IP packet flow with a defined QoS). Its functionally is equivalent to the PS domain of other existing 3GPP networks (GSM and UMTS). EPC is composed of the following main nodes:

- Mobility Management Entity (MME) – it is the main control element of EPC. It is in charge of all Control Plane (CP) functions related to the signalling between the UE and the EPC. Bearer management, connection management and inter-working with other networks are the three main functions supported by MME.

- Serving Gateway (S-GW) – the main function of this node is User Plane tunnel management and switching, being the local mobility anchor for the data bearers when the UE moves between Evolved Nodes B (eNodeBs). The IP packets from all users are transferred through this node, which performs administrative functions, such as collecting information for charging.

- Packet Data Network Gateway (PDN Gateway, P-GW) – it is the edge router between the EPS and external packet data networks. It is responsible for IP address allocation for the UE, as well as QoS enforcement and flow-base charging.

- Policy and Charging Rules Function (PCRF) – it is responsible for Policy and Charging Control (PCC). It is in charge of deciding on how to handle the QoS associated with each service and providing information to the Policy Control Enforcement Function (PCEF) located in the P-GW.

- Home Subscription Service (HSS) – it is a subscription database server that contains all permanent user data, such as the subscribed QoS. It also records the information of users' location in order to access restrictions for roaming.

The access network, E-UTRAN, is composed of a network of eNodeB inter-connected with each other by means of an interface, known as X2.

E-UTRAN is responsible for all radio-related functions, such as:

- Radio Resource Management (RRM) – This covers all functions related to the radio bearers.
- IP Header Compression – This allows to guarantee efficient use of the radio interface.
- Security – Encrypt all data sent over the radio interface.
- Mobility Management (MM) – Control and analyses of radio signal level carried out by the UE.

2.1.2 Radio interface

In this subsection, an overview of multiple access techniques and basic principles of the multi-antenna

transmission in LTE are given, based on [SeTB11] and [HoTo11].

LTE supports both Frequency Division Duplex (FDD) and Time Division Duplex (TDD). In Europe, FDD is the widely adopted duplex mode, and the most relevant bands correspond to 800 MHz, 900 MHz, 1 800 MHz and 2.6 GHz. Portugal's communications sector regulator (ANACOM), followed the trend among other European countries, adopting the 800 MHz, 1 800 MHz and 2.6 GHz bands [ANAC12]. Table 2.1 presents the current spectrum allocation for the Portuguese operators.

Table 2.1. Frequency ranges for UL and DL in LTE in Portugal (extracted from [ANAC12]).

	Uplink [MHz]	Downlink [MHz]
LTE 800	[832, 862]	[791, 821]
LTE 1800	[1 805, 1 880]	[1 710, 1 785]
LTE 2600	[2 630, 2 690]	[2 510, 2 570]

LTE radio interface is based on two multiple access techniques:

- Orthogonal Frequency Division Multiple Access (OFDMA), for DL.
- Single Carrier - Frequency Division Multiple Access (SC-FDMA), for UL.

These techniques provide orthogonality among users, reducing interference and improving network capacity. The resource allocation in the frequency domain takes place with a resolution of 180 kHz of Resource Blocks (RB) in both UL and DL. Each RB consists of a group of 12 sub-carriers spacing is 15 kHz regardless of the total transmission bandwidth.

OFDMA provides good protection against the rapidly varying radio conditions, including fast fading and multipath propagated radio components [Pent11]. The use of OFDMA for DL is important because users can be allocated basically to any of the sub-carriers in the frequency domain. This technique distributes sub-carriers to different users at the same time, so that multiple users can be scheduled to receive data simultaneously. Figure 2.2 illustrates the process of resource allocation.
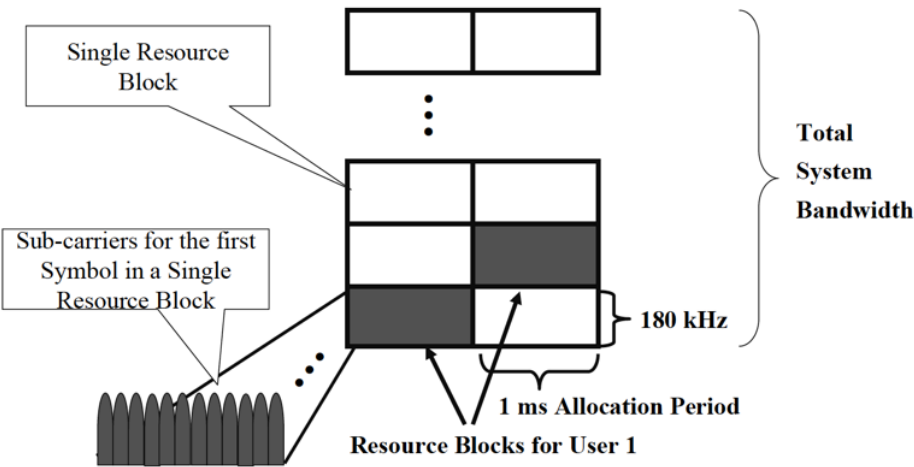
Figure 2.2. Resource allocation in OFDMA (extracted from [HoTo11]).

For UL, the use of OFDMA is not ideal because of its high Peak to Average Power Ratio (PAPR) when the signals from multiple subcarriers are combined [Saut10]. For this reason, SC-FDMA was selected, as the terminal can handle these challenges with more efficiency. The maximum bandwidth that can be allocated is 20 MHz, but the useful channel bandwidth is smaller due to some margin for guard bands. UL transmission resources are defined in the frequency domain with the smallest unit of a resource being a Resource Element (RE). In the UL process, RBs are allocated to each user consecutively in the frequency domain, as shown in Figure 2.3.
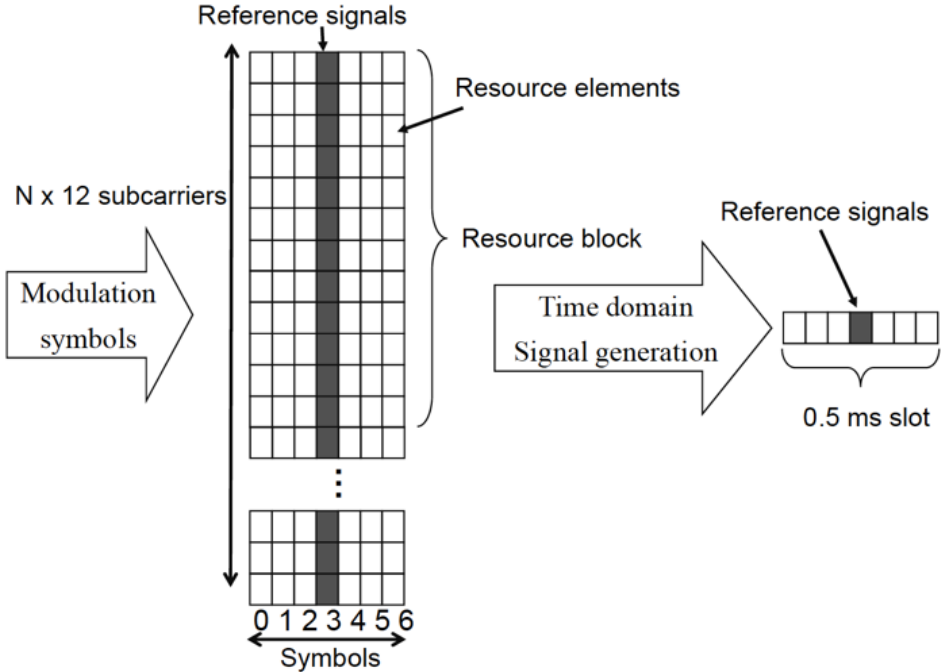
Figure 2.3. Resource allocation in SC-FDMA (extracted from [HoTo11]).

LTE allows up to six different bandwidths for the radio channels. Table 2.2 presents the dependence on the number of sub-carriers and the number of RB.

Table 2.2. Bandwidth, number of sub-carriers and RB relationship (adapted from [Corr15]).

Bandwidth [MHz]	1.4	3	5	10	15	20
Number of sub-carriers	72	180	300	600	900	1200
Number of RB	6	15	25	50	75	100

An important improvement of LTE is Multiple Input Multiple Output (MIMO) operation, which increases the peak data rate by a factor of 2 or 4 for a 2x2 or 4x4 antenna configuration, respectively.

Peak bit rates are directly related to the RB characteristics and bandwidth. The RB relevant features are modulation and coding, bits per symbol and the existence of MIMO. Table 2.3 and Table 2.4 show the peak bit rates in DL and UL, respectively.

In what concerns modulation, LTE uses both Quadrature Phase Shift Keying (QPSK) and Quadrature Amplitude Modulation (QAM): QPSK, 16QAM, 64QAM or 256QAM.

Table 2.3. Downlink peak bit rates in LTE (adapted from [HoTo11]).

Downlink peak bit rates [Mbit/s]								
Resource Blocks			Bandwidth [MHz]					
Modulation and coding	Bits per symbol	MIMO	1.4	3	5	10	15	20
QPSK ½	1	-	1.0	2.5	4.2	8.4	12.6	16.8
16QAM ½	2	-	2.0	5.0	8.4	16.8	25.2	33.6
16QAM ¾	3	-	3.0	7.6	12.6	25.2	37.8	50.4
64QAM ¾	4.5	-	4.5	11.3	18.9	37.8	56.7	75.6
64QAM 1/1	6	-	6.0	15.1	25.2	50.4	75.6	100.8
64QAM ¾	9	2x2	9.1	22.7	37.8	75.6	113.4	151.2
64QAM 1/1	12	2x2	12.1	30.2	50.4	100.8	151.2	201.6
64QAM 1/1	24	4x4	24.2	60.5	100.8	201.6	302.4	403.2

Table 2.4. Uplink peak bit rates in LTE (adapted from [HoTo11]).

Uplink peak bit rates [Mbit/s]							
Resource Blocks		Bandwidth					
Modulation and coding	Bits per symbol	1.4	3	5	10	15	20
QPSK ½	1	1.0	2.5	4.2	8.4	12.6	16.8
16QAM ½	2	2.0	5.0	8.4	16.8	25.2	33.6
16QAM ¾	3	3.0	7.6	12.6	25.2	37.8	50.4
16QAM 1/1	4	4.0	10.1	16.8	33.6	50.4	67.2
64QAM ¾	4.5	4.5	11.3	18.9	37.8	56.7	75.6
64QAM 1/1	6	6.0	15.1	25.2	50.4	75.6	100.8

2.2 Software Defined Networks

In this section, an overview of SDN is given, based on [ONFo12], [JSSA14] and [JZHT14].

SDN is defined by the Open Networking Foundation (ONF) as a network architecture where network control is directly programmable and decoupled from forwarding. The main idea of SDN is to separate the forwarding/data plane from the control one, while providing programmability on the control plane.

In the literature, it is possible to find many block diagrams representing the SDN architecture. A generic architecture for SDN, as shown in Figure 2.4, consists of three layers:

- The Application Layer consists of applications that consume the SDN communications services.
- The Control Layer consists of the controllers that facilitate setting up a tearing down flows and paths in the network.
- The Infrastructure Layer consists, in this representation, of three Autonomous Systems (AS): a legacy access network at the user end, an SND-based Transit-Wide Area Network (WAN), and an SDN enabled data centre network (Cloud).
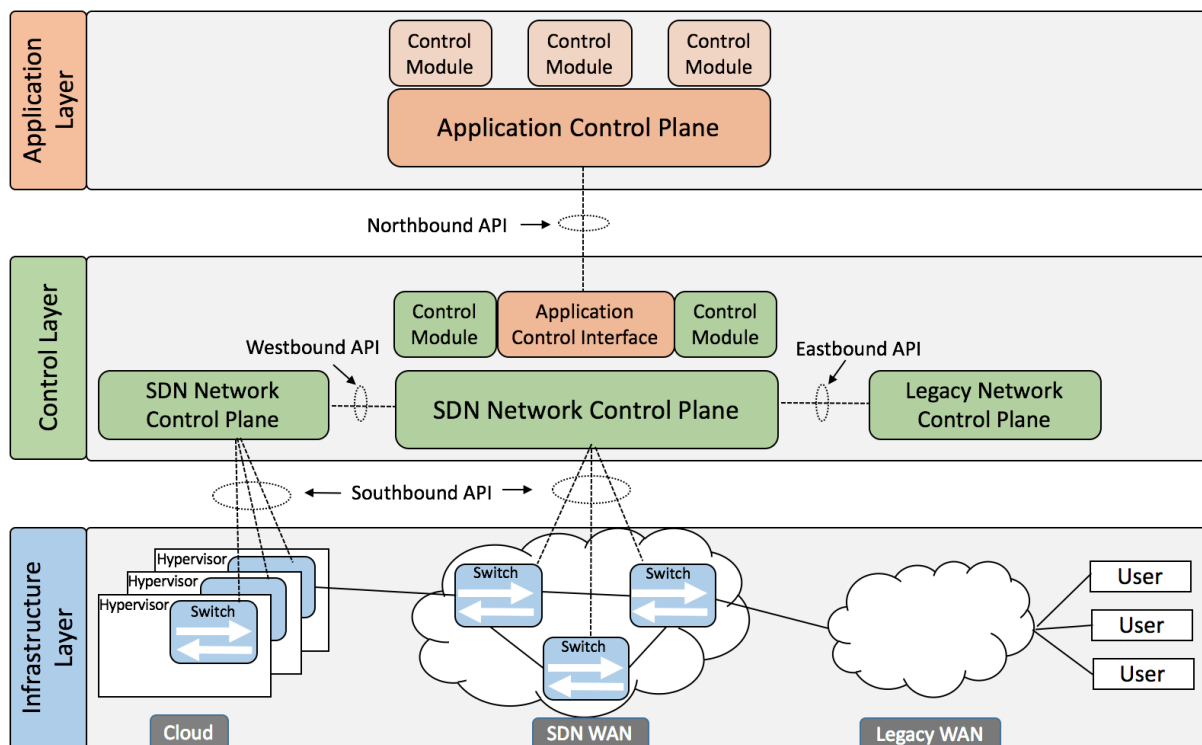
Figure 2.4. Generic SDN architecture (adapted from [JZHT14] and [ONFo12]).

The communication intra- and inter-layers, as Figure 2.4 suggests, are establish by Application Programming Interfaces (APIs). There are four API in this SDN architecture:

- The Northbound API, while the applications running on top of the network, it enables the exchange of information. The definition of this kind of information exchanged, in which form, and how often depends on the kind of application and network. For this reason, there is universal standardised Northbound API.
- The Southbound API represents the interface between control and data planes. It is the enabler

for the externalisation of the control plane. The currently most notable example of implementation of this API is the Open Flow protocol.

- The Eastbound API is responsible for communication with the control planes of non-SDN domains, like Multi-Protocol Label Switching (MPLS) control plane. The implementation of this interface depends on the technology used in the non-SDN domain.

- The Westbound API works as an information channel between SDN control planes of different network domains. It allows for the exchange of network state information to influence routing decisions of each controller, but at the same time enabling the seamless setup of network flow across multiple domains.

In what concerns cellular networks, [LiMR12] presents an SDN architecture where the SDN controller consists of a network operative system running a collection of application modules, such as RRM, mobility management and routeing. The cellular SDN architecture is shown in Figure 2.5.

The success and fast progress of SDN are entirely associated with the success of OpenFlow, which is a standard interface. The interaction between the control and data planes of SDN architecture is simplified by OpenFlow. The OpenFlow-based SDN architecture abstracts the underlying infrastructure from applications by decoupling the network control and data planes. Thus, it allows the network to became programmable and manageable at the scale as the computer infrastructure that it increasingly resembles. The instructions of switch and route the network traffic are provided by the software based access to the flow tables. An OpenFlow-based SDN architecture enables the network to respond to real-time changes at the application, user and session levels. This means that OpenFlow provides extremely granular control.
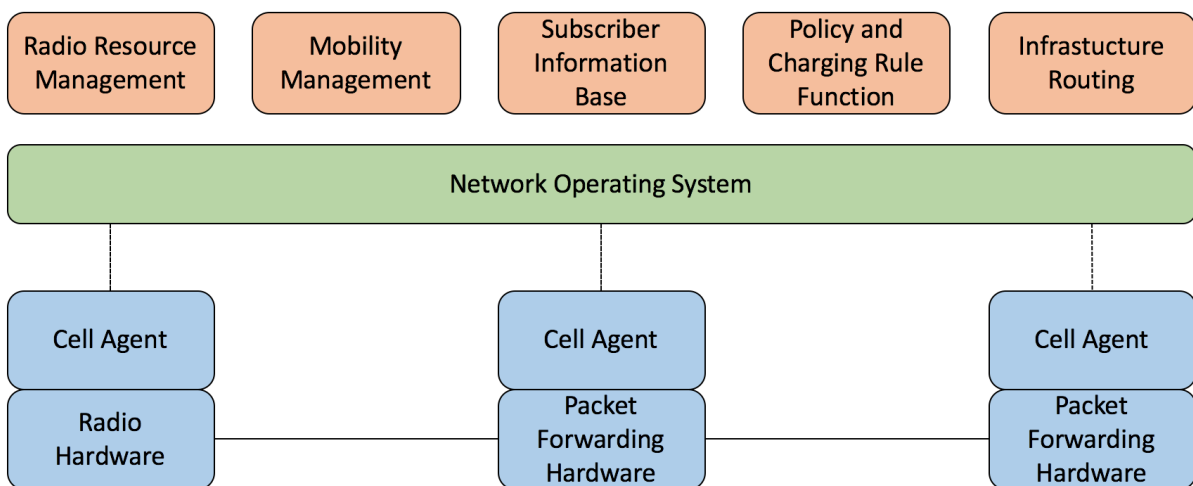
Figure 2.5. Cellular SDN Architecture (adapted from [LiMR12]).

In [BrMe14], the OpenFlow architecture, as Figure 2.6 suggests, consists of three basic concepts:

- The network is built up by OpenFlow-compliant switches that compose the data plane.
- The control plane consists of one or more OpenFlow controllers.
- A secure control channel connects the switches with the control plane.
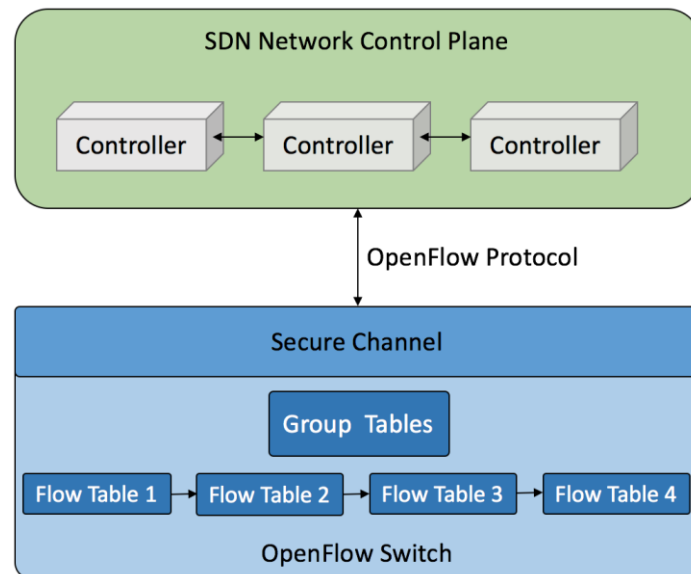
Figure 2.6. Basic OpenFlow Architecture (adapted from [JSSA14]).

An OpenFlow-compliant switch is a basic forwarding device that sends packets according to its flow table, which holds a set of entries, each one consisting of match fields, counters and instructions.

The flow tables of the switches are occupied and manipulated by the controller. The controller can modify the behaviour of the switches with regard to forwarding by insertion, modification and removal flow entries. To this end, the controller uses a secure control channel.

In what concerns flow tables, each entry has three fields:

- Packet Header – it is specific to the flow and defines it.
- Action – it specifies how the flow will be processed, and can be one of the following:
  - o Forward the packet to a given port.
  - o Forward the packet to the controller.
  - o Drop the packet.
- Statistics – it includes information such as the numbers of packets and bytes, among others.

2.3 Background on Virtualisation and Cloud

2.3.1 Network Functions Virtualisation

This subsection addresses NFV aspects, being based on [JSSA14], [ETSI12], [HSMA14] and [HGJL14].

The networking area is not only experiencing the emergence of SDN but also Network Virtualisation (NV) and NFV. The three solutions build an automated, scalable, virtualised and agile networking and cloud environment [JSSA14]. The virtualisation technology has emerged as a way to decouple software applications from the underlying hardware and enable software to run in a virtualised environment.

NV partitions the network logically and creates logical segments in it. It can be viewed as a tunnel connecting any two domains in a network. While NV can be viewed as a tunnel, NFV provides an abstraction and deploys virtual services on it [JSSA14].

Evolving standard high volume servers, switches and storage, which could be located in data centres, network nodes and in end user premises, NFV aims to transform the way that network operators architect networks. It involves the implementation of network functions in software that can run on a range of industry standard server hardware, and that can be moved, or instantiated in, various locations in the network as required without the need for installation of new equipment [ETSI12].

Figure 2.7 illustrates the high-level architecture framework of NFV and its four major functional blocks are [HGJL14]:

- Orchestrator, responsible for the management and orchestration of software resources and the virtualised hardware infrastructure to realise networking services.
- Virtualised Network Functions (VNF) manager, in charge of instantiation, scaling, termination and update events during the lifecycle of a VNF.
- Virtualisation layer, abstracting physical resources, and anchoring VNFs to the virtualised infrastructure.
- Virtualised infrastructure manager, used to virtualise and manage the configurable compute, network and storage resources and control their interaction with VNFs.
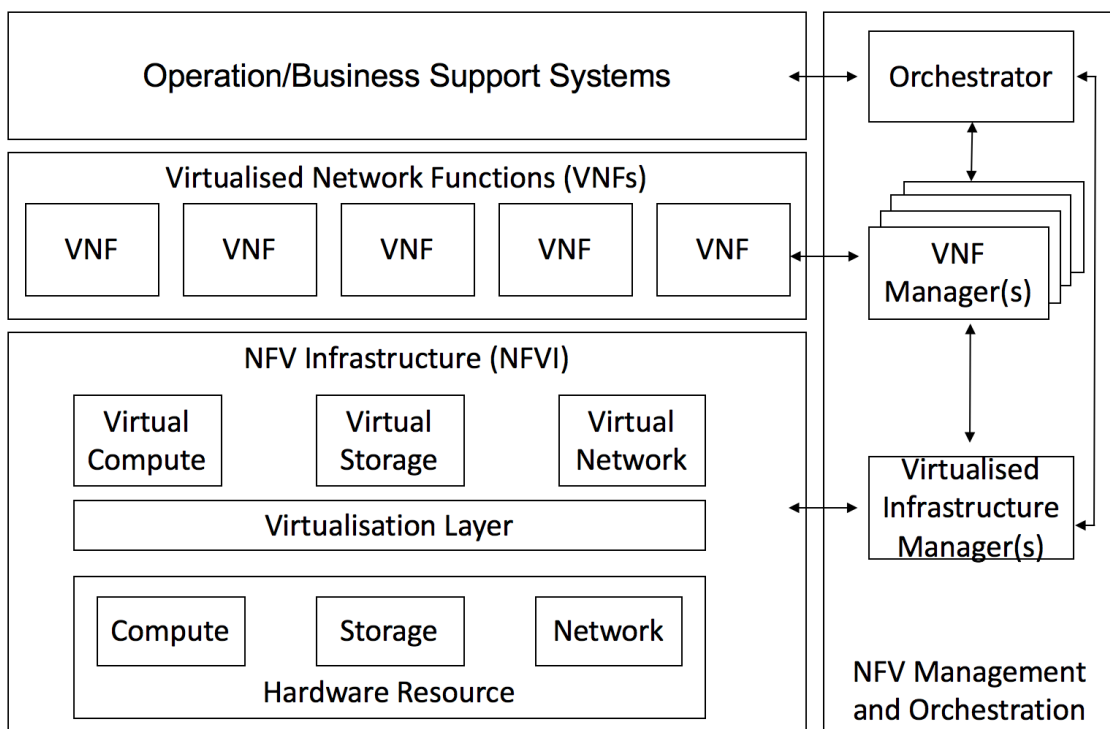
Figure 2.7. NFV architecture framework (adapted from [HSMA14]).

The openness of platforms, scalability and flexibility, operating performance improvement shorter development cycles, and reduced CAPEX and OPEX investments are some of the benefits provided by NFV to the telecommunications industry [HSMA14].

2.3.2 Cloud Radio Access Network

In this subsection, an overview of C-RAN is given, based on [WZHW15] and [CPLR13].

C-RAN is a paradigm that features centralised processing, collaborative radio, real-time cloud computing and power-efficient infrastructure. This new RAN architecture aggregates all BSs computational resources into a central pool. C-RAN aims to reduce the number of cell sites while maintaining similar coverage, and reducing CAPEX and OPEX while offering better services [WZHW15].

According to [PWLP15], the general architecture, illustrated in Figure 2.8, of a C-RAN consists of three main components, namely:

- BBU Pool.
- RRH.
- Fronthaul network

In C-RANs, the traditional BS functions are decoupled into two parts: the distributed installed RRHs, and the BBUs clustered as a BBU Pool in a centralised cloud server.
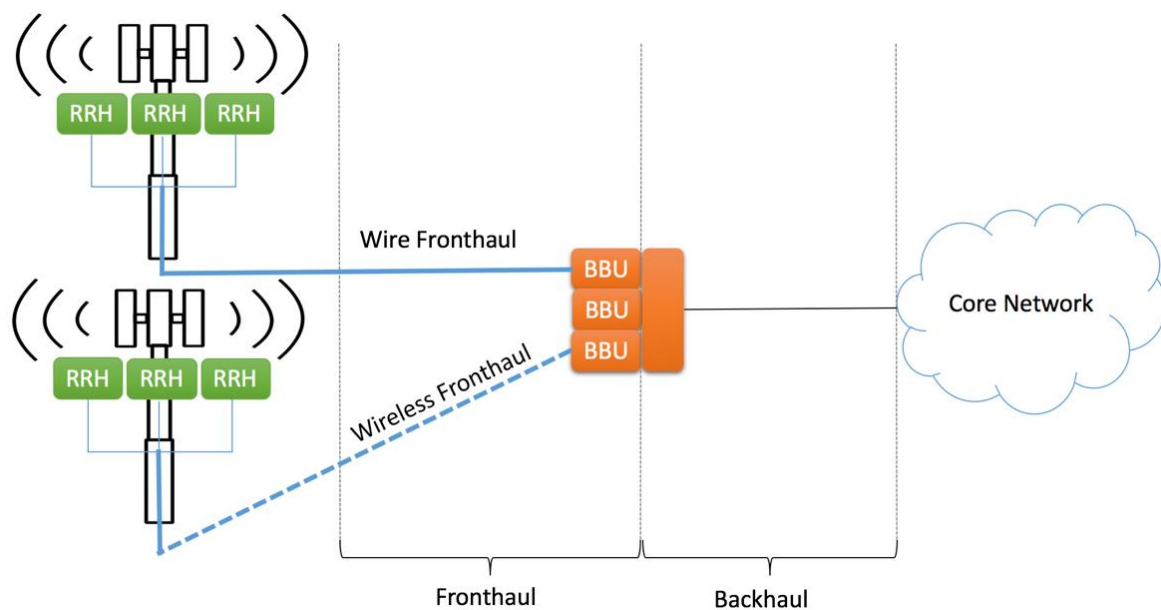
Figure 2.8. C-RAN Architecture (adapted from [CPLR13]).

The RRHs send/receive digitised signals to/from the BBU Pool. Antennas are equipped with RRHs to transmit/receive Radio Frequency (RF). Most signal processing functions are processed in the BBU Pool. For this reason, RRHs can be relatively simple, and can be distributed in a large scale scenario with a cost-efficient method.

While the RRHs perform radio functions, including frequency conversion, amplification, and Analogue/Digital (A/D) and Digital/ Analogue (D/A) conversion, the BBU acts as a digital unit implementing the BS functionality from baseband processing to packet processing.

The link that connects RRH to BBUs with high capacity and low time latency is called fronthaul. According to [PWLP15], its typical protocols include the Common Public Radio Interface (CPRI) and the

Open Base Station Architecture Initiative (OBSAI). CPRI offers maximum latency, near-zero jitter, and a near-zero Bit Error Rate (BER). The fronthaul can be realised via different technologies, such as optical fibre, cellular communication, and even millimetre wave links.

According to the constraints on fronthaul and the distribution of functions between BBUs and RRHs, there are three possibilities for C-RAN structure concerning centralisation, i.e.:

- Full – The functions of the physical layer, the Media Access Control (MAC) layer and the network layer of the conventional BS are moved into the BBU. This solution experiences a high load on fronthaul.

- Partial – The RRH integrates not only the RF functions but also some RF related baseband processing functions, while other functions are still located in the BBU. This solution mitigates the constraints on fronthaul.

- Hybrid – It is considered as a special case of full centralisation, in which partial functions are removed from BBUs and assembled into a separate processing unit in the BBU Pool.

Optical fibre is considered to be the ideal fronthaul for C-RANs, given that it can provide a high transmission capacity at the expense of high cost and un-flexible deployment. In contrast, a wireless fronthaul using cellular transmission or microwave links is cheaper and more flexible to deploy, at the expense of capacity and other restraints.

According to [PCSD15], different radio access standards have different CPRI data throughputs, so different transmission solutions need to be considered. Depending on which option of this protocol is used, a CPRI link rates go from 614.4 Mbit/s up to 10.137 Gbit/s. It is also specified that the BER on the fronthaul link must be lower than 10^{-12}.

The calculation of latency dedicated to fronthaul is not defined by RAN standards, because this network segment is included inside the E-UTRAN eNodeB. In order to calculate it, the concepts of maximum latency and accuracy should be considered. In [PCSD15], the Round Trip Time (RTT) of the fronthaul could reach a maximum latency of 500 μs and an accuracy of ±130.208 ns.

According to [WZHW15] and [CCYS14], the main advantages of C-RAN are:

- Reduced Cost – C-RAN aggregates computations resources in a few big rooms and leaves simpler functions to RRHs, saving on OPEX.

- Energy Efficiency – All processing functionalities are implemented in a remote data centre, being possible to do significant savings in OPEX due to much lower power consumption of RRH.

- Spectrum Utilisation – C-RAN enables the sharing of channel state information of each BS to mobile terminal link.

- Business Model Transformation – The cloud concept will generate more business models, such as cellular infrastructure sharing.

- Adaptability to Non-Uniform Traffic and Scalability – In C-RAN, baseband processing of multiple cells is carried out in the centralised BBU Pool, so, the overall utilisation rate can be improved. The required baseband processing capacity of the pool is expected to be smaller than the sum of single BSs.

2.4 State of the Art

Regarding the fronthaul link critical role in delivering C-RAN performance and cost benefits, [SARS15] establishes a novel and flexible fronthaul that supports one-to-one, as well as one-to-many, logical mappings between BBUs and RRHs. FluidNet is a flexible C-RAN for the small cells that allocates an intelligent and dynamically reconfigurable controller, based on network feedback, in the BBU Pool. For [ArSR15], FluidNet is an example of a C-RAN with a reconfigurable Software Defined Fronthaul (SDF). It adopts a two-step approach: first, it determines the optimal combination of configurations needed to support traffic, i.e., Distributed Antenna Systems (DAS) and Fractional Frequency Reuse (FFR) strategies; then, it employs a novel efficient algorithm. FluidNet allows desirable features such as co-existence of multiple mobile operators and technologies in the same C-RAN. While reducing the compute resource usage in the BBU Pool by 50% compared to baseline schemes, the strategies of FluidNet provides a 50% improvement in satisfying traffic demands.

According to [MHLW15], the fronthaul employs the CPRI protocol but the traditional transmission using bare fibre might not work efficiently anymore. The authors present four different optical solutions for fronthaul link: direct dark fibre, coloured CPRI, Wavelength Division Multiplexing - Passive Optical Network (WDM-PON) and Active WDM. Compared with bare fibre, optical WDM solution could save trunk fibre, extend the transmission reach and provide protection schemes. CPRI transmissions have physical requirements, such as 400 μs for maximum roundtrip latency and maximum BER of 10^{-12}. To fulfil the requirements, dark fibre is the default solution. However, due to large centralisation, optical solutions are desired to save fibre usage, and provide protection and management at the same time. WDM is the main technology to transmit many CPRI links over a single fibre. CPRI over Optical Transport Network (OTN) is able to monitor BER in real time and switch to the protected channel while performance is degraded. The key feature of WDM-PON, which can take advantage of the tree topology when massively installed, is a colourless transceiver. Colourless transceivers are mature with 2.5 Gbit/s, which is sufficient for CPRI option 3. Nevertheless, an advanced data rate up to 10 Gbit/s is still under development. For active WDM, using CPRI options from 3 (2.5 Gbit/s) up to 7 (10 Gbit/s), the roundtrip latency of OTN increases with the introduction of Forward Error Correction (FEC) and also with the decrease of the data rate. On the other hand, transparent WDM has ultimately a low latency as 0.5 μs.

The potential of Heterogeneous Networks (HetNets) has been proved to satisfy the increasing data rates, proximity to end user, efficient spatial spectrum reuse and indoor coverage. According to [CLZW15], the most efficient physical link in the fronthaul of HetNet is Radio-over-Fibre (RoF). It simplifies the distribution of Millimetre-Wave (MMW) signals, which minimise interference with existing wireless services in HetNet. To support MMW small cells, the authors propose a local centralised optical Coordinated Multipoint (CoMP) thought RoF fronthaul using only local information and local high capacity RoF links.

[DKYK15] also presents an approach focused on the fibre - MMW link. Experimental results show that the effect of fibre dispersion is negligible when the fibre length is shorter than 50 km. The MMW-wireless link was limited to 3 m, because of space limitations and of the use of a low-gain antenna. Nevertheless,

it is expected that it can be significantly increased to an appropriately long range if a high-gain antenna is used. This technology is an attractive method for realising broadband radio signal delivery where broadband wireless infrastructure and fibre cables are not available.

Traffic distribution can change in case new cells are added to the network, or if existing cells change their traffic profile. Therefore, [ChHC14] proposes using a packet-based fronthaul based on Ethernet that RRHs can be dynamically assigned to BBU Pools. Consequently, the overall multiplexing gain of the BBU Pools can be maximised. The optimal gain can be obtained connecting 20-30% of office BSs and 70-80% of residential ones to the BBU Pool.

This optimal gain achievable in C-RAN for a given traffic profile equals 1.6. Regarding this packet based fronthaul, [CJCB15] states that reusing existing Ethernet is a promising solution and an important matter to study. However, transverse the asynchronous Ethernet without losing synchronisation is the main challenge. A possible solution for delivering synchronisation is to equip CPRI2Ethernet (CPRI2Eth) gateways or Future RRH (RRH++) with Global Positioning System (GPS), that assures both frequency and phase delivery. Another solution could be to implement Institute of Electrical and Electronics Engineers (IEEE) 1588 slave in CPRI2Eth gateways or RRH++. It assures lower equipment cost, however, it will be affected by variable network delay present in Ethernet networks.

When deploying fibres is not the best choice, high capacity MMW links provide a fast and flexible alternative. However, the link was designed for a fixed data rate, and it is not possible to adapt radio systems to different data rates without hardware changes. For this reason, [CHLS15] presents a novel differential encoding scheme for Differential Quadrature Phase Shift Keying (D-QPSK) modulation, which enables adaptable data rate in CPRI transmission, without modifying a standard receiver. It was implemented and tested for data rates up to 10 Gbit/s, limited by the bandwidth of the microwave components. It also fulfils CPRI specifications, having a maximum BER less than 10^{-13} and latency bellow 0.1 μs.

Besides consuming power for operation, support equipment sites remain unused as traffic load varies throughout the day. For this reason, [ACHC15] states that, unless the mobile operator already owns a large fibre infrastructure, the deployment of fibre exclusively for C-RAN may not be cost-effective unless a majority of sites remain served by radio links. The cost of fibre in a C-RAN deployment constitutes one of the largest CAPEX components, hence, to solve this issue, the usage of microwave links to replace fibre is warranted for population densities of over 8 000 users/km2 when considering cheap fibre.

Cloud computing and virtualisation techniques are considered an opportunity to reduce operation costs and provide flexible and dynamic systems. For this reason, [WeGP13] focus on multiplexing gains induced from user load and data traffic heterogeneity. Here, the evaluation shows the increase of the multiplexing gain when a higher number of sectors are aggregated in a single fronthaul link. In fact, the aggregation of five sectors saves 9% of the computational resources.

The power efficiency of a BS is a fundamental constituent to maintain the sustainability of future networks. Regarding this subject, [DeDL15] presents an advanced power model that supports a broad range of network scenarios and BS types, features and configurations. The estimated power

consumption over the technology generations 2014-2020 is illustrated over different BS types operating at full load, resulting in a power gain of 50% and 20% for pico-cell and 2x2 macro-cell BSs, respectively. The proposed model also supports BS sleeping functionality during reduced traffic load.

From an economical viewpoint, [ATPH15] proposes a model to compare the local BBU with three strategies for BBU hoteling, such as BBU staking, BBU Pooling and C-RAN. The model includes cost comparisons and sensitivity analysis with respect to pooling and virtualisation gain. A scenario handling 100 cells was created to do the model assessment. In terms of relative cost, CAPEX and OPEX decrease as the level of resource sharing increases.

Due to user mobility and network usage, the traffic load in mobile networks is an issue to needs to take into consideration the variations during the day. Therefore, [ChCB13] presents the energy and cost savings in C-RAN, evaluated numerically using OPNET. Here, a real case scenario was built upon the mobile traffic forecast for the year 2017. It is stated that C-RAN enables a reduction of user data signal processing resources 4 times comparing with the traditional architecture.

Cost issues related to deploying C-RAN were investigated by [HCAC15] in order to find the most feasible configurations and choice of technologies. The proposed model minimises the length of fibre while at the same time maximises the statistical multiplexing gain for each BBU Pool.

Chapter 3

Models and Simulator Description

A description of the model used in this thesis is provided in this chapter. An overview of the model, metrics and implementation details are present as well. The chapter ends with the model assessment.

3.1 Model Overview

The model described in this section in a high-level perspective that aims at drawing insights about the connections between the RRHs and BBU Pools in a network configuration. It takes into consideration different ways to analyse connections, based on traffic profile, positioning and delay characteristics of the network resources needed to support the set of cell sites available countrywide. Furthermore, it also analyses the costs of a C-RAN architecture implementation.

The main objective of this thesis is to develop and study a solution for C-RAN implementation in a certain area with a focus on the fronthaul link, whether it be through fibre or microwave, which is the key aspect related to the investment [ACHC15]. Therefore, the model intends to analyse the network configuration with different specifications, regardless of the studied scenario, in order to get a weighed result.

The model can be basically divided into three layers, as shown in Figure 3.1:

- Physical.
- Technical.
- Costs.
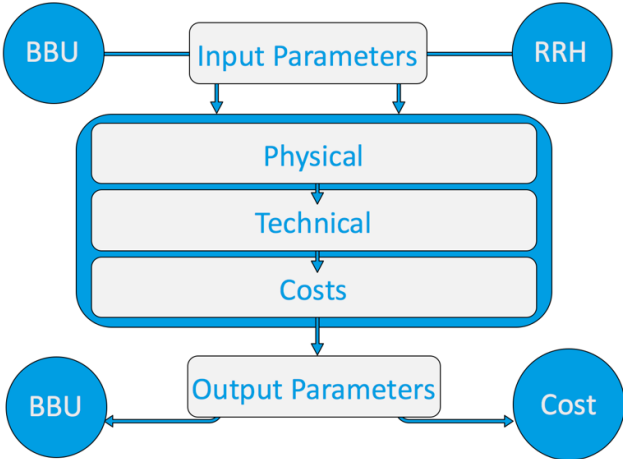
Figure 3.1. Model Overview.

The input parameters are divided into three main classes and the output parameters are divided into two main classes, both summarised in Table 3.1 and Table 3.2, respectively:

Table 3.1. List of inputs for the model.

Inputs	
RRH	Locations
	Temporal traffic load
BBU	Locations
	Maximum latency/distance for each BBU Pool
	Maximum number of RRH for BBU Pool
	Maximum capacity of each BBU Pool
External	Maximum radius
	Timestamps to analyse
	Algorithm

Table 3.2. List of outputs for the model.

Outputs	
For each BBU	Index of the RRHs connected
	Location of the RRHs connected
	Type of connection with the RRH (fibre or microwave)
	Fronthaul Delay of the RRHs connected
	Fronthaul Distance of the RRHs connected
	Costs associated
Costs	Total costs of the new configuration

Each layer of the model is used to analyse different parameters of the network, as Figure 3.2 suggests.
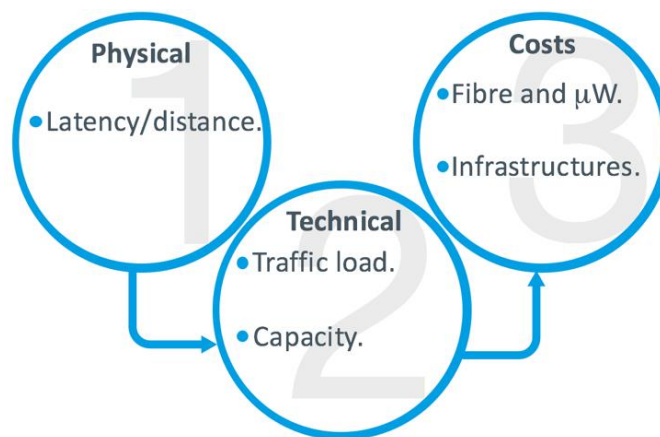
Figure 3.2. Model Layers.

The first layer aims at computing the distances between RRHs and BBUs. Associated to this calculation, the possible connections that one RRH can have with all BBUs are also computed. This assignment is based on the maximum latency that a fronthaul link can have, taking the different propagation velocities both in fibre and in microwave links into account.

The second layer deals with five different algorithms, highlighted in Subsection 3.3.2:

- Minimise Delay.
- Number of RRH per BBU Balance.
- Minimise Number of BBU Pools.
- Flatness.
- Capacity Load Balance.

This layer is responsible for determining the most accurate assignment within the existing possibilities, taking the algorithm into account. The different algorithms focus on different network aspects, such as fronthaul distance and delay, the number of RRHs that one BBU handle, the number of used BBUs, the traffic load of each RRH and consequently of each BBU, and the capacity of the BBU. After weighting the options, the model produces the connections between RRHs and BBU Pools.

The costs layer is divided into two, each one with steps: one layer is related to CAPEX and the other

with OPEX, as shown in Figure 3.3. This decision is justified by the fact that, both costs analyses are one of the motivations to work on C-RAN (see section 1.1 and 2.3).
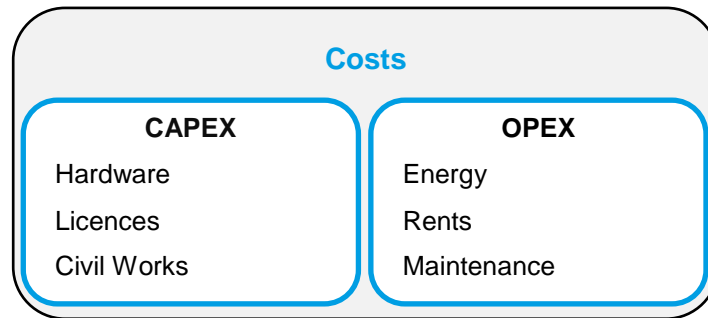
Figure 3.3. Costs layer diagram.

In what concerns the CAPEX layer, it is considered that the needed equipment is related to the BBU Pool and the fronthaul, which are the new components in the C-RAN architecture, assuming that the cell sites already have RRHs instead of eNodeB. The investment related to the hardware includes the telecom equipment to process the baseband, which includes the equipment related to the air conditioning to guarantee that the BBU Pool is not overheated. The licences are related to the amount of traffic generated from the RRHs that needs to be processed in the BBU Pool. It also considers the need to build not only the infrastructure for the BBU Pool, but also for the fronthaul, such as new fibre paths and radio links.

From the OPEX viewpoint, expenses are associated with the fees related to the energy consumption that the equipment generates, all in processing, transmitting and cooling. Rents are only related to the place occupied by each BBU Pool. To guarantee the good performance of the equipment, both in the BBU Pool and in the fronthaul link, some maintenance needs to be done.

3.2   Model Parameters

3.2.1 Latency

There are several applications that do not require a very high data rate but rather a very low delay. Latency is one of the main constraints for the fronthaul in a C-RAN architecture, determining the maximum length of the link between RRH and BBU Pool.

It is important to note that usually latency is represented by the measure of RTT, which has a more meaningful impact on Quality of Experience (QoE) than One-Way Delay (OWD). For simplicity, the present work assumes that RTT is given by:

$$\delta_{RTT} = 2 \cdot \delta_{OWD} \tag{3.1}$$

where:

- δ_{RTT} – Round Trip Time.

- δ_{OWD} – One-Way Delay.

The length of the fronthaul link is dictated by its characteristic speed and by the fronthaul OWD, hence:

$$d_{fronthaul\,[km]} = v_{[km/ms]} \cdot \delta_{fronthaul[ms]} \tag{3.2}$$

where:

$d_{fronthaul}$ – Fronthaul distance.

v – Transmission speed in the link.

$\delta_{fronthaul}$ – Fronthaul OWD.

Equation (3.2) can also be used to obtain the RTT in the fronthaul as a function of the length of the fronthaul link.

Splitting the BSs functionalities between BBUs and RRHs and centralising BBUs into a few centres brings many benefits, in terms of costs and RAN performance. However, this requires a proper network to transport the new fronthaul traffic, exchanged by BBUs and RRHs [PCSD15], in addition to the conventional backhaul traffic. Transporting fronthaul traffic over access networks is critical from the latency viewpoint. Strict latency constraints must be met when transporting fronthaul, thus, the physical distance between BBUs and RRHs is limited, and a trade-off between higher BBU consolidation and fronthaul latency requirements arises.

As specified in [3GPP14], the maximum total round-trip latency $\delta_{RTT,BBU-RRH}$ is 2 ms. Regarding different latency contributions, presented in Figure 3.4, the following condition must be held:

$$\delta_{RTT,BBU-RRH} = 2\delta_{fronthaul} + \delta_{RRH,UL} + \delta_{BBU,UL} + \delta_{RRH,DL} + \delta_{BBU,DL} + 4\delta_{SW} \leq 2\text{ ms} \tag{3.3}$$

where:

$\delta_{RTT,BBU-RRH}$ – Fronthaul RTT delay.

$\delta_{RRH,UL/DL}$ – RRH UL/DL delay.

$\delta_{BBU,UL/DL}$ – BBU UL/DL delay.

δ_{SW} – Switch delay.

The maximum $\delta_{RTT,BBU-RRH}$ directly translates to a maximum admissible OWD for every CPRI flow or, equivalently, to a maximum length of its route. The range of maximum length is typically between 20 km and 40 km [MBCT15].
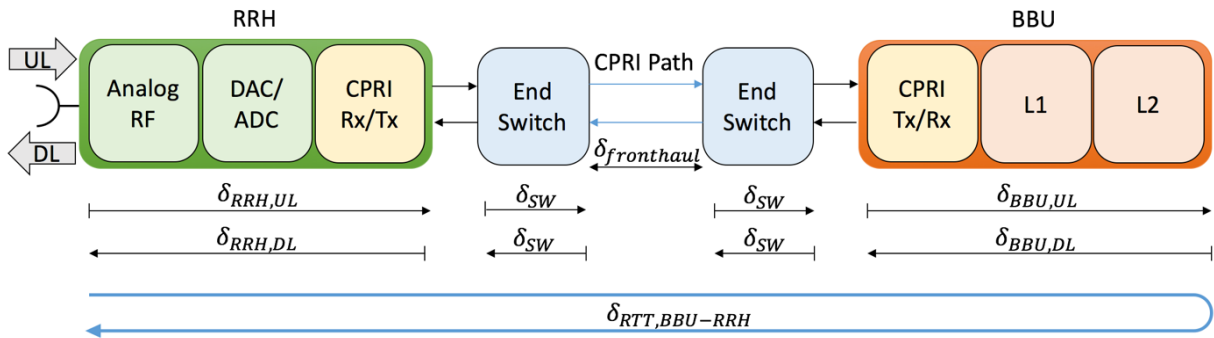
Figure 3.4. Delay contributions along the fronthaul (adapted from [MBCT15]).

3.2.2 Processing Power

The BBU Pool enables the use of virtualisation techniques in order to create multiple instances of a Virtual Base Station (VBS) in a single physical data centre. In order to achieve an efficient load balancing of traffic, the processing power has to be quantified.

The total processing power that is used by the BBU Pool is measured in Giga Operations Per Second (GOPS), and can be expressed as:

$$P_{pool\,[\text{GOPS}]} = P_{fixed\,[\text{GOPS}]} + \sum_{i=1}^{N_{BBU}} P_{BBU,i\,[\text{GOPS}]} \tag{3.4}$$

where:

- $P_{BBU,i}$ – required processing power per BBU.
- P_{fixed} – fixed processing power required for scheduling and signalling functions, which does not depend on the number of BBUs.
- N_{BBU} – number of BBUs.

A proposed method to calculate the required processing power of a BS, for both DL and UL, is presented in [DeDL15], considering both analogue and digital functions. The following expression describes the total scaled power:

$$P_{BS} = \sum_{i \in I} P_{i,ref} \prod_{x \in X} \left(\frac{x_{act}}{x_{ref}} \right)^{s_{i,x}} \tag{3.5}$$

where:

- $P_{i,ref}$ – Complexity associated with each function.
- x_{act} – Actual value for the input parameter.
- x_{ref} – Reference value for the input parameter.
- $s_{i,x}$ – Scaling exponent for sub-component.

Taking into consideration the C-RAN architecture, it is assumed that the RRH only performs the radio functions while the BBU performs all baseband operations. The present work focuses only on the digital functions, which are the ones that are related to the BBU processing power. The complexity associated with each function and the scaling exponents of each sub-component are presented in Annex B.

3.2.3 Fronthaul Capacity

Fronthaul link capacity depends on the maximum traffic demand that can be supported by the corresponding cell site, which depends on the number and type of RRHs that the cell site possesses. As mentioned in Chapter 2, the most widely used protocol for fronthaul communication is CPRI, hence, the data rates concerning a single RRH presented in Table 2.3, which were used for the fronthaul capacity. The value denoted for an LTE 100 MHz 8x8 RRH was inferred from the three preceding values in Table 2.3, which evidence that either an increase in bandwidth or in the MIMO order by a certain

factor cause a CPRI data rate increase by that same factor.

The calculation of data rate per CPRI link is based on the following expression:

$$R_{b\,[bits/s]} = N_{ant} S_{r\,[sample/s]} S_{w\,[bits/sample]} 2\frac{I}{Q} C_w C_l \tag{3.6}$$

where:

- N_{ant} – Number of antennas per sector.
- S_r – Sampling rate used for digitisation.
- S_w – Sample width.
- $2\frac{I}{Q}$ – Multiplication factor for in-phase (I) and quadrature-phase (Q) data.
- C_w – Factor of CPRI control word.
- C_l – Line coding factor (either 10/8 for 8B/10B coding or 66/64 for 64B/66B coding).

3.2.4 Cost Functions

Due to the centralisation, collateral systems, such as cabinets, racks, power supplying, cooling, and aggregation gateways, can be re-implemented to save energy and costs. Cloud computing and virtualisation, technologies introduced on a C-RAN approach, provide an effective way to share the processing resources.

In order to face the high traffic demand that requires an increase in computational resources and transmission capacity, mobile operators are investigating novel solutions for cost-effective network expansion and upgrade. In [ATPH15], the authors propose a model to compare, in terms of costs, the local BBUs and the three different strategies for BBU hoteling: BBU stacking, BBU Pooling, and C-RAN.

Given that the obtainable data do not fulfil all the parameters of the cost model proposed by [ATPH15], which are related to specific components and technologies currently unknown, it was necessary to make some changes in order to adapt it to the available information.

The adapted model is divided into two main costs functions, one for CAPEX and the other for OPEX,

$$C_{Total[€]} = C_{CAPEX[€]} + N_{years} C_{OPEX[€/year]} \tag{3.7}$$

where:

- C_{Total} – Total cost of the architecture.
- C_{CAPEX} – Total cost of CAPEX.
- C_{OPEX} – Total cost of OPEX per year.
- N_{years} – Number of years considered for OPEX.

The adjustment just takes into consideration the recent technology available in the network (local) and the futuristic one (C-RAN), which are the first and the last proposed by [ATPH15], respectively.

The aspects to take into account for the CAPEX calculation are the cost of the hardware, licences and civil works. In this way, the costs for the local architecture is:

$$C_{CAPEX,local[\text{€}]} = N_{BB10}C_{BB10[\text{€}]} + N_{BB20}C_{BB20[\text{€}]} + N_{cab,l}C_{Cabinet,local[\text{€}]} + N_{site}C_{site,local[\text{€}]}$$
$$+ N_{fl} C_{fibre\,[\text{€}]}$$

(3.8)

where:

- $C_{CAPEX,local}$ – CAPEX for a local architecture.
- $C_{BB10/20}$ – Cost of construction of a 10/20 MHz cell.
- $C_{Cabinet,local}$ – Cost of a local cabinet.
- $C_{site,local}$ – Cost of a local site.
- C_{fiber} – Cost of dark fibre per kilometre.
- $N_{BB10/20}$ – Number of 10/20 MHz cells.
- $N_{cab,l}$ – Number of aggregation points in a local architecture.
- N_{site} – Number of sites.
- N_{fl} – Number of kilometres of the fibre link.

Since the C-RAN architecture has a virtualisation approach and an additional cost for the fronthaul, the CAPEX is:

$$C_{CAPEX,C-RAN[\text{€}]} = V\big(N_{BB10}\,C_{BB10[\text{€}]} + N_{BB20}C_{BB20[\text{€}]}\big) + N_{cab,c}C_{Cabinet,C-RAN[\text{€}]} + N_{site}C_{site,C-RAN[\text{€}]}$$
$$+ N_{fl_{[km]}}C_{fibre\,[\text{€}/km]} + 2N_{ml}C_{microwave[\text{€}]}$$

(3.9)

where:

- $C_{CAPEX,C-RAN}$ – CAPEX for a C-RAN architecture.
- $C_{Cabinet,C-RAN}$ – Cost of a C-RAN cabinet.
- $C_{site,C-RAN}$ – Cost of a C-RAN site.
- $C_{microwave}$ – Cost of microwave equipment.
- $N_{cab,c}$ – Number of aggregation points in a C-RAN architecture.
- N_{ml} – Number of the microwave link.
- V – Virtualisation factor.

Regarding the estimation of fixed costs per year, the OPEX takes into consideration three main factors:

$$C_{OPEX[\text{€}]} = C_{energy[\text{€}]} + C_{renting[\text{€}]} + C_{maintenance[\text{€}]} + C_{fibfronthaul[\text{€}]} + C_{mwlicences[\text{€}]}$$

(3.10)

where:

- C_{energy} – Cost of the energy consumption.
- $C_{renting}$ – Cost of renting.
- $C_{maintenance}$ – Cost of a maintenance of infrastructures.
- $C_{fibfronthaul}$ – Cost of maintenance of fibre fronthaul.
- $C_{mwlicences}$ – Cost of microwave fronthaul licences.

Energy consumption is related to air-conditioning and telecom equipment associated with each RRH to BBU connection. The virtualisation in a local approach is 1. This factor exists in a C-RAN architecture, which has energy savings due to centralisation,

$$C_{energy[€]} = 24 \cdot 365 \cdot E_{BBU[\text{kWh}]} C_{fee[€/(\text{kWh})]} N_{RRH,con} V \tag{3.11}$$

where:

- E_{BBU} – Energy consumed per hour for a BBU.
- C_{fee} – Energy fee.
- $N_{RRH,con}$ – Number of RRH connected.

The term related to renting considers the average price per m² per month in different areas:

$$C_{renting[€]} = 12_{[\text{month}]} A_{[\text{m}^2]} V \left(N_{DU} C_{DU[€/\text{m}^2/\text{month}]} + N_U C_{U[€/\text{m}^2/\text{month}]} + N_R C_{R[€/\text{m}^2/\text{month}]} \right) \tag{3.12}$$

where:

- $C_{DU/U/R}$ – Cost of rent a square metre per month in a dense urban/urban/rural area.
- $N_{DU/U/R}$ – Number of RRHs in a dense urban/urban/rural area.
- A – Area occupied by an RRH.

The conditions that allow the prediction of maintenance are related to network deployment, the hardware that is not related to baseband processing, and the computer boards responsible for dealing with signal processing. Therefore, maintenance is computed by a multiplication among the different aspects of CAPEX and different coefficients,

$$C_{maintenance[€]} = 0.01 C_{CAPEX,deployment[€]} + 0.1 C_{CAPEX,hardware[€]} + 0.25 C_{CAPEX,computer[€]} \tag{3.13}$$

where:

- $C_{CAPEX,deployment}$ – Cost of deployment investment.
- $C_{CAPEX,hardware}$ – Cost of hardware investment.
- $C_{CAPEX,computer}$ – Cost of computer investment.

The fibre infrastructure also requires maintenance, which is a percentage of the investment in fibre links:

$$C_{fibfronthaul[€]} = 0.06 N_{fl_{[\text{km}]}} C_{fibre\,[€/\text{km}]} \tag{3.14}$$

To compute the licences costs due to the microwave transmission, it is necessary to consider three factors: the link distance, the transmission frequency band, and the bandwidth. One should consider also a Cross Polarisation Cancellation Interface (XPCI) factor, [ANAC16]. The reference values to compute microwave licencing are presented in Annex C.

$$C_{mwlicences[€]} = k_{1[€/\text{MHz}/\sqrt{\text{km}}]} \sqrt{d_{fronthaul[\text{km}]}} B_{[\text{MHz}]} \phi_{XPCI} \tag{3.15}$$

where:

- k_1 – Factor related to the bandwidth.
- B – Bandwidth.
- ϕ_{XPCI} – XPCI factor.

3.2.5 Multiplexing Gain

To evaluate the performance of the C-RAN architecture concerning traffic fluctuations, [ChHC14] proposes a metric to weigh the benefits from the statistical multiplexing gain viewpoint. The statistical multiplexing gain compares the resources needed in a traditional RAN to those in a C-RAN. As the number of baseband resources is proportional to the traffic they need to process, the sum of traffic peaks in a traditional RAN is compared to the peak in a BBU Pool in a C-RAN:

$$G_{mux} = \frac{\sum_{i=1}^{N_{RRH}} T_{peak,i \, [\text{MB/h}]}}{\sum_{j=1}^{N_{BBU}} T_{peak,j \, [\text{MB/h}]}}$$

(3.16)

where:

- N_{RRH} – Number of RRHs.
- T_{peak} – Peak of traffic during the day.

3.2.6 Fairness Index

In order to estimate the load balancing strategy, [RaWW15a] suggests a parameter to monitor load, denominated as fairness index. This parameter is measured by using the load distribution of all collected RRHs. The fairness index can be defined as:

$$F_{index} = \frac{\left(\sum_{i=1}^{N_{RRH}} L_i\right)^2}{N_{RRH}\left(\sum_{i=1}^{N_{RRH}} L_i^2\right)}$$

(3.17)

where:

- L_i – Load of the RRH i.

The range of the fairness index is between 0 and 1, with the higher value indicating a more balanced load distribution among BBUs.

3.3   Model Implementation

In this section, a detailed explanation of the model is presented, followed by the developed algorithms.

3.3.1 Workflow

The model has the objective of analysing the network configuration, based on locations and traffic profile, to better understand the fronthaul connections and the type of fronthaul links deployed over a C-RAN architecture. In Figure 3.5, it is possible to see a detailed perspective of the overall model workflow.
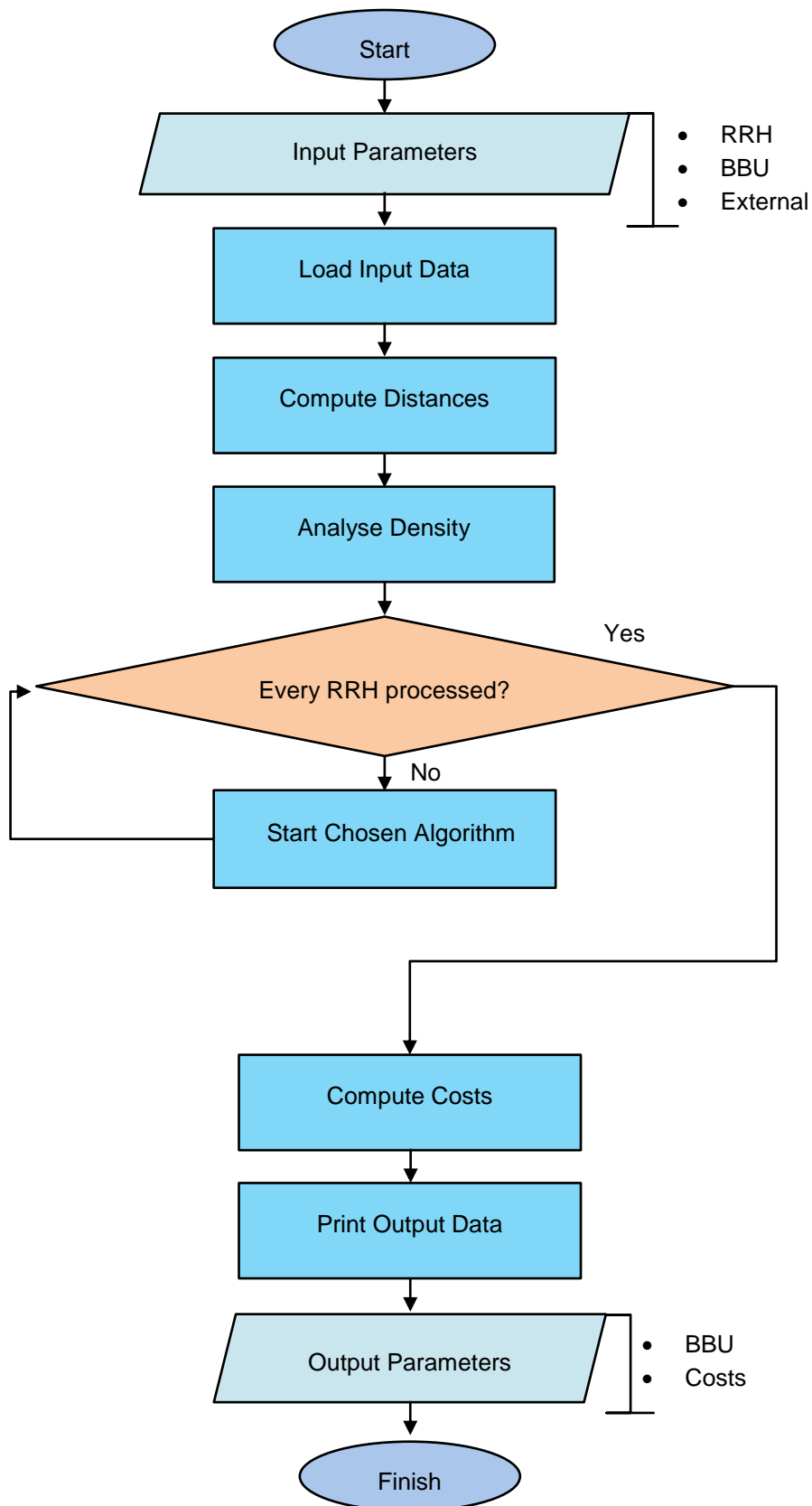
Figure 3.5. Model Flowchart.

As depicted in Figure 3.5, the first step is to compute the distances between all RRHs and all BBU Pools. Associated with that calculation, the number of possible connections between one RRH and all BBU

Pools is also computed, based on the maximum distance/delay of the fronthaul link. This is performed in order to have all the potentials connections to weight the most appropriate option.

After that, the model starts a cycle until there are no more RRHs in the network to analyse. The technical layer occurs in this cycle, which is the core of the model. This means that the critical decisions are made in this layer, and they will influence the final C-RAN configuration according to the algorithm introduced in the input parameters. When all RRHs are dealt with, they may be assigned to just one BBU Pool or none, but never connected to two or more.

In the last step of the model, with the network configuration established, both CAPEX and OPEX are computed.

3.3.2 Algorithms

The technical layer is the one where the decisions of the connections between the most appropriated BBU Pool to each RRH are made, which depend on the algorithm that is chosen at input parameter. Depending on the chosen algorithm, there are several key aspects to analyse, such as traffic curves, the distance between BBU Pools and RRHs, the number of BBUs, and load balance. The algorithms can only be selected one in a time. To illustrate how the algorithms work, a scenario with 2 BBU Pools and 10 RRHs was created, Figure 3.6, being assumed that both BBU Pools do not have capacity limits and that all RRHs can connect to both BBU Pools, which means that there are no restrictions concerning distance/latency.
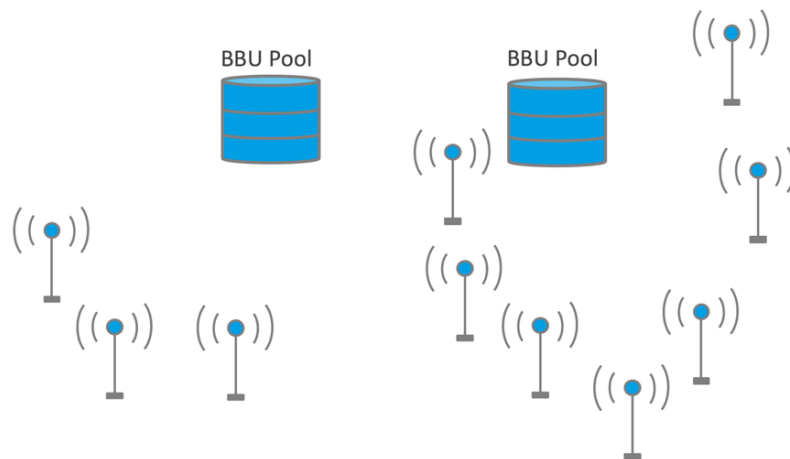
Figure 3.6. Scenario to explain algorithms diagram.

The first four algorithms have the same principle, differing in the key aspect to analyse, as Figure 3.7 shows. There are three kinds of RRHs, based on the maximum fronthaul distance, in what concerns the number of possible BBU Pools connections:

- The ones that cannot be connected to any BBU Pool, which means that they do not respect the distance requirement.
- The ones that may be connected to one BBU Pool, which means that they respect just the distance requirement of that BBU Pool.
- The ones that respect the distance requirement to more than one BBU Pool, which means that

they will evaluate the options to connect to the most appropriate BBU Pool for each algorithm.

To connect an RRH to a BBU Pool, there are two network requirements that must be fulfilled: the first is maximum fronthaul distance, and the second is the maximum capacity of the BBU Pool, both specified by input parameters. Thus, the RRHs that do not respect at least one of the restrictions cannot be connected to any BBU Pool. For this reason, they will have their own BBU decentralised, which means that the BBU stays as in the traditional RAN.
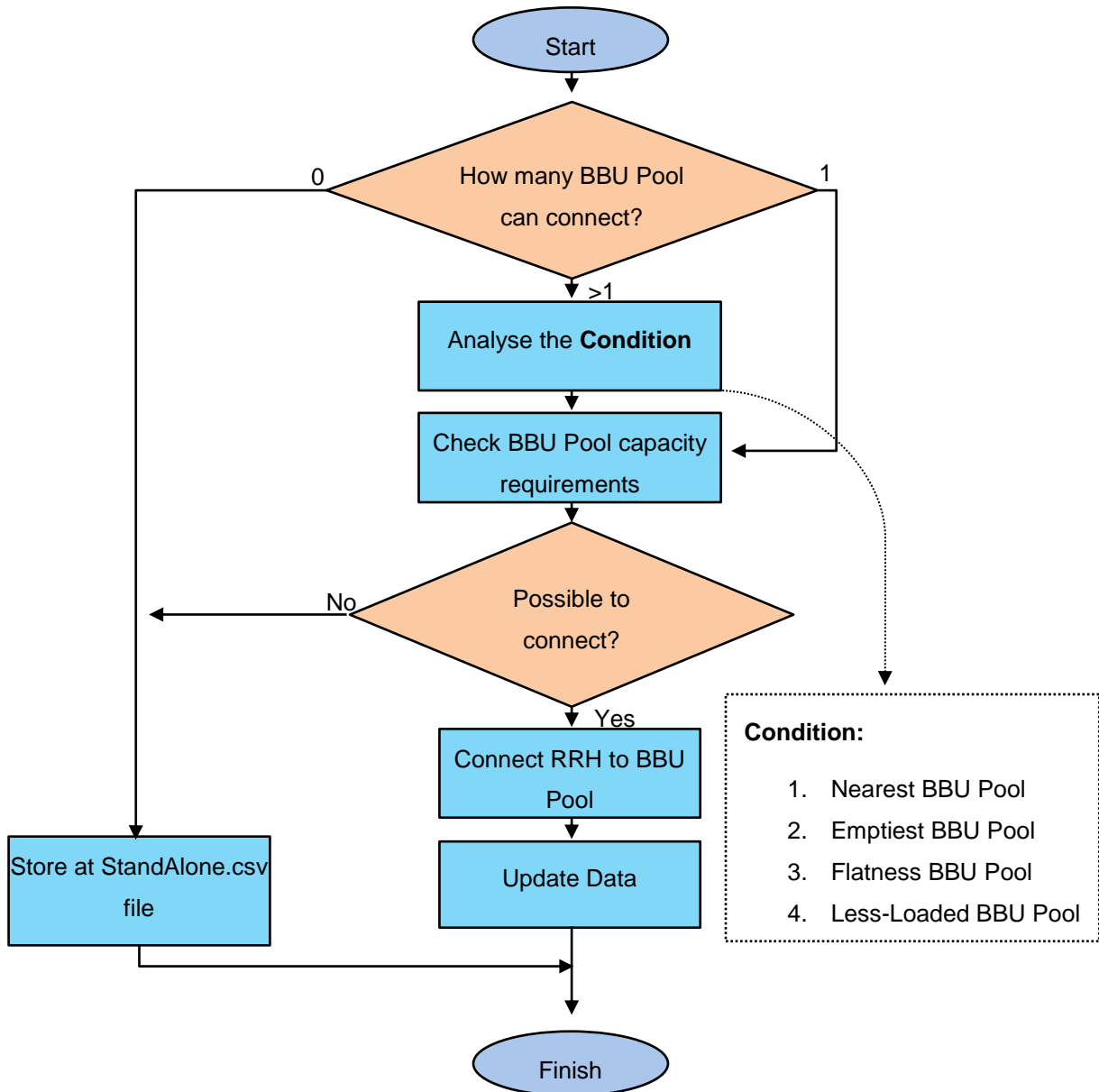
Figure 3.7. Algorithms Flowchart.

The **Minimise Delay Algorithm** aims to connect the RRH **closer** to the possible BBU Pool location, as Figure 3.8 illustrates. Each RRH has possible locations of BBU Pools to connect, thus, knowing all the distances between possible connections, the algorithm checks the capacity requirement of the RRH to the nearest BBU Pool until it is able to start the connection. In Figure 3.7, this algorithm is associated to condition number one.
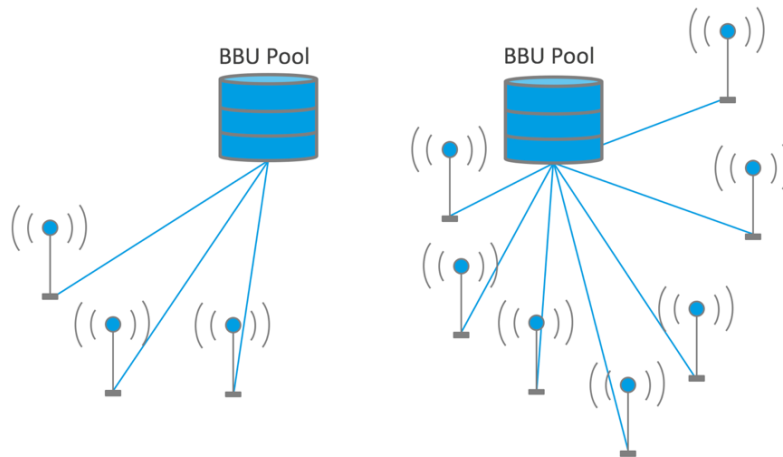
Figure 3.8. Minimise Delay algorithm diagram.

The **Number of RRH per BBU Balance Algorithm** aims to balance the number of RRHs in every BBU Pools. The information on the number of RRHs that each BBU Pool has is always available and updated, thus, each RRH, before evaluating the decision, has the information to analyse the possible connections, thus, the RRH will check the maximum capacity of the BBU Pool with less RRHs already connected, until it is capable of performing the connection. With this approach, as Figure 3.9 suggests, it is guaranteed that BBU Pools have almost the same number of RRHs. In Figure 3.7, this algorithm is associated to condition number two.
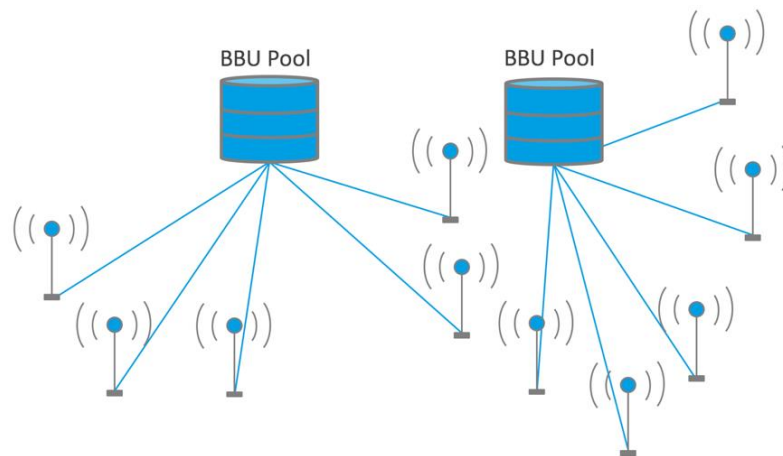
Figure 3.9. Number of RRH per BBU Balance algorithm diagram.

The **Flatness Algorithm** aims to force a horizontal traffic profile in every BBU Pool, with the objective to avoid traffic peaks, taking into consideration the three types of RRHs: residential, commercial and mixed. These types have specific time intervals throughout the day regarding traffic behaviour. The ideal BBU Pool traffic profile should have a constant traffic load throughout the day, in order to obtain multiplexing gains and energy efficiency in a C-RAN approach, comparing with the traditional RAN. The algorithm takes the selected hours of the day at input parameters, which must be a vector of integers ranging between 1 and 24.

Since the information of the traffic profile of each BBU Pool is always updated, each RRH evaluates the possible connections, based on hours' vectors. The RRH, before connecting to one BBU Pool, considers the traffic load, assuming that the connection is made, doing a linear regression in between the points

of time in the vector, the regression that has a lower slope being the one that provides higher gains. Thus, until there are no more BBU Pools to analyse, and taking into consideration the maximum capacity limit of each BBU Pool, the RRH connects to the BBU Pool with the lowest slope provided by the linear regression. With this decision, as Figure 3.10 shows, it is ensured that the BBU Pools has constant traffic throughout the day. In Figure 3.7, this algorithm is associated to condition number three.
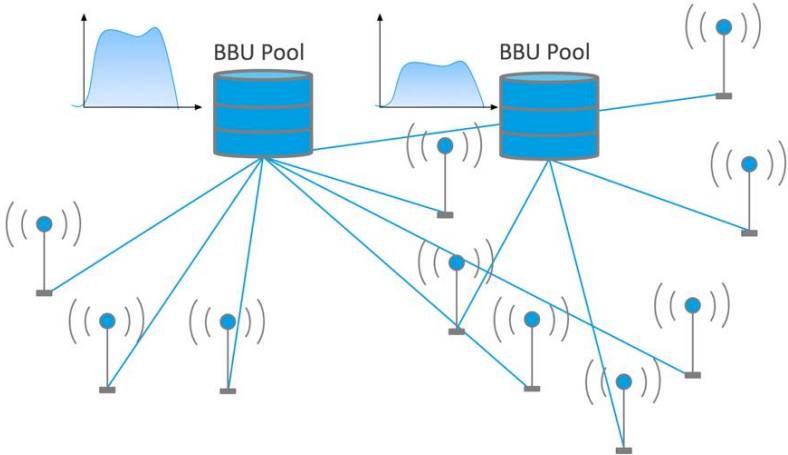
Figure 3.10. Flatness algorithm diagram.

The **Capacity Load Balance Algorithm** aims to balance traffic load in every BBU Pool. The information of traffic load of each BBU Pool is always available and updated. Before evaluating the decision, each RRH has the information of traffic of the possible BBU Pools connections, thus, the RRH will check not only the maximum capacity limit of the BBU Pool, but also the possible load if the connection occurs. The possible BBU Pool connection that has the lower traffic load after the link happens starts the connection. With this approach, as Figure 3.11 indicates, it is guaranteed that the BBU Pools have a balance in what concerns to traffic load. In Figure 3.7, this algorithm is associated to condition number four.
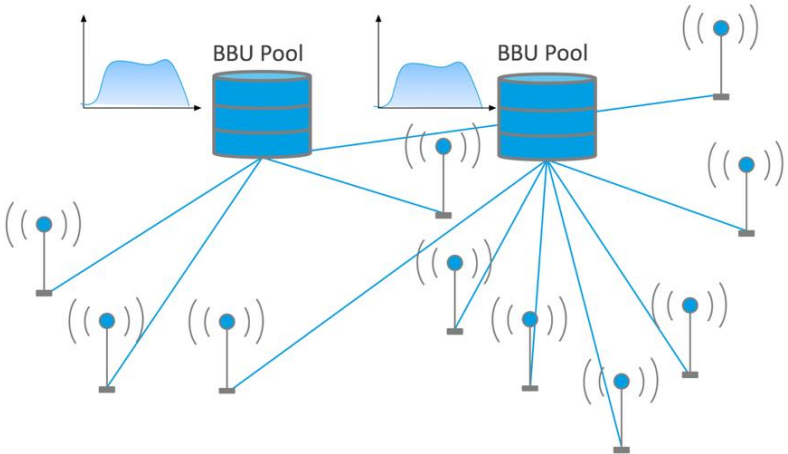
Figure 3.11. Capacity Load Balance algorithm diagram.

The **Minimise Number of BBU Pools Algorithm** aims to minimise the number of BBUs. The key aspect of this algorithm is to understand, for each RRH, the possible BBU Pools that are already in use. This information is always available and updated. There are three hypotheses on the number of possibilities, based on number of BBU Pools that are already in use for each RRH, as Figure 3.12 suggests:

- The RRHs that only can connect to one BBU Pool already in use, which means that the RRHs may be connected to that BBU Pool.
- The RRHs that can connect to more than one BBU Pool already in use, which means that the RRHs will weigh the options to connect to the most appropriate BBU Pool.
- The RRHs that cannot connect to any BBU Pool already in use, which means that the RRHs will evaluate the options and may connect to an unused BBU Pool.
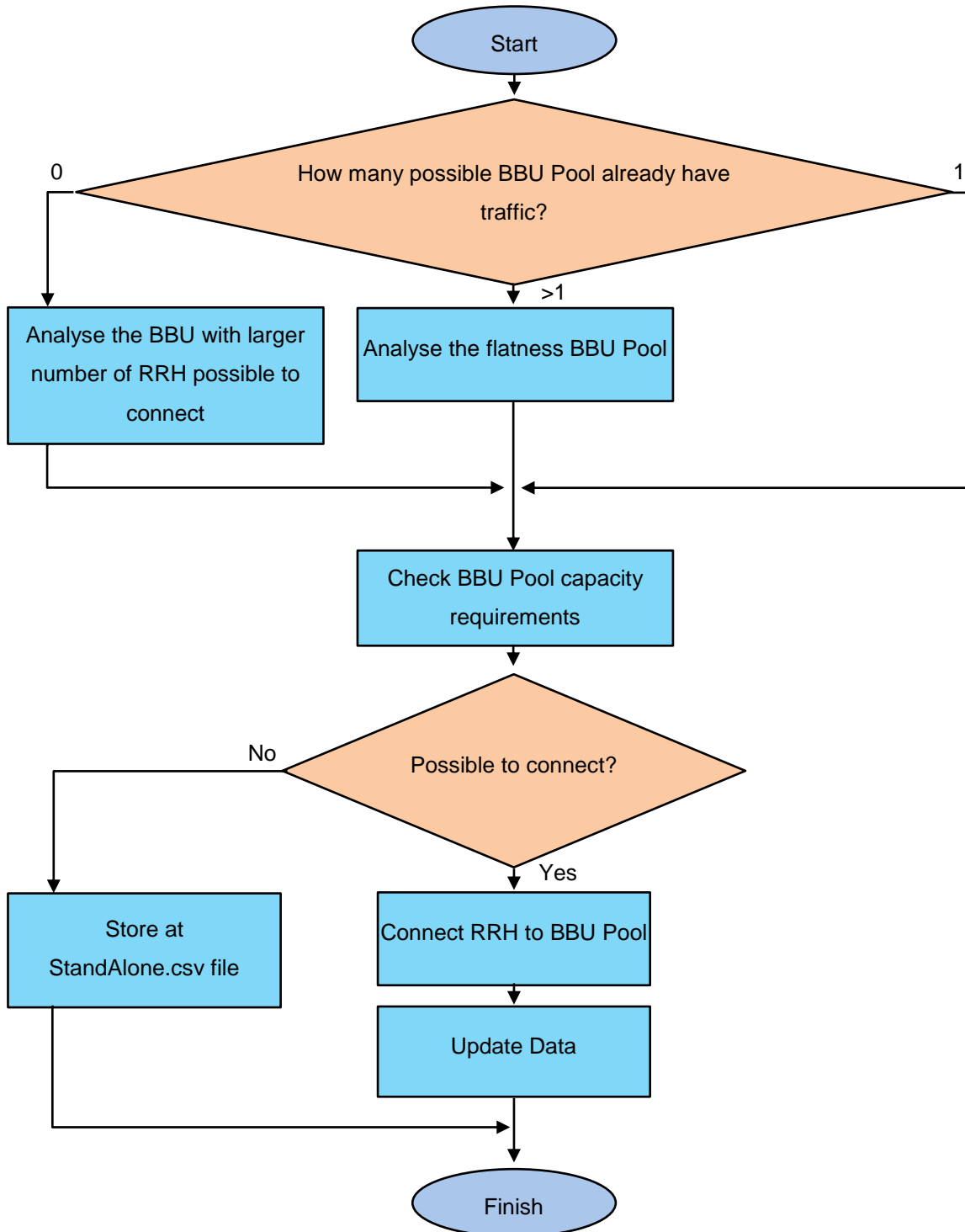
Figure 3.12. Minimise Number of BBU Pools algorithm flowchart.

To evaluate the connections that have more than one possibility, the RRHs check the maximum capacity limit of each possibility, and connect to the one that has a traffic load Flatness, based on the third algorithm. The remaining ones that do not have the possibility to connect to a BBU Pool already in use are forced to connect to the BBU Pool that has the possibility to connect to the larger number of RRHs. With this approach, as Figure 3.13 suggests, it is guaranteed that the number of BBU Pools is minimised. In Figure 3.12, it is illustrated that, like the algorithms explained above, the RRH that does not respect at least one of the requirements, distance or capacity limits, cannot be connected to any BBU Pool. For this reason, it will have its own BBU decentralised, i.e., the BBU stays as in the traditional RAN.
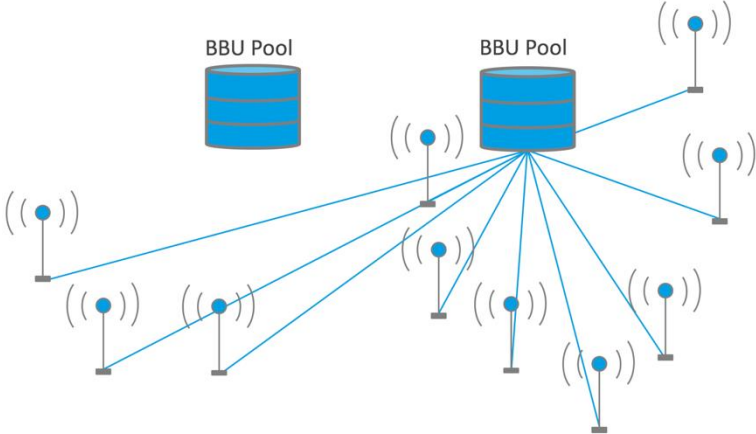
Figure 3.13. Minimise Number of BBU Pools algorithm diagram.

3.4 Model Assessment

In order to validate the model implementation, during its development, the outputs were subjected to a set of empirical tests. Basically, as the scripts were under construction, a careful examination of all variables was performed, in order to check for coherence and accuracy from a theoretical viewpoint.

To validate the performance of critical parameters, such as distance and capacity limits, which are the main responsible for the possibility to start a connection, a scenario with 374 RRHs in different locations and with 45 possible BBU Pools, also with different locations, was created. In order to test the variation, in percentage, of the number of RRHs that are successfully connected to one BBU Pool, a variation in the maximum fronthaul distance and BBU maximum capacity was considered, shown in Figure 3.14 and Figure 3.15, respectively. The figures correspond to the Capacity Load Balance algorithm. In Figure 3.14 there are no capacity limits from the BBU Pool viewpoint, and it is possible to understand that, at the point of maximum distance for the fronthaul the percentage of RRH connected are 100%, but the curve reaches the saturation point at the mean distance of the fronthaul.

In Figure 3.15 there are no distance limits from the fronthaul viewpoint, and it is possible to understand that, at the point of maximum BBU Pool capacity the percentage of RRH connected are 100%, but the curve reaches the saturation point at the mean BBU Pool capacity.

Table 3.3. List of empirical tests that were made to validate the model implementation.

Number	Description
1	Validation of the input file read, by verifying if the type of variable (string or number) is correct.
2	Validation of the network input file read, by verifying if the number of RRHs and BBUs coordinates' pairs loaded to Matlab was equal to the number of rows of the file.
3	Scatter plot of the RRHs and BBUs locations, in order to visually inspect their geographical rightness.
4	Validation of the coverage areas: • Check if the set of circles form coverage areas was covering the geographical area.
5	Validation of maximum delay and distance constraint: • Check there are not connections that do not respect the constraint.
6	Validation of maximum capacity of the BBU: • Check there are not connections that do not respect the constraint.
7	Validation of the BBU computational and link capacity tables update: • Check if it is happening every time an RRH is connected to a BBU Pool. • Check if the values are correctly computed and stored.
8	Verification of cell site connection completion: • Check if the number of loaded pairs of coordinates equals the number of connected cell sites.
9	Verify if the process of handling disconnected RRH: • Check if there are no sites unexamined.
10	Verification of the correct plot of all outputs.
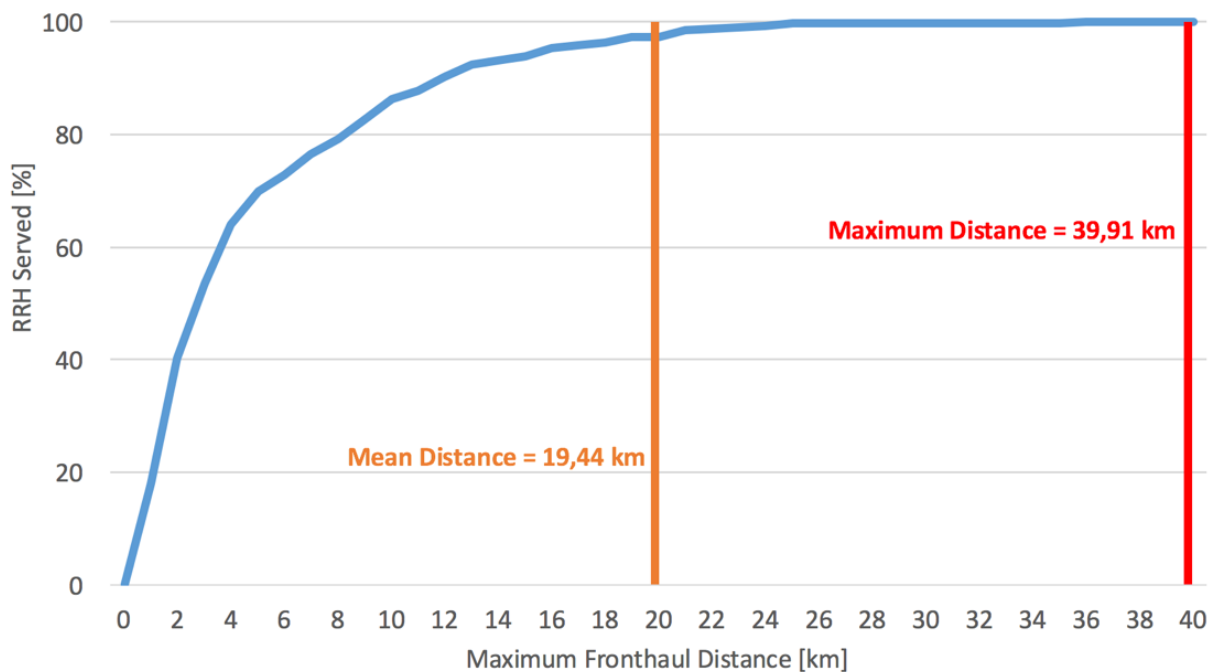
Figure 3.14. RRH Served evolution with maximum fronthaul distance.
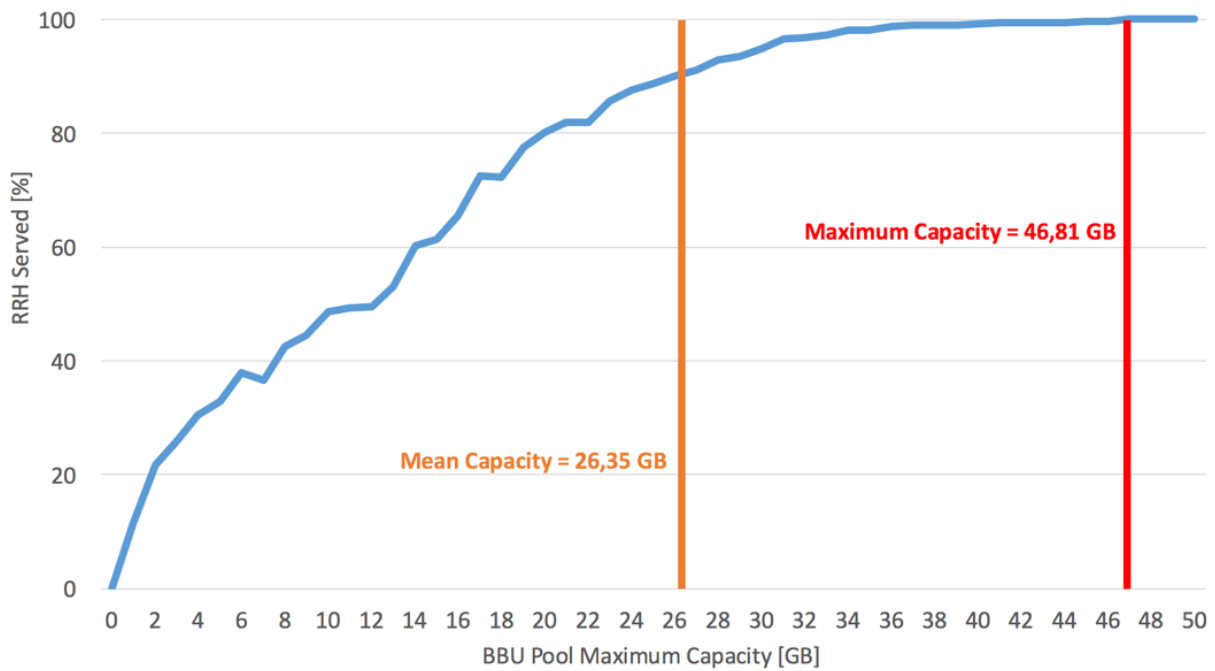
Figure 3.15. RRH Served evolution with BBU Pool Maximum Capacity.

Analysing both Figures 3.14 and 3.15, it was verified that the algorithm was properly running and that the aggregation between the RRHs and the BBU Pools was properly performed.

There are two scenarios for this master thesis, each one with two possible variants: the aggregation points locations, taking into account that one aggregation point corresponds to one RRH and the RRHs locations. The number of RRHs ranges between 374 and 8 065, which means that in each simulation took between 1 minute and 6 hours, respectively. The simulations were performed in a 2.2 GHz Intel Core i7.

Chapter 4

Results Analysis

This chapter presents the considered scenario along with the associated results and respective analysis.

4.1 Scenarios

To study the performance of a C-RAN architecture when it is implemented on a large scale, this thesis has two different scenarios, based on data provided by NOS for Minho and public data for Portugal.

4.1.1 Minho Scenario

The Minho scenario, as illustrated is Figure D.1, is located in the north-west of Portugal, taking into consideration the regions of Porto, Braga, Viana do Castelo, and Vila Real; the whole area has around 3.4 million inhabitants in 11 651 km². Although the average population density is 288 inh./km², the Porto metropolitan area is the second biggest urban area in the country with around 940 inh./km², which reveals the area with more mobile traffic.

As mentioned in Section 3.4, each scenario has two variants, related to the RRHs and cell sites, which means that the cell sites do not take sectors into account, and consequently the RRHs, of each LTE cell site location. The scenario information concerning the number of RRHs and cell sites, as well as the number of BBU Pools, is summarised in Table D.1.

Regarding the information available in Table D.1, it is possible to understand the difference between the number of RRHs and the number of cell sites taking into consideration the percentage of sectors per cell site summarised in Table 4.1.

Table 4.1. Percentage of sectors in Minho.

Number of Sectors	Percentage [%]
1 and 2	8.82
3	74.87
4,5 and 6	16.31

In order to classify RRHs per areas, such as dense urban, urban and rural, one has established metrics based on the density of RRHs. Analysing the number of neighbours in a 2 km radius, two thresholds were defined to split the three types of areas based on empirical tests to correspond to a real case scenario. Consequently, Figure D.2 shows the distribution of RRHs in the Minho scenario.

In what concerns the traffic profile of RRHs, there are three intervals to analyse:
- Dawn – between 00:00 and 08:00.
- Labour – between 08:00 and 17:00.
- Night – between 17:00 and 24:00.

RRHs are divided into three classes, according to the hours of the day with higher traffic load:
- Commercial – if traffic in the labour period is substantially higher than the night one.
- Residential – if traffic in the night period is substantially higher than with the labour one.
- Mixed – if the difference between traffic in the labour and night periods is not significant.

The percentage of traffic type in RRHs is presented in Table 4.2.

Table 4.2. Percentage of RRHs traffic type in Minho.

Type of RRH	Percentage [%]
Commercial	42.78
Residential	25.40
Mixed	31.82

The distribution of the different types of traffic in RRH in Minho is shown in Figure D.3.

For this scenario, not only the total traffic but also its different types according to RRHs average DL profile is taken, as illustrated in Figure 4.1:
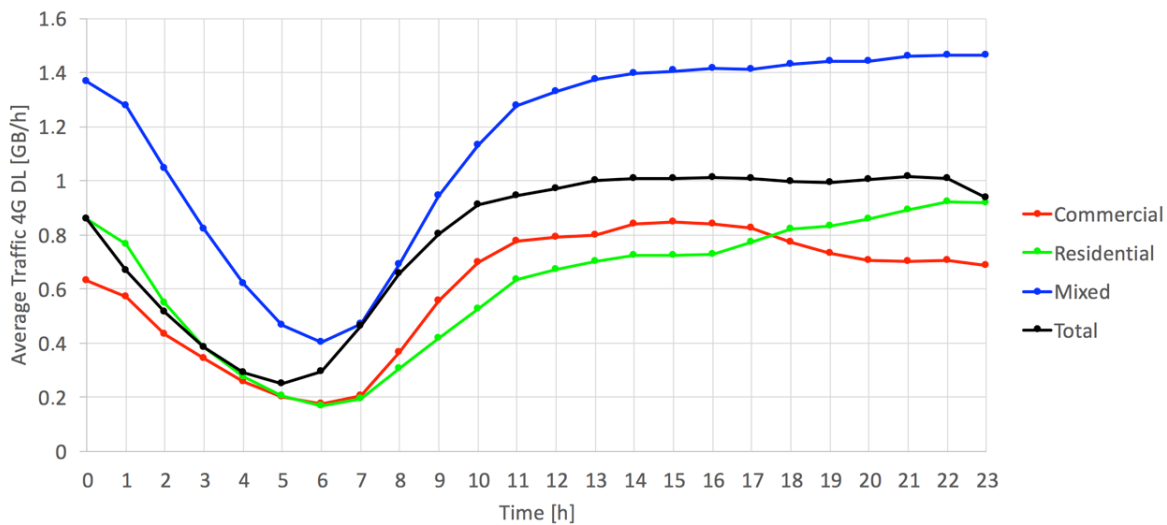
Figure 4.1. Average DL traffic for Commercial, Residential and Mixed RRHs in Minho.

4.1.2 Portugal Scenario

The Portugal scenario is, as illustrated in Figure 4.2, is the whole country one, with an area of 92 090 km^2 and around 10.5 million inhabitants. The population density is approximately 115 inh./km^2, which obviously does not reflect that most of the population lives in coastal areas, and that roughly a quarter lives in Lisbon's Metropolitan Area. There is a lower density of population in the countryside, in comparison with coastal areas, which means that the mobile network has the same behaviour.

As similar to the Minho scenario, the information related to the number of RRH and cell sites for each variant in Portugal is summarised in Table 4.3.

Table 4.3. Number of RHHs and possible BBU Pools in Portugal.

Variant	Number of RRHs	Number of BBU Pools
Cells sites	2755	86
RRHs	8065	86
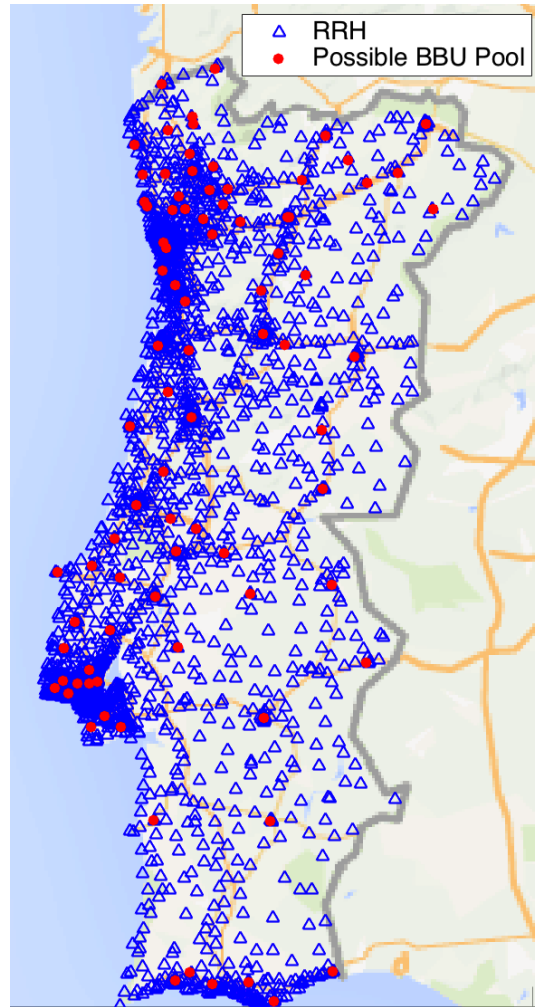
Figure 4.2. Portugal map with RRHs and possible BBU Pools locations.

For Portugal, the percentage of sectors per cell site is summarised at Table 4.4.

Table 4.4. Percentage of sectors in Portugal.

Number of Sectors	Percentage [%]
1	0,94
2	5,38
3	93,68

The classification the RRH per areas is the same principle as in the Minho scenario. It is noticeable, based on RRHs neighbourhood, that the cities of Lisbon, Setubal, Porto, Coimbra and Braga are the ones with higher RRHs density. Figure D.4 shows the distribution of RRHs in Portugal:

Given the general traffic characterisation for this scenario, the type of traffic for the RRHs is based on the density and the number of RRHs per site, in order to take it similar to a real case scenario, Table 4.5.

Table 4.5. Assumptions to characterise the RRHs traffic profile in Portugal.

	1 Cell	2 Cells	3 Cells
Dense Urban	Mixed	Commercial	Commercial
Urban	Residential	Mixed	Commercial
Rural	Residential	Residential	Mixed

The percentage of RRHs traffic type, in Portugal scenario, is presented in Table 4.6.

Table 4.6. Percentage of RRHs traffic type in Portugal.

Type of RRH	**Percentage [%]**
Commercial	22.23
Residential	55.28
Mixed	22.49

The distribution of the different types of traffic in RRHs is illustrated in Figure D.5.

The average DL traffic profile is illustrated in Figure 4.3.
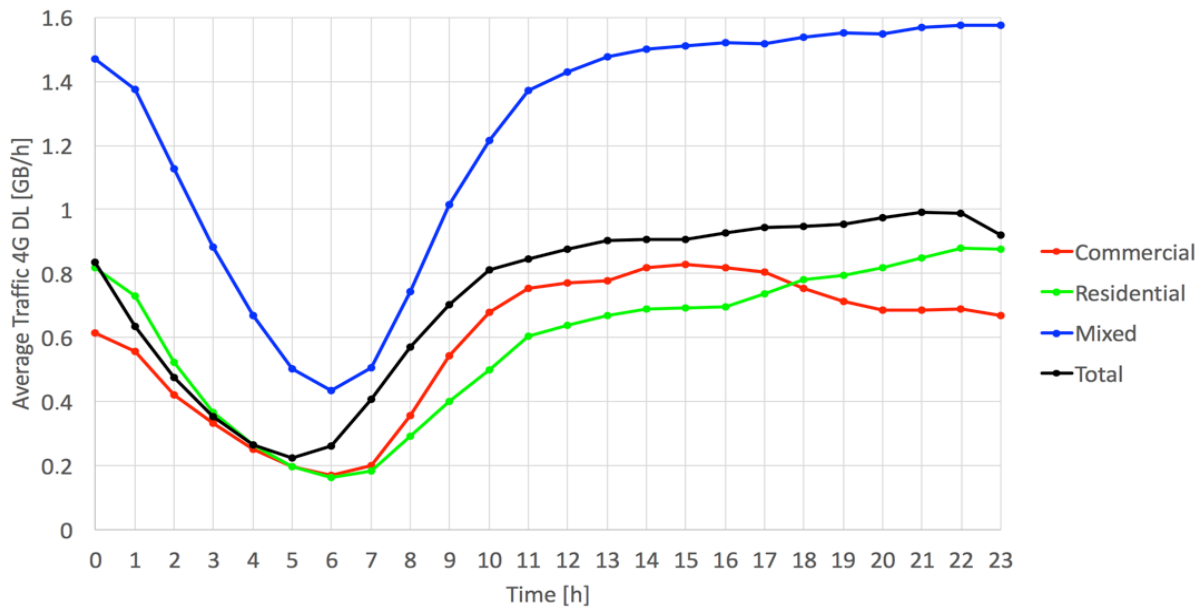
Figure 4.3. Average DL traffic for Commercial, Residential and Mixed RRHs in Portugal.

4.1.3 Reference Configurations

To analyse the model performance parameters, reference configurations were created. For the network configuration, the scenarios use different RRHs configurations according to the type of RRHs:

- Dense Urban – uses the 2 600 MHz band, 20 MHz bandwidth, and 2x2 MIMO configuration.
- Urban – uses the 1 800 MHz band, 10 MHz bandwidth, and 2x2 MIMO configuration.
- Rural – uses the 800 MHz band, 10 MHz bandwidth, and 2x2 MIMO configuration.

The reference parameters related to the maximum distances allowed by the fronthaul due to latency constraints are set according to the two transmission technologies:

- Fibre link – maximum distance of 40 km and propagation speed of 200 km/ms.
- Microwave link – maximum distance of 1.5 km and propagation speed of 300 km/ms.

Regarding the BBU Pool maximum capacity, in the reference configuration no limit was established, being considered infinite. This condition considers that a BBU Pool can lead to all traffic provided from every RRH. RRHs generate both DL and UL traffic in all radio technologies. As reference, the LTE DL traffic was used, being analysed in GB/h in the BBU Pool.

Both scenarios are assumed to have some assumptions in order to test the model, mostly related to costs. The C_{fee} value is based on the energy fee available for low voltage tariffs in EDP [ERSE16]. The C_{DU}, C_U and C_R data are based on statistical information from housing companies for the different regions of Portugal [Imov16]. The fact that the C-RAN architecture is cheaper than the local one is justified by the fact that when one rents a square meter alone the value increases. The area occupied by a cabinet is based on the size of the BTS3900A cabinet, which consists of an RF cabinet and a power cabinet [HUAW12]. The virtualisation factor depends on the algorithm and network specifications, being considered independent for each BBU Pool. The remaining values were provided by NOS.

Table 4.7. Assumption values in reference scenarios.

	Local	C-RAN
$C_{BB10[€]}$	300	
$C_{BB20[€]}$	600	
$C_{site[€]}$	5 500	1 500
$C_{Cabinet[€]}$	300	450
$C_{fibre\,[€/km]}$	5 000	
$C_{microwave[€/link]}$	6 000	
$C_{fee[€/kWh]}$	0.16	
$C_{DU[€/m^2/month]}$	15	13
$C_{U[€/m^2/month]}$	10	8
$C_{R[€/m^2/month]}$	5	4
$E_{BBU[kWh]}$	0.6	
$A_{[m^2]}$	4	3
V	1	$\dfrac{1}{G_{mux}}$

Due to the expensive cost of fibre deployment, and to make the reference assumptions closer to a real case scenario, although the fibre cost remains the same, it is assumed that NOS already owns a fibre infrastructure corresponding to 85% of the investment, since it has a fibre network spread all over the

country. The already existing fibre links are presented in the network as the backhaul, making the connection between E-UTRAN and EPC. For this reason, some of the total investment in fibre is already done. Thus, taking advantage of their own fibre infrastructure this scenario is closer to a real one. Otherwise, considering that the operator needs to spend 100% of the costs to deploy a new fibre network becomes unbearable, being too pessimistic and unreal.

4.2   Analysis of the Reference Scenario

The reference scenario is the Minho one, with 1 176 RRHs and 42 possible BBU Pools locations. In order to have reference values to compare and analyse in the following sections, one analysed the reference scenario with the reference configuration. Initially, some tests on the performance parameters were made in order to evaluate the most consistent algorithm.

In Table 4.8, the fronthaul constraints are shown in terms of distance. By adopting the proposed model with different algorithms, there are two algorithms that are not within the average values of the five proposed algorithms. On the one hand, once the Minimise Delay algorithm intends to connect the RRHs to the nearest BBU Pool, it is expected that the mean value of OWD, and hence the distance mean value, are below the average values. On the other hand, the Minimise Number of BBU Pools algorithm aims to increase the number of RRHs per BBU Pool, thus, RRH-BBU connections have longer distances, being above average values. This represents a reasonable trend, avoiding some maximum delay conditions from the operator's viewpoint, for reasons of system reliability and redundancy.

Table 4.8. Fronthaul distances for different algorithms in the reference scenario.

Algorithm		Minimise Delay	Number of RRH per BBU Balance	Minimise Number of BBU Pools	Flatness	Capacity Load Balance
Fronthaul distance	Min [km]	0.01	0.01	0.01	0.01	0.01
	Max [km]	35.37	39.98	39.96	39.97	39.97
	Mean [km]	4.84	20.02	26.76	18.81	19.26
Fronthaul fibre distance	Min [km]	1.53	1.59	1.62	1.64	1.72
	Max [km]	35.37	39.98	39.96	39.97	39.97
	Mean [km]	6.46	20.82	27.23	19.42	19.99
Fronthaul microwave distance	Min [km]	0.01	0.01	0.01	0.01	0.01
	Max [km]	1.50	1.50	1.40	1.46	1.50
	Mean [km]	0.81	0.89	0.83	0.95	0.97

Figure 4.4 illustrates the distribution of the RRHs connected in reference conditions for different fronthaul distance intervals. One can easily understand the distribution of shared RRHs along the distance for the different algorithms. On the one hand, the Minimise Delay algorithm has a decreasing trend in the percentage of shared RRHs, but on the other hand, it increases in the Minimise Number of BBU Pools algorithm. This tendency in the Minimise Number of BBU Pools algorithm is justified by the fact that when an RRH is away from the closer BBU Pool, the algorithm is forced to use that distant BBU Pool to minimise the data centres. The other algorithms do not have a specific trend, remaining with an almost constant tendency. These algorithms are responsible for balance, and for this reason, they take advantage of all BBU Pools to provide an equilibrium.
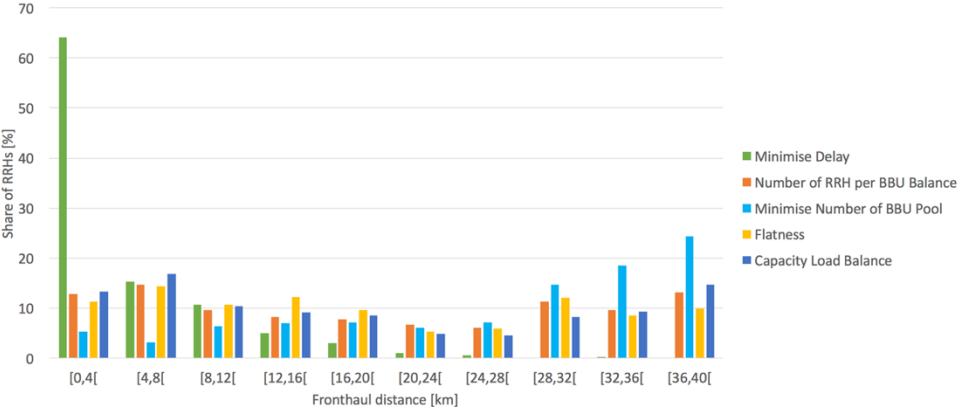
Figure 4.4. Shared RRH at different fronthaul distances in different algorithms.

Another aspect to be analysed is the load of BBU Pools and the impact that each algorithm has in this parameter. Figure 4.5 shows the maximum traffic values related to the BBU Pool with minimum and maximum traffic loads for the different algorithms. Regarding the Minimise Number of BBU Pools algorithm, the maximum and the minimum traffic loads are above the other algorithms, because the same traffic has to be divided among a smaller number of BBU Pools. The existence of one RRH that can connect only to one BBU Pool, due to delay constraints, makes the minimum load of the Minimise Delay algorithm to stay below the remaining ones, because that BBU Pool only has one connected RRH generating traffic.
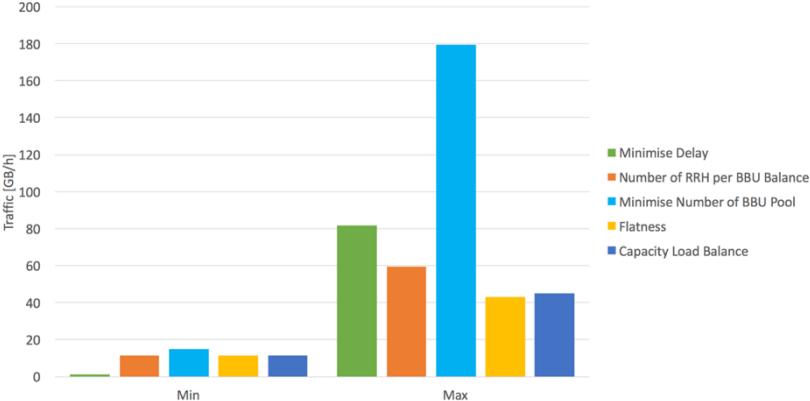
Figure 4.5. Minimum and maximum traffic load in one BBU Pool in different algorithms.

Another interesting parameter to analyse is the multiplexing gain, which can be studied in two perspectives: considering the traffic in GB/h, which means that the gain is only related to the traffic generated from the user, and considering the traffic in GOPS, which means that the gain considers not

only the user traffic but also non-traffic related operations that the BBU Pool constantly performs.

The multiplexing gain considers the traffic load in GB/h, according to the different algorithms, being presented in Table 4.9. The Minimise Number of BBU Pools algorithm has the higher gain, because with less BBU Pools the processed traffic is centralised and the gain is enhanced. The Minimise Delay algorithm has the BBU Pool with a higher gain, because it is designed to have the lower fronthaul distance possible. This distance makes dense urban RRHs, which have a more pronounced and specific traffic curves, to be connected to the same BBU Pool, taking advantage of gain. In contrast, it has also one BBU Pool with no gain; in fact, this BBU Pool has only one connection due to the distance effect, since that RRH may not be centralised, having his local BBU. Comparing the remaining algorithms, the Flatness has the greater mean multiplexing gain and the lower standard deviation, which means that all BBU Pools are well distributed concerning the constant traffic load along the day. Nevertheless, the Capacity Load Balance algorithm offers a mean user multiplexing gain as well as a lower standard deviation similar to the Flatness algorithm.

Table 4.9. DL user multiplexing gain for different algorithms in the reference scenario.

Algorithm		Minimise Delay	Number of RRH per BBU Balance	Minimise Number of BBU Pools	Flatness	Capacity Load Balance
User Multiplexing Gain	Min	1.00	1.02	1.02	1.02	1.02
	Max	1.52	1.34	1.22	1.22	1.26
	Avg	1.10	1.12	1.13	1.12	1.12
	Std	0.13	0.07	0.07	0.06	0.06

The multiplexing gain, taking into consideration the traffic load in GOPS, is presented in Table 4.10 according to the different algorithms. It is possible to see that, as expected, the multiplexing gain is lower comparing with the traffic load in GB/h, due to the fact that this multiplexing gain does not only apply to user processing resources and also to cell processing that does not depend on the user. Nevertheless, the trend among algorithms remains with the same behaviour as the user multiplexing gain.

Table 4.10. DL user and cell multiplexing gain for different algorithms in reference scenario.

Algorithm		Minimise Delay	Number of RRH per BBU Balance	Minimise Number of BBU Pools	Flatness	Capacity Load Balance
User and Cell Multiplexing Gain	Min	1.00	1.01	1.01	1.01	1.01
	Max	1.07	1.08	1.06	1.07	1.07
	Avg	1.04	1.04	1.05	1.04	1.04
	Std	0.02	0.01	0.02	0.01	0.01

One algorithm should be chosen, based on the previous tests. For this reason, by analysing the previous parameters, one may evaluate advantages and disadvantages in between algorithms. Concerning fronthaul distance, the Minimise Delay has the most promising results in contrast to the Minimise Number of BBU Pools. The remaining algorithms are balanced, not having a meaningful difference in values. Considering the BBU Pools traffic load, the Flatness and the Capacity Load Balance algorithms are the most favourable ones, having the lower amount of traffic values in the most loaded BBU Pool. The multiplexing gain analysis shows that the more stable algorithms, having the lower standard deviation, are also the Flatness and Capacity Load Balance ones. From the operator viewpoint, the network should be balanced and reliable in order to provide QoS to the user. It means that, although some algorithms apparently fit in some parameters tests, in other tests they reveal an inconsistency in order to have benefits for the network. For this reason, one chooses the Capacity Load Balance algorithm, because although it has a similar behaviour as the Flatness one, the maximum traffic balance in the network is forced to be constant in this algorithm, thus, the C-RAN architecture has similar BBU Pools in different locations.

The maximum and minimum traffic loads vary with the different BBU Pools. With the Capacity Load Balance algorithm, Figure 4.6, it is possible to observe the variations, in GB/h, of the traffic load in the network. One can clearly see that although some BBU Pools are more or less loaded, the majority, around 81%, have maximums between 25 GB/h and 35 GB/h.
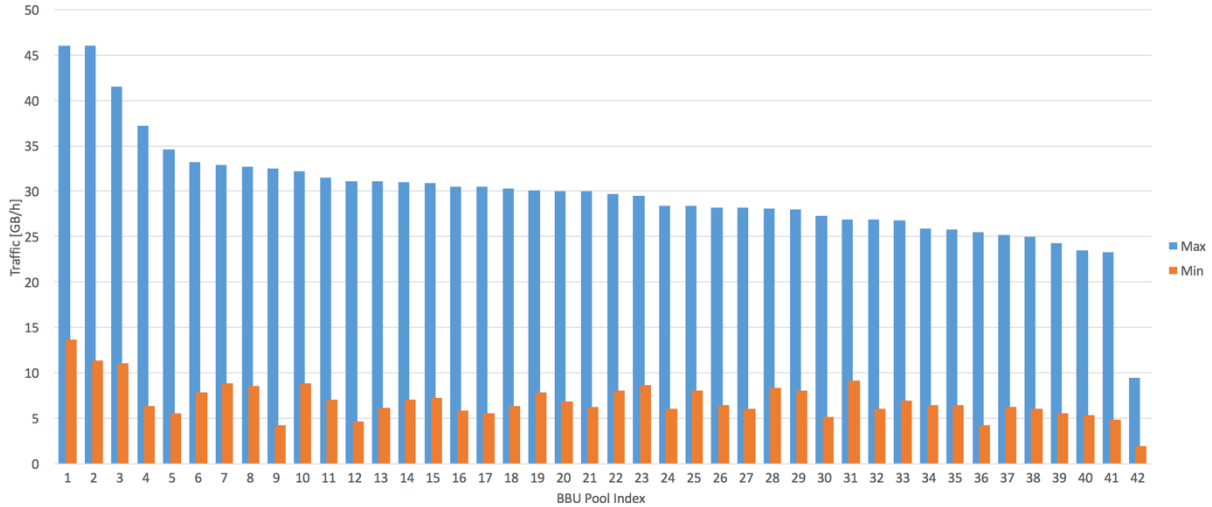
Figure 4.6. Minimum and maximum traffic in GB/h per BBU Pool with capacity balance.

The maximum and minimum loads processed in the BBU Pools with the same algorithm, but analysing the traffic in TOPS, is illustrated in Figure 4.7. One should notice that the minimum traffic is closer to maximum one due to the operations processed that are independent of traffic. This operation implies that load is more equally distributed among BBU Pools. Regarding the fact that the analysis in TOPS is less dependent on the user traffic generated, user impact is not as noticed as in the study in GB/h, thus, connections between BBU Pools and RRHs may be different, and load balance in the BBU is more consistent. So, 95% of the BBU Pools have a maximum traffic load between 3.0 TOPS and 4.5 TOPS.
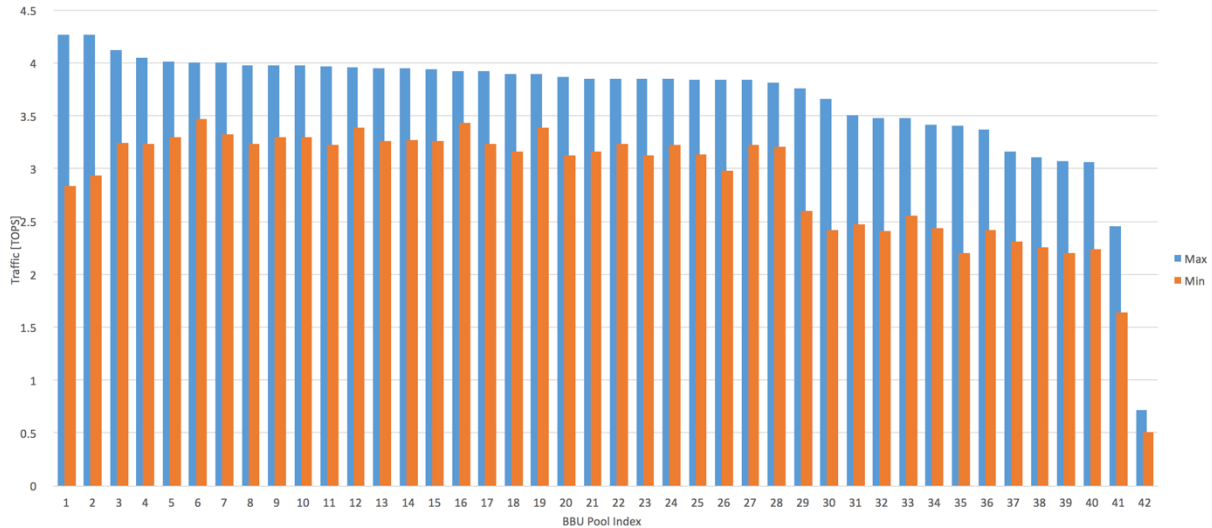
Figure 4.7. Minimum and maximum traffic in TOPS per BBU Pool with capacity balance.

CAPEX and OPEX are important parameters when a network is deployed. By adopting the proposed model, CAPEX reduction using a C-RAN instead of a traditional RAN, as Figure 4.8 suggests, is 14% considering the haul component, and 51% not considering the investment in these connections. The main component of the CAPEX analysis is, as expected, the haul. The backhaul has almost the same cost as the fronthaul, nevertheless, comparing the local architecture with the C-RAN one, the haul increases around 0.2% due to the fronthaul microwave links. The fact that the microwave link can only be established for distances below 1.5 km contributes to the increasing cost. Since each microwave link costs 12 k€ and one kilometre of fibre costs 6 k€, fibre links are advantageous from an economical viewpoint for distances bellow 2 km. The haul factor, due to the expensive cost of fibre in long distances, appears as the most significant element, even though it is assumed that the operator owns 85% of the infrastructure. Furthermore, by analysing the cost without the haul, one can see that the sites construction represents the CAPEX main component, due to the fact that the BS is the most expensive factor of a wireless network infrastructure. The variation of 59% in this element takes into consideration the difference in costs between a local and C-RAN architectures assumed in the reference parameters. Regarding cabinets cost, it is important to observe that, as expected, it increases 50% in C-RAN. Since the cost of a cabinet normalised per cell in C-RAN is 1.5 times higher than in a local architecture, it is expected that the total cost of this component remains with the same trend. In the BB component, the fact that virtualisation is considered makes a 14% cost reduction in C-RAN comparing to the local approach. Virtualisation is the key feature in this component, because the cost of a BB unit is basically the same in both architectures, with either 10 MHz or 20 MHz in a cell.

OPEX reduction by using C-RAN instead of a traditional RAN, as Figure 4.9 suggests for one year, is 13% considering the haul component, and 30% not considering these connections. As in the CAPEX analysis, the most significant influence is also the haul, because its value is a percentage of the initial investment considering the fibre, which is the most significant transmission link. Leaving aside matters related to the haul, the most obvious reduction is in renting, around 37%, due to the fact that the area considered to be occupied per cell in C-RAN is lower comparing with the local architecture. Moreover, the cost ratio in different geographical areas is also considered in renting, which also increases savings.

Due to the fact that the reduction in power consumption between the two architectures is related to virtualisation, the cost saving in energy is approximately 14%. The cost reduction of 17% in the maintenance component is based on the reduction of BB hardware and computers virtualised in the BBU Pools. Centralisation also influences the savings in what concerns to civil work.
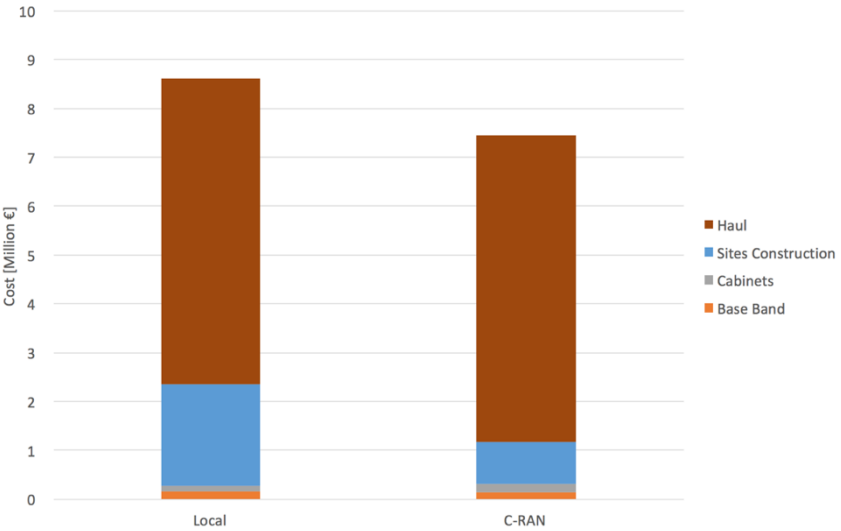
Figure 4.8. Local and C-RAN CAPEX with its components in the reference scenario.
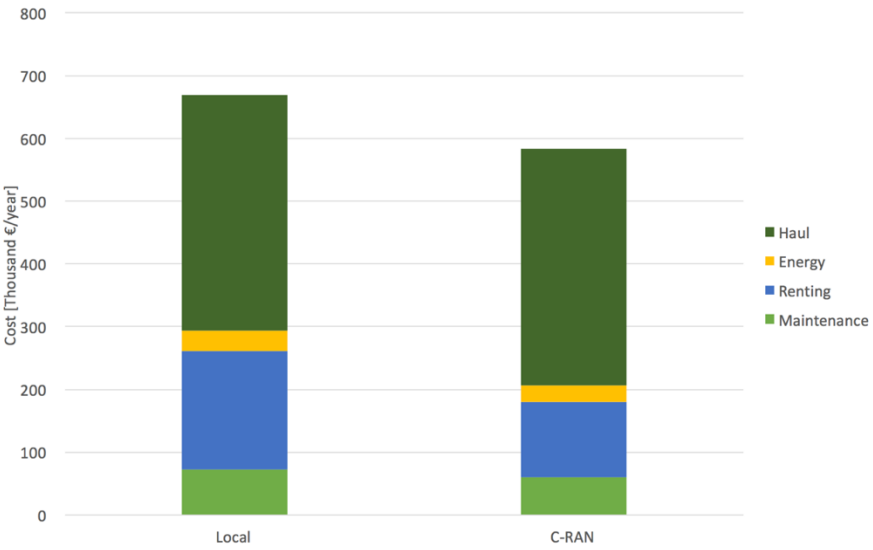
Figure 4.9. Local and C-RAN OPEX per year with its components in the reference scenario.

As highlighted in Subsection 1.2, the percentage of CAPEX and OPEX of a network was divided into different components. With the proposed model, a similar approach was taken. CAPEX, referring to network construction BB hardware, installation and civil work cost in local and C-RAN architectures, corresponding to Figure 4.10, and OPEX covering the cost needed to operate the network, such as site rental, energy, and maintenance as well in local and C-RAN architectures, corresponding to Figure 4.11. One should note that these figures do not take into consideration the haul intervention due to the high percentage that it represents. In Figure 4.11, the reduction is notorious, in percentage, of sites construction, and in contrast, the BB and cabinets components show a higher relevance on cost.

(a) Local   (b) C-RAN
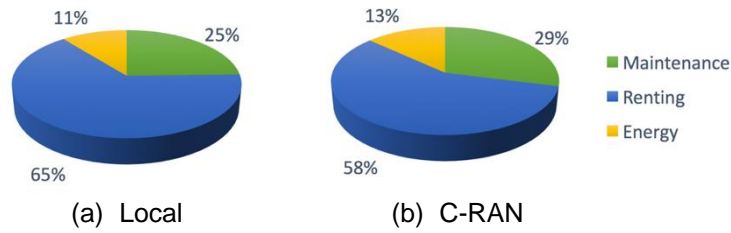
Figure 4.10. Comparison of CAPEX component for a local and C-RAN architecture.

(a) Local   (b) C-RAN
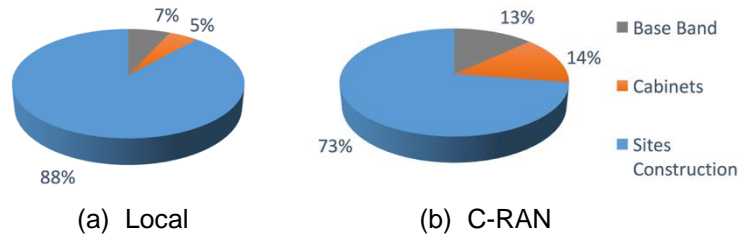
Figure 4.11. Comparison of OPEX per year component for a local and C-RAN architecture.

4.3 Analysis of Minho Scenario

4.3.1 Latency Impact

To determine the effect of the imposed maximum fronthaul delay, several outputs were analysed for different values of this constraint, namely the percentage of RRHs type, the fronthaul distance, and the percentage of connected RRHs.

The first insight on latency is the expected decrease in the percentage of dense urban RRHs and an increase in the percentage of rural RRHs as the maximum fronthaul delay increases. The Figure 4.12 depicts this evolution of the percentage of RRHs type of area, according to the Capacity Load Balance algorithm. One also sees a dominance of rural RRHs above a 10 km radius to the centre of the BBU Pool positions. One can clearly understand that with the increase of the percentage of connected RRHs, the rural ones can also increase with the same trend. One should notice that there are BBU Pools in rural areas, which means that the centralisation in a denser scenario may have a different tendency.
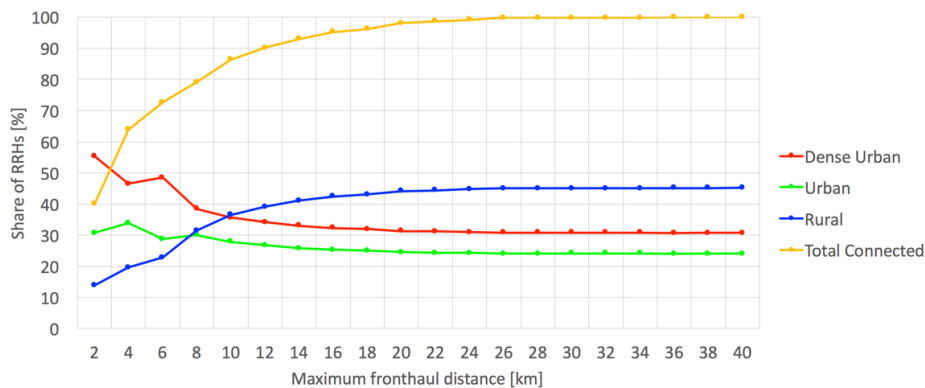
Figure 4.12. Area type of shared RRHs with different fronthaul distances in Minho.

The manipulation of the maximum fronthaul distance constraint has a direct impact on the multiplexing gain. Figure 4.13 shows, with the Capacity Load Balance algorithm, the variation of user multiplexing gain in BBU Pools positioned in dense urban, urban and rural areas considering the fronthaul link length. The classification of dense urban, urban and rural BBU Pool was based on the percentage of these type of areas that have RRHs connected to that BBU Pool. Each BBU Pool is classified according to the higher percentage of the connected RRHs type. One can easily see that the total multiplexing gain does not have a significant variation, only 3% when the fronthaul distance increases. This behaviour reaches a maximum value between the 4 km and 6 km, and a minimum at 16 km, due to the distribution of commercial, residential and mixed traffic, represented in Figure D.3. and Figure 4.14. When the percentage of mixed RRHs increases, the total multiplexing gain decreases. This algorithm is computed to make the BBU Pools balanced in terms of traffic and, as the fronthaul distance increases, the percentage of mixed RRHs also increases. This kind of RRHs, having a non-well established traffic profile, introduces a negative impact in terms of multiplexing gain. Since the dense urban percentage decreases, as illustrated in Figure 4.12, the percentage of BBU Pools characterised as dense urban also decreases, consequently, the multiplexing gain in dense urban BBU Pools decreases. The multiplexing gain in urban BBU Pools reaches a maximum value at 4 km, when the percentage of urban RRHs also reaches its maximum; after that, the gain remains almost constant, varying 2% as the fronthaul distance increases. As expected, rural BBU Pools have a minimum gain at 2 km, where the existence of rural RRHs is at a reduced number. The majority of rural RRHs have mixed traffic profile. For this reason, when the fronthaul distance increases, as well as the percentage of rural RRHs and consequently the mixed RRHs, the multiplexing gain keeps the trend, having a variation of almost 2%.
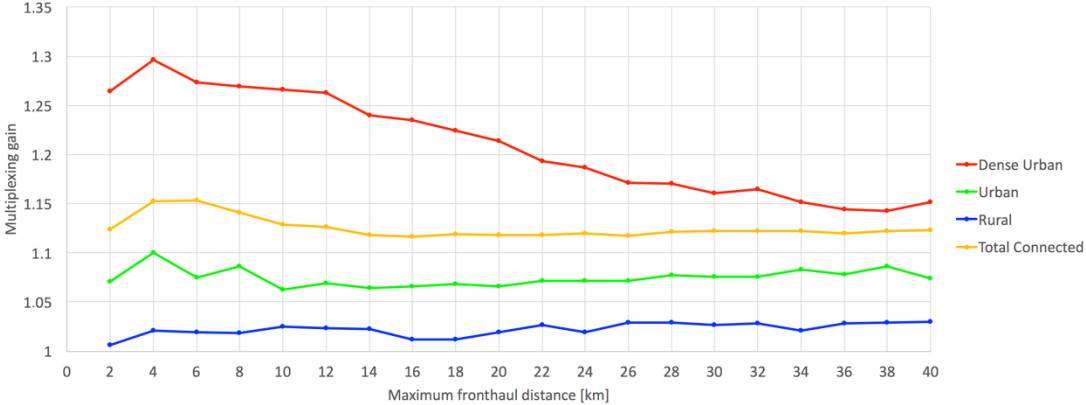
Figure 4.13. Multiplexing gain in variation for different fronthaul distances.
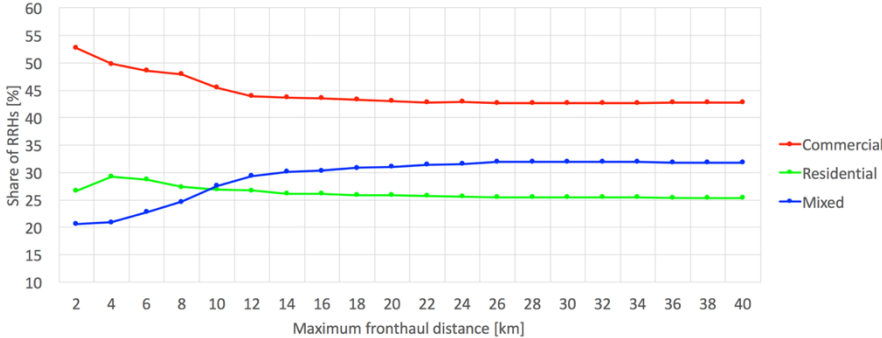
Figure 4.14. Traffic type of shared RRHs with different fronthaul distances.

As expected, an imposed growth of maximum fronthaul distance increases the average fronthaul distance, as Figure 4.15 confirms. One can clearly see that the average distance is lower than the maximum imposed one, approximately half of the maximum value established, showing that this algorithm (Capacity Load Balance) does not take into consideration the distance between RRHs and the BBU Pools. An increase in standard deviation when the maximum distance increases is also evident, which is coherent with the fact that BBU Pools provide connectivity to nearby sites as well as sites further away, causing a higher dispersion of delay values. A linear model was used to fit all three cases.
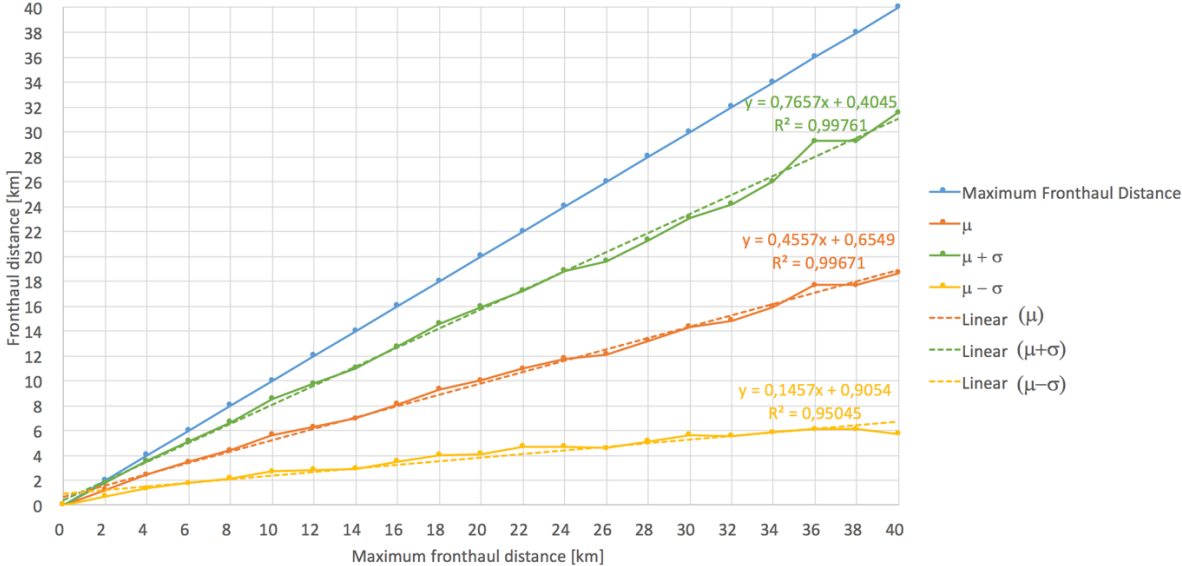
Figure 4.15. Fronthaul Distance variation with fronthaul distance.

A decrease in the percentage of possible microwave links is expected, caused by the increase in the maximum fronthaul distance. This possibility is an option that occurs when the fronthaul distance is below 1.5 km, assuming that is line of sight. It is important to understand the different behaviours of the Minimise Delay and Capacity Load Balance algorithms. In fact, Figure 4.16 shows that, as the maximum distance increases from 10 km to 40 km, the percentage of possible microwave links decreases approximately 5% in both algorithms. This means that the saturation of the percentage of possible microwave fronthaul links starts at 10 km. In the Minimise Delay algorithm, since the connections are made between the BBU Pool and the closer RRH, it is guaranteed that above 1.5 km all possible microwave fronthaul links are established at the first point of the graph. As the maximum fronthaul increases, the number of connections also increases, justifying the decrease of percentage in microwave links. However, using the Capacity Load Balance algorithm, connections do not have a specific trend regarding distance variation, as explained with the standard deviation in Figure 4.15. In this algorithm, between some points, the tendency is contrary to the descending trend. By increasing the maximum imposed distance, each BBU Pool may have more possible RRHs to connect to. The additional possibilities provided by the increase in the fronthaul distance are above 1.5 km, but each BBU Pool already has possibilities below 1.5 km. The algorithm allows a balanced distribution in capacity among BBU Pools, thus, to increase the distance constraint, the number of possible connections per BBU Pool may also increase, providing more options to do a more balanced network, not considering the fronthaul distance in the decision. If one considers that microwave technology could

only support the traffic demand of the considered RRHs for shorter distances (e.g., 1 km or less), it would reduce these percentages, even if the curve exhibits a similar behaviour. A polynomial model was used for the fitting, since it was the one with the higher correlation.
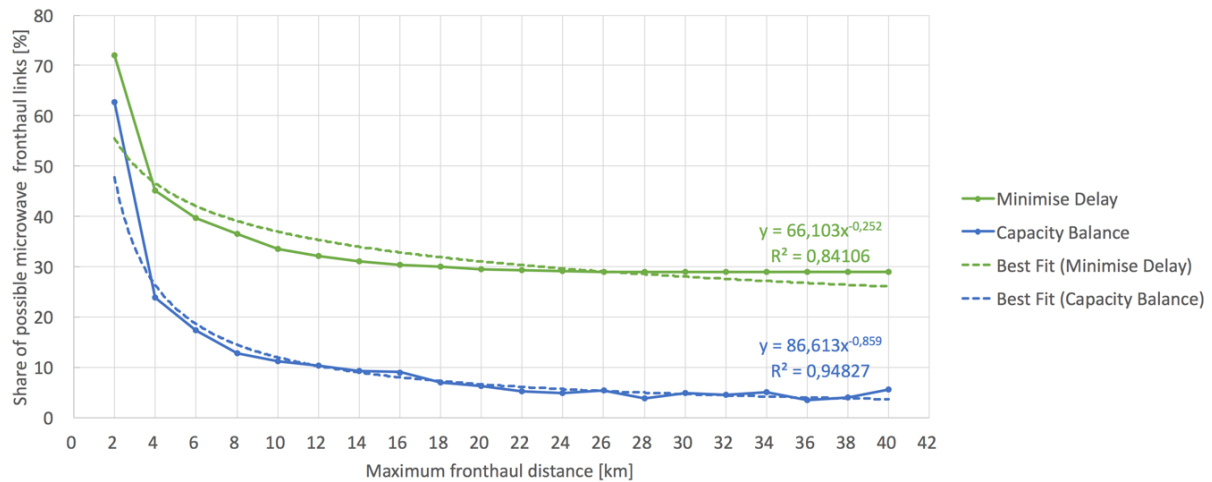
Figure 4.16. Shared possible microwave links for different fronthaul distance.

Of interest as well is the analysis on the number of needed BBU Pools using the Minimise Number of BBU Pools algorithm. Figure 4.27 depicts this evolution of the number of required BBU Pools. As expected, a decrease of the number of BBU Pools exists as the maximum fronthaul distance increases, because if the maximum fronthaul distance increases, the maximum length of fronthaul links increases as well. This implies an increase in the BBU Pool coverage area, which leads to a scenario where fewer BBU Pools are needed to cover the same total area. As the coverage area increases, the percentage of shared RRHs also increases, because there are no capacity limits. It should be noted that the maximum number of BBU Pools is never reached. A logarithmic model was used for the fitting, since it is the one with the higher correlation.
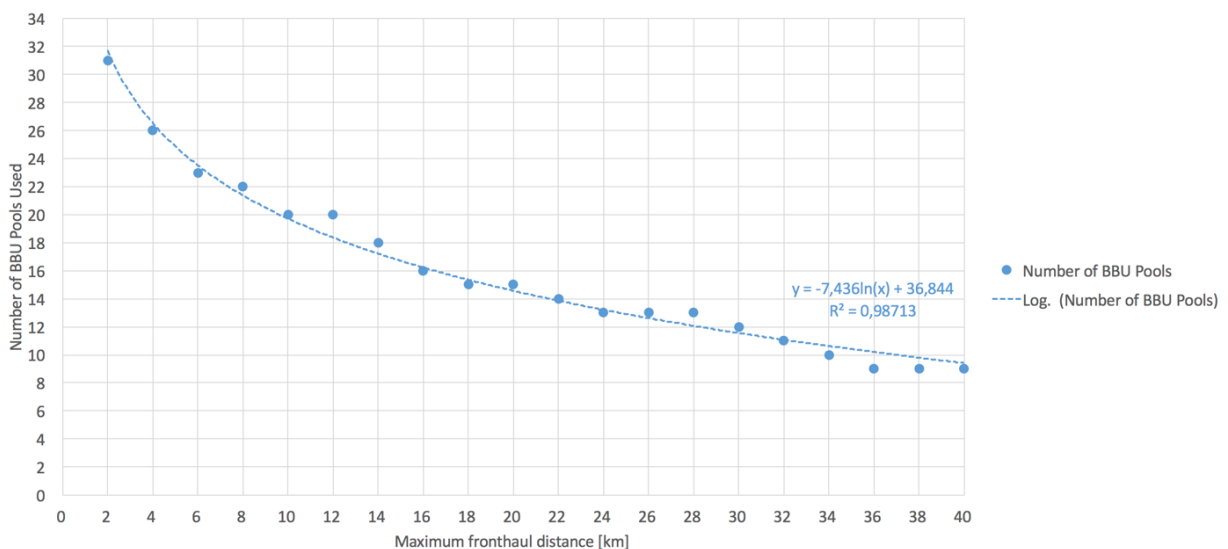
Figure 4.17. Number of BBU Pools Needed for different distance limits in Minho.

Regarding BBU Pool capacity, Figure 4.18 illustrates the trend of the BBU Pool with the maximum and the minimum capacities required versus the maximum fronthaul distance constraint. The maximum

capacity is the load of the most loaded BBU Pool and the minimum capacity is the load of the less loaded one. These values were obtained for different deployment distance constraint and algorithms, such as Capacity Load Balance and Minimise Number of BBU Pools. Observing the trend of the Capacity Load Balance algorithm, it is possible to conclude that regardless of the maximum fronthaul distance, both the maximum and the minimum capacities are almost constant. This fact is justified by the algorithm target. In this approach, as the maximum fronthaul distance increases, the total traffic processed by the BBU Pools increases as well. Nevertheless, from 10 km the maximum traffic of the most loaded BBU Pool remains almost constant. Concerning the maximum traffic at the Minimise Number of BBU Pools algorithm, one can observe that the load grows linearly with the distance constraint in some intervals, because when increasing the fronthaul distance constraint, each BBU Pool is able to serve a larger number of RRHs and consequently more traffic. Another important observation that can raise from Figure 4.18 is the fall of the maximum load, which can be explained by the fact that the BBU Pool positioning, due to the scenario characteristic, generates discontinuities, which can result in gaps in the overlapping regions covered by more than one BBU Pool as the fronthaul distance constraint increases, as it can be observed in the results from 24 km to 26 km. Furthermore, when the algorithm has more than one possibility to connect to, it uses the Flatness algorithm, balancing load in the BBU Pools and also justifying the decrease in load.
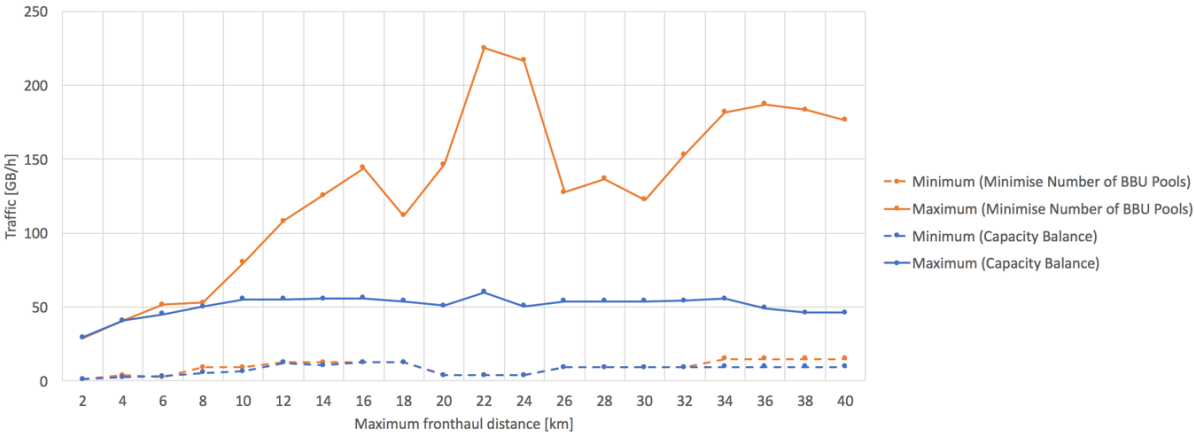
Figure 4.18. Traffic variation for different fronthaul distance in two algorithms.

With the increase of the maximum fronthaul distance, both CAPEX and OPEX associated with the development of a network with a C-RAN architecture are influenced. To better understand the cost saving related to the change from a local architecture to a C-RAN one, only the components corresponding to the RRHs are considered. As expected, due to the high cost of a new fibre infrastructure related to the haul, meaning back- and fronthaul in local and C-RAN architectures, respectively, the costs analysis is divided into two main components, considering or not the haul.

In Figure 4.19, one can clearly understand, as expected, that as the fronthaul distance increases, CAPEX also increases, due to the intensification of the percentage of connected RRHs as distance increases. This intensification also allows connections with a higher distance, which leads to a growth in the haul cost and consequently in CAPEX. When the maximum fronthaul distance increases, although the cost value increases, the savings between the two architectures decreases 9%, meaning that the

savings are 23% at 2 km and 14% at 40 km. From the four components considered in Figure 4.19, the CAPEX predominant factor, whether in local or C-RAN architectures, is related sites construction at the first kilometres, being respectively almost 75% and 59% of the total CAPEX of each architecture at 2 km; with the expensive costs of fibre, as the maximum fronthaul increases, sites construction loses predominance. Due to the lower cost of sites construction in C-RAN comparing with the local approach, the dominance of the haul is initiated earlier: in C-RAN, the dominance starts at 4 km, representing 46% of the total CAPEX, and it is always increasing up to 84% at 40 km; in the local architecture, the dominance starts at 12 km, representing 47% of the total CAPEX, and it is always increasing up to 73% at 40 km. Since, by reference, the cabinet cost per cell in C-RAN is 1.5 times higher than in a local architecture, this factor remains constant along distance. The variation in BB costs between the two architectures is related to the multiplexing gain, which is the distinctive feature due to virtualisation in C-RAN. A polynomial model was used for the fitting in both architectures, since it is the one with the higher correlation, thus, one can easily estimate CAPEX per km.
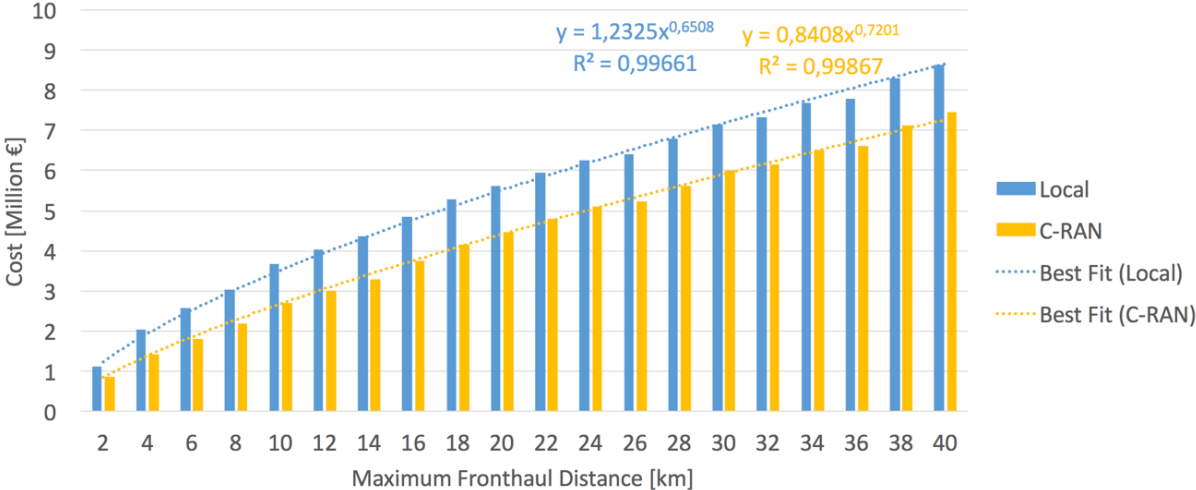
Figure 4.19. CAPEX variation for different fronthaul distance.

Regarding OPEX, as the maximum fronthaul distance constraint increases the cost also increases, as Figure 4.20 suggests. Similar to the CAPEX analysis, four components are presented, i.e., renting, maintenance, energy and haul. Although OPEX has a growth trend, its saving margin behaves in the opposite tendency, having at 2 km a saving margin of 25% and at 40 km it reaches 13%. Considering all components, there are two that have a higher percentage of the total OPEX; renting and the haul. Taking short distances, renting represents the main component, due to the reduced length of the fibre and significant percentage of connected RRHs. In a local architecture, this factor is predominant up to 12 km, from which the haul takes dominance, taking 47% of the total OPEX. Haul OPEX being a percentage of CAPEX, it rises as the fronthaul link distance increases as well, due to the expensive fibre costs. In the C-RAN architecture, justified by the lower costs of renting comparing with the local one, the dominance of the haul appears at 6 km with 49% of the total OPEX. The variations in energy costs between the two architectures are related to the multiplexing gain, which is the distinctive feature due to virtualisation in C-RAN. The energy has a peak of saving of 23% at 4 km, with 14% at 40 km. Maintenance has a decreasing trend with a variation of 3% as the maximum fronthaul distance increases. By ascending order, as proposed in Subsection 3.2.4, the influence of CAPEX in

maintenance OPEX is related to deployment, hardware and computers. Although sites construction has an increasing trend, regarding cost saving, the fact that the BB component has a decreasing trend implies a declining influence. A polynomial model was used for the fitting in both architectures, since it is the one with the higher correlation. Thus, one can easily estimate OPEX per km.
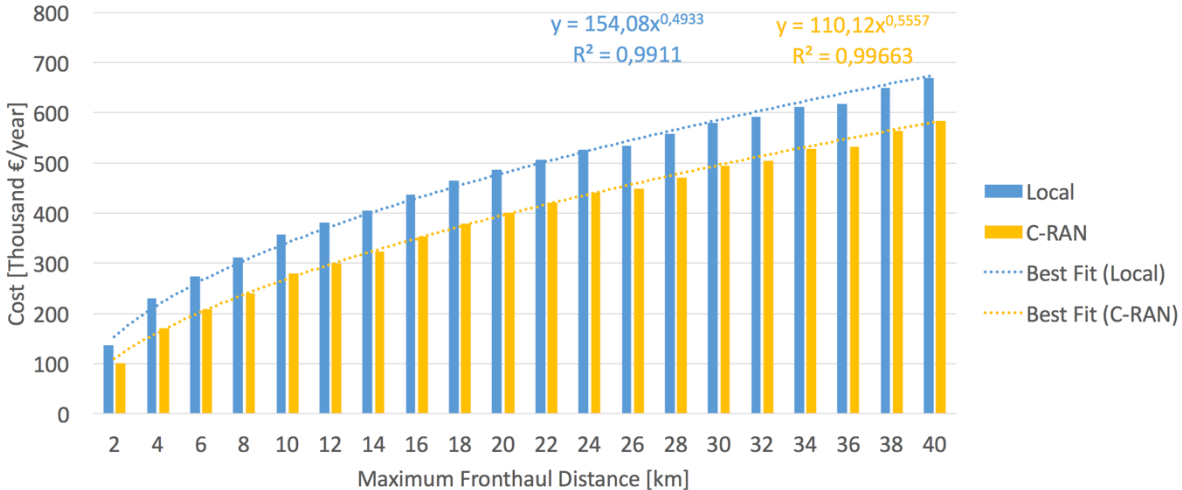
Figure 4.20. OPEX per year variation for different fronthaul distance.

4.3.2 Capacity Impact

The influence of the maximum traffic generated per RRH is an important perspective to analyse in order to design the BBU Pools to deal with all traffic. For this reason, it is important to understand the percentage of RRHs considering different maximum traffic intervals, as Figure 4.21 suggests. In fact, one can clearly see that the majority of RRHs has peaks of traffic between 0 GB/h and 2 GB/h, and a lower percentage between 12 GB/h and 14 GB/h.
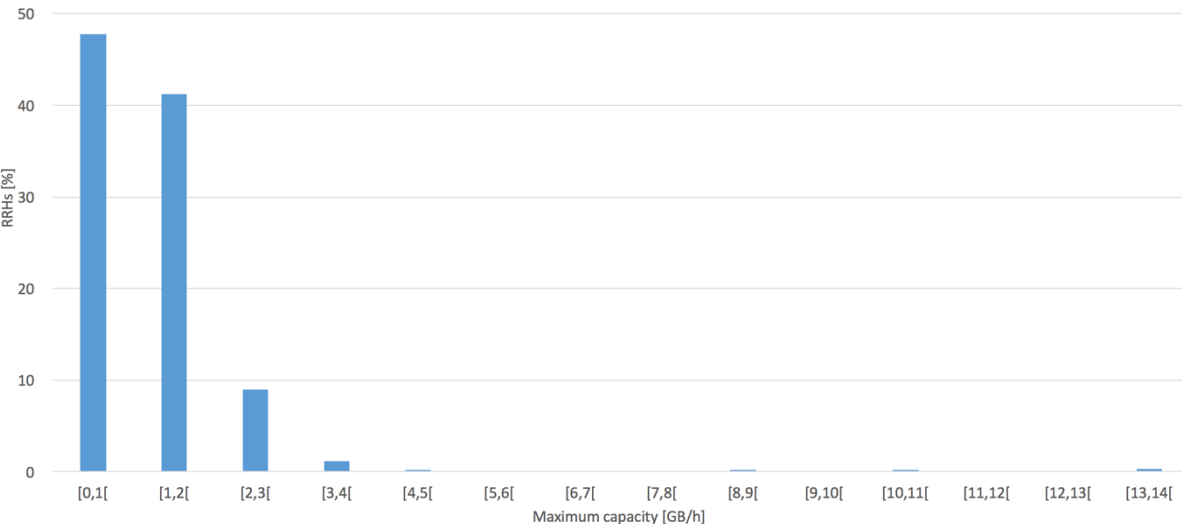
Figure 4.21. Percentage of RRHs between capacity limit intervals.

Using the Capacity Load Balance algorithm, the impact caused by the increase of the maximum capacity limit per BBU Pool on the percentage of connected RRHs with the respective type of area is illustrated in Figure 4.22. As predictable, as the capacity limit increases, a growth in the percentage of connected

RRHs is noticeable. In fact, with the growth in this constraint, BBU Pools improve the capability to deal with a higher amount of traffic, which means that a greater number of RRHs is able to be connected. RRHs with lower traffic peaks are located in dense urban areas, due to the highly deployed zone, meaning that, by having more RRHs in a dense urban area, traffic will be specific to that zone and it will have lower peak values compared with the other areas. For this reason, the percentage of dense urban connected RRHs is higher than the other type of RRHs, when BBU Pools have a lower value for the maximum capacity. As the capacity constraint increases, the percentage of rural RRHs also increases and the urban RRHs one decreases. Since rural RRHs are the more representative, it is expected that as BBU Pools have the capability to connect more RRHs, the percentage of rural ones is more important. The opposite occurs by analysing urban RRHs, which have the lower percentage in the network. This shows that rural RRHs are the ones with high peaks of traffic, followed by urban ones. One can clearly see that with 25 GB/h of maximum BBU Pool capacity, the percentage of connected RRHs reaches almost 90%. A saturation point exists, concerning the variation of percentage in the different connected RRHs type of area.
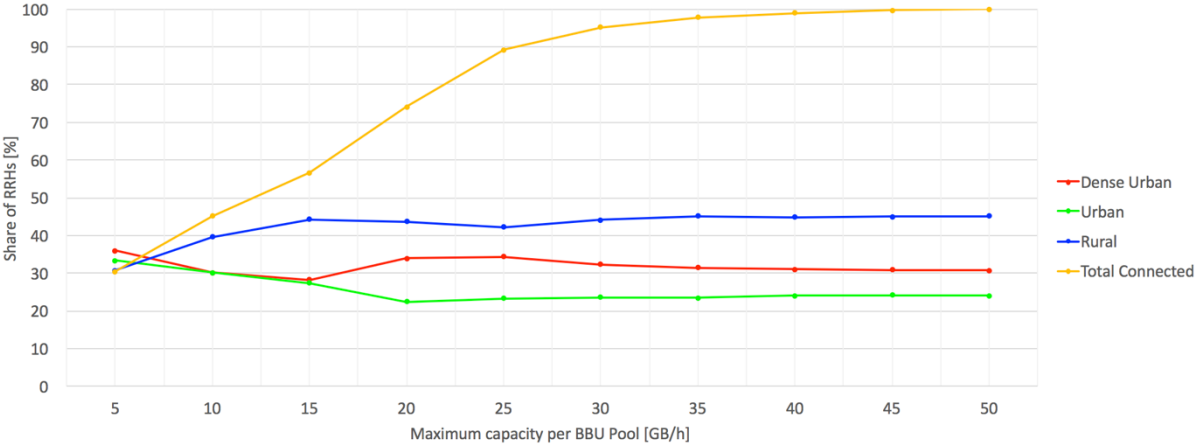
Figure 4.22. Area type of shared RRHs with different capacity limits in Minho.

To evaluate how the different type of RRHs evolves as the capacity limits increases, the Capacity Load Balance algorithm was chosen. The percentage of the connected type of traffic RRHs are represented in Figure 4.23. As expected, the percentages of connected RRHs of the different characterisations stabilises from a certain capacity limit constraint. In fact, with the lower capacity limit established, 5 GB/h, the percentage of mixed cells is the minor one. Thus, one can conclude that RRHs with higher peaks of traffic are the mixed ones, having a growing behaviour as the capacity limit increases. This fact matches with the rural RRHs in the previous analysis, because, RRHs having a non-well established traffic profile, the mixed ones are representative in rural areas. Commercial RRHs, with the opposite behaviour, are always the ones with the higher percentage of connections. This RRHs are the ones with lower peaks of traffic. The decreasing gap between the commercial RRHs and the remain ones, with a focus in the mixed, shows the higher percentage considering the lower values of the constraint. Thus, it justifies the lower peaks of traffic comparing with the other type of RRHs. The percentage of residential RRHs remains almost constant, having variations of 2%, as the maximum capacity increases. Residential RRHs do not represent a restrictive RRH type when the BBU Pool capacity limit is a constraint.
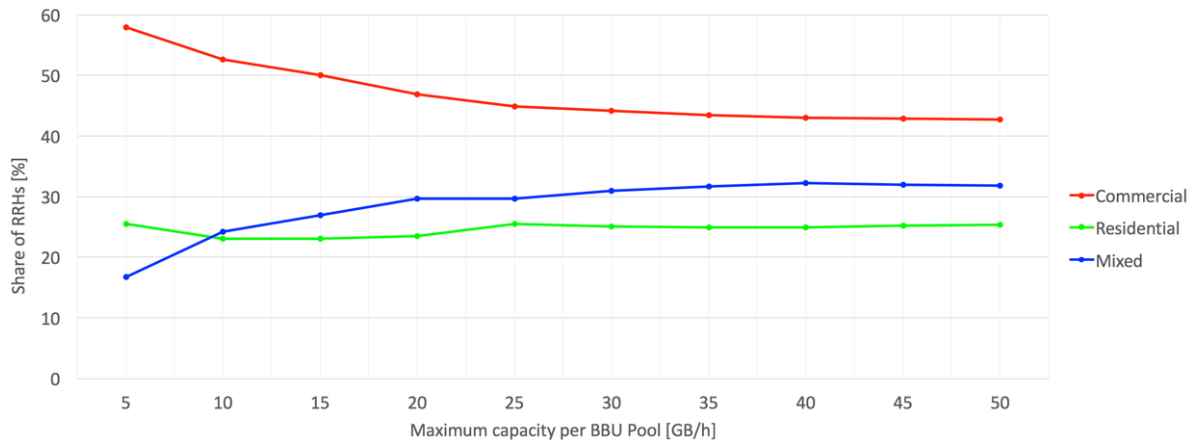
Figure 4.23. Traffic type of shared RRHs with different capacity limits in Minho.

Using the Minimise Number of BBU Pools algorithm, Figure 4.24 shows the trend of the required number of BBU Pools for different values of maximum capacity. It can be observed that the percentage of BBU Pools needed to handle the traffic of the connected RRHs decreases from 100% to 21,4%, meaning that almost 80% of the BBU Pools are not necessary when considering no capacity limits and having the reference of 40 km of maximum fronthaul distance. In fact, one should notice that the maximum required capacity increases approximately 360% comparing with the Capacity Load Balance algorithm. This fact considers that 100% of the network RRHs are connected. An exponential model is used for the fitting, since it is the one with the higher correlation.
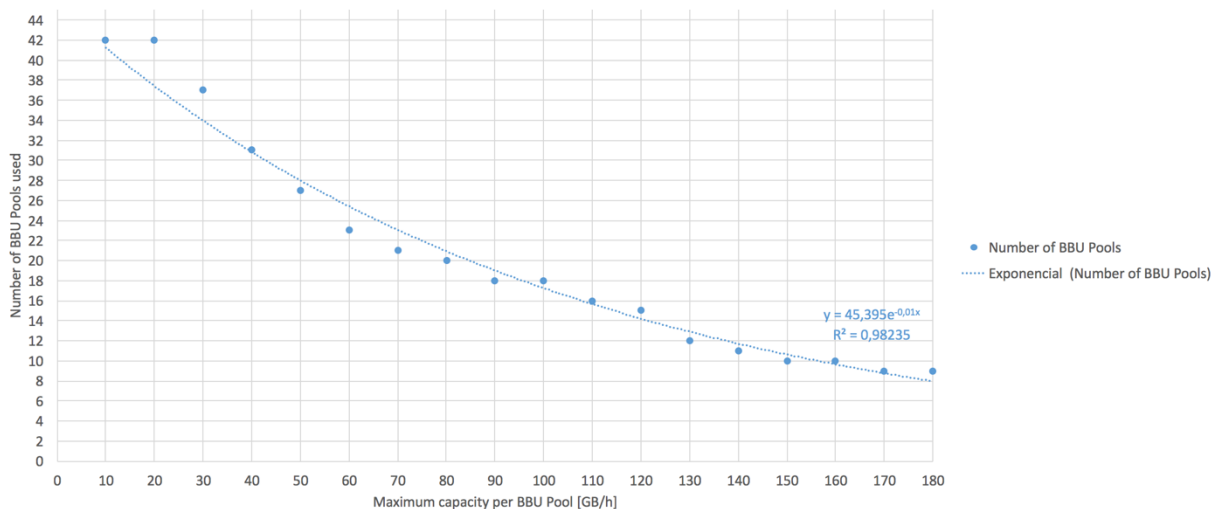
Figure 4.24. Number of BBU Pools Needed for different capacity limits in Minho.

Traffic growth, due to smartphones, as suggested in Chapter 1, is expected to reach a value 12x higher in 2021, comparing with 2015. For this reason, and to have a futuristic view of the network, a multiplication factor was created in order to evaluate traffic growth along the years. The total mobile data traffic is expected to rise at a compound annual growth rate of around 50% [Eric15]. This multiplication factor assumes that the traffic profile along the day remains with the same characteristics for each RRH and that it does not change geographically. In [Mont16], a proliferation analysis with a factor of the same order of magnitude is proposed with multiple traffic estimation strategies. The work is mostly focused on small cells to cover the new traffic demand and their repercussion in centralised deployment.

Table 4.11. Traffic multiplication factor among the years.

Year	2016	2017	2018	2019	2020	2021
Factor	1	1.5	2.25	3.38	5.06	7.59

The maximum capacity of a BBU Pool needs to be designed with a margin considering the planned consumption, allowing to deal with higher traffic peaks if they occur, and to account with forecasted traffic growth, as Figure 4.25 suggests: using the Capacity Load Balance algorithm, one shows the maximum traffic of the BBU Pool with the highest peak of traffic and with the lowest one; the margin was not taken into consideration, which needs to be considered in a real design, together with the percentage of the maximum peak of traffic, which is usually between 10% and 20%. The fitting represents an exponential model with a coefficient of determination $R^2=1$, which proves that the two quantities are directly proportional, as intuitively expected.
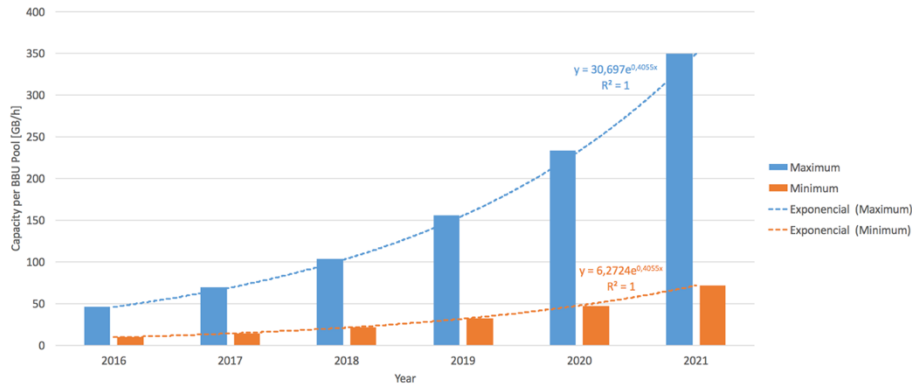
Figure 4.25. Maximum and minimum traffic variation in the BBU Pools for until 2021.

When BBUs are aggregated in a Pool, such a margin can be shared, allowing additional pooling gain in the C-RAN architecture compared to a traditional RAN. In Figure 4.26, one can see that by establishing a capacity limit per BBU Pool, the network takes advantage of that possibility, reaching almost the maximum value; from 5 GB/h to 30 GB/h, the maximum capacity is almost equal to the maximum established one, but with 50 GB/h the margin is 8%. For this reason, such an additional margin is especially applicable to resources required to support traffic peaks in different cells. In other words, in C-RAN, capacity can be scaled and designed based on peak utilisation in all BBU Pools, rather than all RRHs peak utilisation.
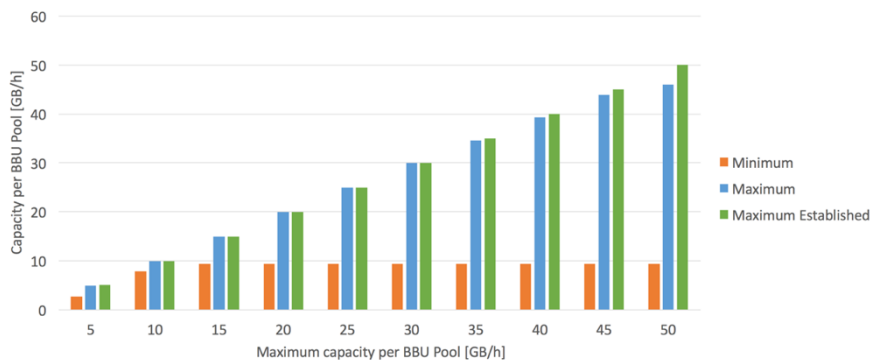
Figure 4.26. Maximum and minimum traffic for different capacity limits per BBU Pool.

The different design of BBU Pools maximum capacity influences cost directly, both CAPEX and OPEX. In fact, this influence is produced by the amount of RRHs that are connected as the maximum BBU Pool capacity increases. One should remember that this analysis takes 40 km of maximum fronthaul distance as reference. To better understand the costs saving related to the change from local to C-RAN architectures, only the components corresponding to the connected RRHs are considered. In other words, only the RRHs connected in C-RAN are considered for the comparison with local architecture.

Concerning the initial investment viewpoint, Figure 4.27 illustrates the variation of the total CAPEX imposing a maximum capacity per BBU Pool in GB/h. Four factors are considered for the total CAPEX, i.e., BB, cabinets, sites construction, and haul. One should keep in mind that the haul refers to back-and fronthaul in local and C-RAN architectures, respectively. The first insight that one can extract is, as predictable, the growth tendency in cost as the maximum capacity per BBU Pool increases in both architectures. The most significant factor is the haul, representing around 72% and 83% of the total CAPEX in local and C-RAN architectures, respectively. This percentage has variations of 2% in local and 6% in C-RAN, for the different maximum capacity values. Another aspect related to the total CAPEX is that there is an increasing percentage of cost savings comparing the local with C-RAN approaches. This rising trend starts at 5 GB/h with 6%, and ends at 50 GB/h with 14%. So, as the maximum capacity per BBU Pool increases, the total CAPEX saving also increases. This costs saving is justified by the sites construction factor. It should be noted, as already discussed, that the cost of construction of a local RRH is, by reference, around 3 times higher in local comparing with C-RAN architectures, thus, in sites construction, there is 31% of cost savings as the constraint increases, starting with 28% at 5 GB/h and ending with 59% 50 GB/h. Haul savings are almost equal to 0%, because not only the cost of fibre is the same, but also the size of the links remains equal in both architectures. The microwave component in the C-RAN fronthaul has a negative impact, because the limit distance does not allow the microwave link to be profitable comparing with fibre, representing approximately 0.02% of saving loss. Cabinets generate a negative impact in terms of saving, being always 1.5 times more expensive in C-RAN comparing with local architectures. BB has a decreasing variation of 2% in cost savings as the constraint increases. A polynomial model was used for the fitting in both architectures, since it is the one with the higher correlation. Thus, it is possible to estimate CAPEX per km.

Figure 4.27. CAPEX variation for different capacity limits.

Concerning OPEX, Figure 4.28 illustrates its evolution for different values of maximum capacity per BBU

Pool. As expected, as the constraint increases, OPEX has an increasing behaviour due to the number of connected RRHs, which increases as well. Four components were taken into consideration for the total OPEX, i.e., maintenance, renting, energy and haul. Haul being a percentage of CAPEX, it is the predominant factor in local and C-RAN architectures, representing approximately 55% and 64% of the total OPEX, respectively. The variation of this percentage for the different maximum capacity per BBU is 2% on both architectures. Apart from the percentage of the total OPEX of the most significant component, it is important to analyse the savings of C-RAN comparing with local approach in the different factors that influence OPEX. From a global perspective, the total OPEX saving has a stable behaviour as the maximum capacity per BBU increases, around 13%. This constant trend is justified by the behaviour of the different factors. One component that has an increasing trend as the constraint increases is maintenance, with savings from 10% to 17%. The influence of this component came from the reduction in CAPEX sites construction. Although sites construction is the component with a lower percentage in maintenance, the significant growth in CAPEX savings justifies the 7% increase in OPEX savings. The energy component, having virtualisation as the differentiator factor between both architectures, remains with similar savings around 14% with a variation of 2%. Renting has an increase of 1% in what concerns OPEX savings. This slight growth behaviour is justified by the reference cost assumptions, and Figure 4.22. The cost of a dense urban, urban and rural, are respectively 1.15, 1.25 and 1.25 times higher in local comparing with C-RAN architectures. Therefore, as the percentage of rural RRHs increases, the gap between both architectures is higher, increasing savings. In the same way as the CAPEX, the haul component has almost 0% saving. In fact, it has a negative impact on savings around 0.1% due to the higher cost of microwave licences comparing with the corresponding fibre links in the local architecture. A logarithmic model was used for the fitting in both architectures, since it is the one with the higher correlation. So, it is possible to estimate OPEX per km.
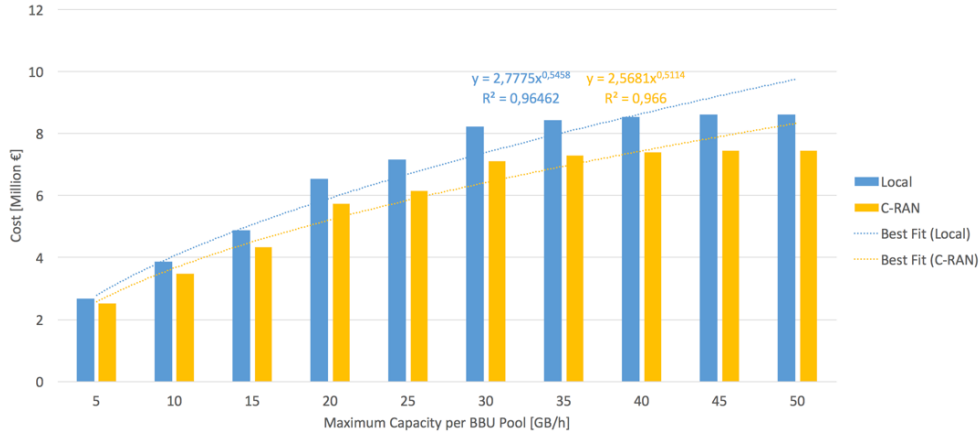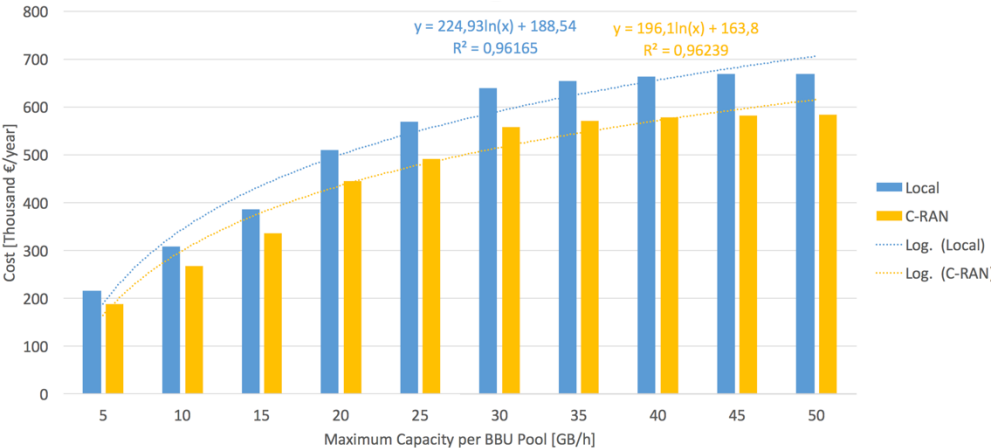

Figure 4.28. OPEX per year variation for different capacity limits.

4.4 Analysis of Portugal Scenario

In this section, the proposed model is applied to the Portugal scenario, which comparing with Minho on

the number of RRHs and area, is respectively 7 and 8 times larger. One should remember that some of the characteristics of this scenario were taken from the Minho one, such as traffic profiles and type of RRH characterisation. Although the assumptions do not respect the real trend of traffic in Portugal, the scenario is close to a real case.

The first observation, due to the scenario dimension where latency is a key aspect in connections, is the variation of connected RRHs for different maximum fronthaul distances supported by C-RAN, as Figure 4.29 illustrates. One should keep in mind that the algorithm that is used in this analysis is the Capacity Load Balance one. It should be noted that, in this case, there are no capacity limits per BBU Pool. As it can be seen, as expected, the growth behaviour is evident as the maximum fronthaul distance increases, which is related to the coverage area of the BBU Pools. The maximum fronthaul distance determines the radius of coverage of every BBU Pool. As this radius increases, the coverage area also increases and the RRHs included in this area are connected. One should notice that at the maximum value of distance associated with latency constraints of LTE, it is not possible to connect all RRHs with the BBU Poll locations available in this scenario. Considering the type of area, from the around 3.4% of RRHs that cannot be connected in a C-RAN architecture, all of them are rural. Concerning the traffic profile classification, 53% are residential and 47% are mixed.
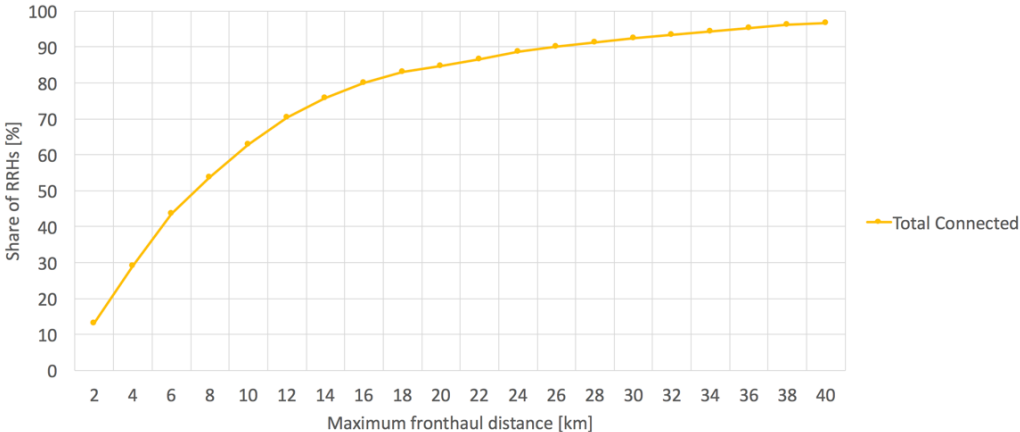
Figure 4.29. Total shared RRHs for different maximum fronthaul distance in Portugal.

The variation of RRHs type area for different maximum fronthaul distance is represented in Figure 4.30. The impact that distance has in the different type of connected RRHs taking into consideration their region is shown. As a result of the country characteristics, the percentage of rural areas is higher than the sum of dense urban and urban ones from 24 km of maximum fronthaul distance. Considering Figure D.4, it is expected, due to the highly deployed RRHs in dense urban areas, that the percentage of this type of RRHs is higher compared with the other types for short distances of fronthaul. The peak is reached at 4 km, because metropolitan areas are not fully covered with 2 km. Urban area RRHs reach their maximum percentage at 2 km, because rural RRHs become more representative as the distance increases. This growth behaviour of rural RRHs occurs since the increase of the coverage area allows the connection of this type of RRHs. The decreasing trend of dense urban is justified by the increasing trend of the rural area. At the same time as the number of dense urban RRHs does not change, the growth of the coverage area generates the connection of rural RRHs, which are the ones with the higher percentage from 10 km of fronthaul.
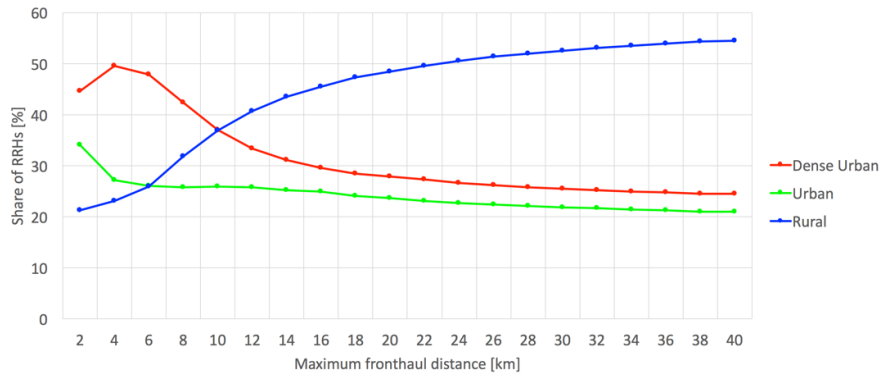
Figure 4.30. Area type of shared RRHs for different fronthaul distances in Portugal.

Another interesting analysis is how the behaviour of the traffic type is affected by the fronthaul distance, illustrated in Figure 4.31. One should notice that this characterisation is extrapolated from the assumptions explained in Subsection 4.1.2. Commercial RRHs are characterised by being more representative in dense urban areas, hence, this kind of RRHs has a decreasing trend as the fronthaul distance increases. In the opposite trend are the mixed RRHs, having a non-well established traffic profile, typically located in rural areas. Since it is a type of RRH that is also located in rural areas, the urban ones have a growth tendency. One should keep in mind that, as represented in Subsection 4.1.2, the percentage of mixed RRHs is higher that the commercial ones, which is not shown in Figure 4.31, due the RRHs that are not connected.
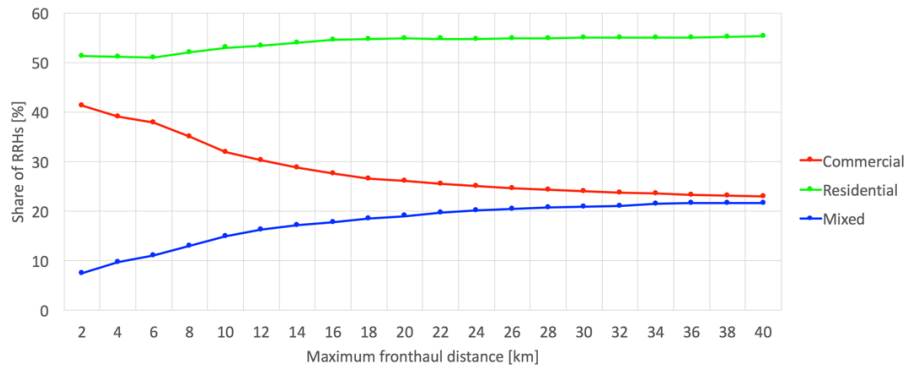
Figure 4.31. Traffic type of shared RRHs for different fronthaul distances in Portugal.

Taking the possible 86 BBU Pools, and considering that are no capacity limits in any data centre, by using the Minimise Number of BBU Pools algorithm, one shows in Figure 4.32 the number of BBU Pools for different values of the maximum fronthaul distance. As expected, the number of BBU Pools that are needed in the network show a decreasing trend as the maximum fronthaul distance increases, because as the coverage areas increase the overlapped areas also increase, making some BBU Pools locations redundant to cover the same region. The minimum number of BBU Pools needed for Portugal is 44, almost 5 times more than in Minho; this number allows only for the connection of 96.6% of the total RRHs. One should notice that the total number of BBU Pools never reaches the maximum number of possibilities, and by using less BBU Pools CAPEX and OPEX will rise due to the increase of the fronthaul links length. A linear model was used for the fitting in both architectures, since it is the one with the higher correlation. It should be noted that by increasing the scenario in 8 times, the number of possible BBU Pools only increases twice.
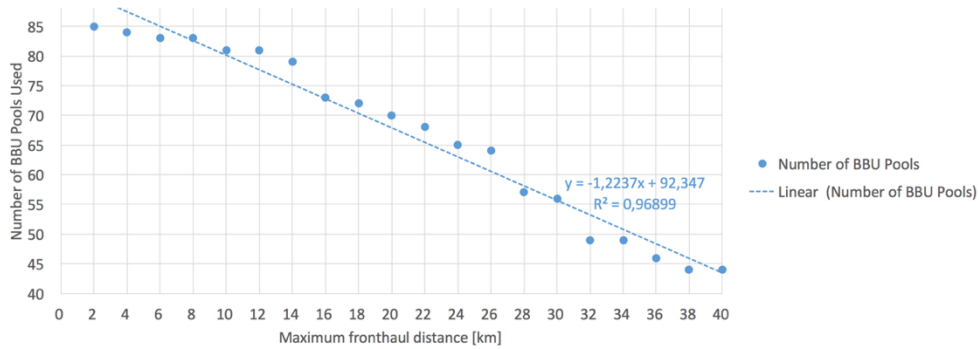
Figure 4.32. Number of BBU Pools Needed for different distance limits in Portugal.

After analysing the impact of the fronthaul distance, the main technical issue when developing a C-RAN architecture in Portugal, it is important to understand the investment that needs to be done, taking into consideration the network in Portugal and the reference configuration presented in Subsection 4.1.3.

The key concern of a C-RAN dimensioning is to provide a network that is cost-effective for the operator, and this fact aggravates when the scenario is whole country. Figure 3.33 illustrates the total CAPEX for local and C-RAN architectures. One should remember that haul refers to the backhaul in local and fronthaul in C-RAN. It is assumed in this comparison that the operator owns 85% of the haul infrastructure. The first insight is the 13% of cost savings using C-RAN. It is noticeable that the component with higher relevance is the haul, representing 78% and 90% of the total CAPEX in local and C-RAN architectures, respectively. This component does not contribute positively to savings, around 0.08% more expensive in C-RAN, due the cost of the microwave fronthaul links in comparison with the corresponding fibre backhaul links. In fact, the key factor for saving is sites construction, which is 69%. This large percentage of savings are related to the fact that in a local architecture, the cost of sites construction is, by reference, 3 times higher than in C-RAN. CAPEX in both architectures being 1% of the total, the baseband component introduces 4% of savings introduced by the multiplexing gain, that exists in C-RAN in contrast with the local approach. This low multiplexing, and consequently low percentage of saving in this component, is justified by the fact that in this scenario only three curves of traffic are considered. This three traffic profiles are based on the average traffic in Minho, so, the diversity of traffic profile is poor, which generates low and unreal multiplexing gains. The cabinets component is characterised by being 1.5 times more expensive in C-RAN comparing with local architecture. Thereby, it represents a negative impact of 50% in terms of saving.
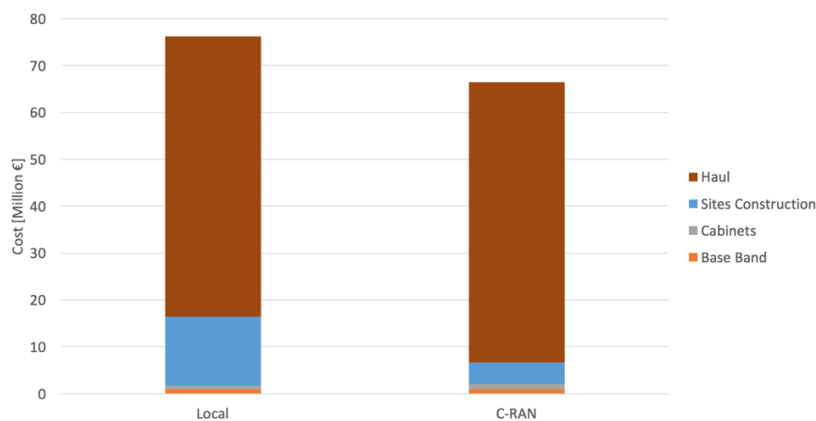
Figure 4.33. Local and C-RAN CAPEX with its components in Portugal.

Apart from the initial investment, it is important to keep the network providing a reasonable QoS for users along the years. In order to do so, a continuous investment is needed in order to maintain the network under the intended conditions. For this reason, Figure 4.34 shows the OPEX per year in a local and in a C-RAN architectures. It is possible to see, as expected, a reduction in OPEX using a C-RAN architecture comparing with the local one, representing 10% of cost savings. It is also evident that the main component in both architectures is the haul. It is also assumed that the network operator owns 85% of the haul, which represents 64% of the total CAPEX. Comparing the savings using C-RAN and local approaches, the haul represents a negative impact of 0.07% considering that the licences of the fronthaul microwave links are high-priced compared to the maintenance of the correspondent backhaul fibre links. The component that introduces a high percentage of savings, approximately 38%, is the renting. As already discussed, the cost of a dense urban, urban and rural square metre, are respectively 1.15, 1.25 and 1.25 times higher in local comparing with C-RAN architectures. When the scenario is Portugal, where the number of RRHs is relative to the country and the percentage of rural is higher than the sum of dense urban and urban, the savings in renting become notorious. The maintenance also contributes positively to savings, having 15% of cost reduction. The influence of this component is related to the reduction in CAPEX sites construction. Although the sites construction is the component with the lower percentage in the maintenance, the fact that sites construction is the second most significant factor in CAPEX contributes to savings in OPEX. As introduced in Subsection 3.2.4, the differentiator feature in the energy component is virtualisation. The fact that the traffic curves that are used in Portugal are based on the average ones of Minho, creates only three types of traffic profiles, thus, the multiplexing gain is low, and consequently, the virtualisation factor is near to,1 providing only a 4% savings in energy.
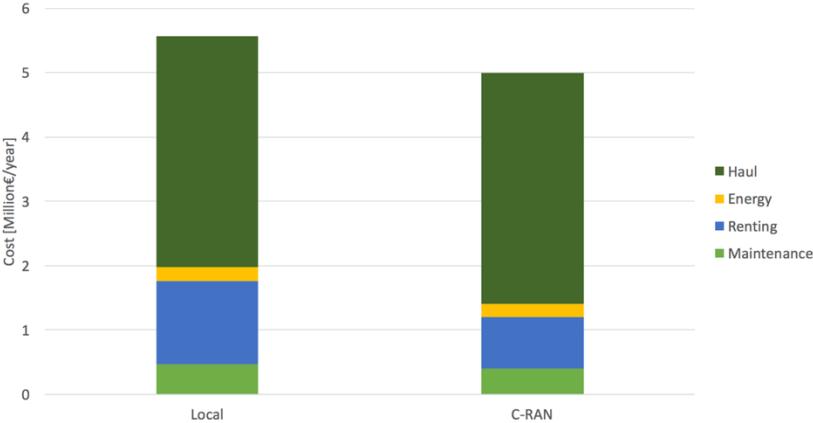
Figure 4.34. Local and C-RAN OPEX per year with its components in Portugal.

Chapter 5

Conclusions

This chapter finalises this report and presents the conclusions.

The main goal of this thesis was to design a C-RAN architecture in an LTE network. This design has analysed the advantages, introducing the separation of eNodeB into RRHs and BBU Pools, both in a technical and in an economical viewpoint. A study of the critical parameters that influences the implementation of this new architecture with the main focus on the fronthaul link, namely the delay, the capacity and the costs was made based on a model which allow the analysis of different network configurations.

In the first chapter, a global view of mobile communication systems challenges in terms of traffic growth forecast and economic sustainability for the operators is presented. The motivations for the present work are illustrated and a mobile cloud network is introduced as a solution for future radio access networks.

Chapter 2 introduces a theoretical background on LTE's network architecture, identifying the main components and their functionalities. It is followed by the radio interface, which addresses the main aspects of spectrum distribution, multiple access schemes, resource blocks organisation and used modulation. An overview of the SDN paradigm is given, including its founding principles, main interfaces and generic and cellular architecture. A high-level description of the most prominent SDN protocol, the OpenFlow standard, is also given in this chapter. A background on Virtualisation and Cloud is provided, including the main benefits and characteristics of NFV. It is also introduced an overview of the C-RAN architecture, explaining the main differences between a centralised and decentralised one, its main components and their functionalities (RRHs, BBUs and fronthaul), different ways to split functions between the components and concludes with the advantages and constraints of these type of architecture. The last section is the state of the art, describing the latest developments on C-RAN, focusing on aspects relative to fronthaul link and some performance enhancements relative to the normal architecture.

In Chapter 3, the model is described, starting with a global perspective and followed by the parameters introduced in the model. After the parameter definition, a deeper overview and implementation details are presented, ending with a model assessment. The segmentation of the model is based on the definition of three layers, such as physical, technical and costs.

The model parameters are mathematical factors considered to build the model. Starting with latency, which is the constraint that is responsible for limiting the fronthaul distance between, followed by a description of how capacity can be processed in GOPS. To evaluate the investment that needs to be made when developing a C-RAN architecture, a mathematical function was created with the objective to compute the costs both in CAPEX and OPEX. As performance parameters of the model, the multiplexing gain was defined in order to understand the traffic variations grouped in a BBU Pool and the fairness index indicates how balanced the load in the BBUs are.

The model implementation starts with a detailed explanation of the model. This description focuses in a complete workflow of the different layers of the model. Introduced in the model overview and treated in the model implementation, the used algorithms are explained in this section. There are five algorithms, namely Minimise Delay, the Number of RRH per BBU Balance, Minimise Number of BBU Pools, Number of RRH per BBU Balance and Capacity Load Balance.

The final section of Chapter 3, where the developed model was applied to a certain number of tests in order to check if it was correctly implemented, is the model assessment. The model behaviour had output parameters consistent with expectations. Consequently, the implementation was validated, allowing to proceed for any scenario analysis.

Chapter 4 starts by providing a description of the used scenarios in this thesis, the Minho region and the continental part of Portugal. This description takes into consideration the geographical distribution of RRHs and possible BBU Pools of NOS network. Regarding the locations of the RRHs, three classes of RRHs were defined based on the geographical density of the RRHs, namely dense urban, urban and rural. Based on the traffic profile of each RRHs, also three classifications were made, namely commercial, residential and mixed.

Before the analysis of the results, in order to establish a reference scenario, the assumptions used in the model are proposed. First, in order to define the RRHs characteristics, it was suggested a classification of the frequency and bandwidth used in dense urban, urban and rural RRHs. Following by the constraints of the model, namely the fronthaul distance and the maximum capacity per BBU Pool. In the reference assumptions, the maximum fronthaul distance for fibre is 40 km and for the microwave is 1.5 km. In what concerns to the BBU Pools, it is assumed, by reference, that there are no capacity limits. To conclude this section, an overview of the costs assumptions are described and differentiated as local and C-RAN architecture costs.

The reference scenario is based on the locations of Minho, having 1 176 RRHs and 42 possible BBU Pools. For maximum fronthaul distance it was established 40 km, where until 1.5 km the fronthaul link is based on microwave transmission. The BBU Pools have no capacity limit by reference. In order to understand the robust algorithm, the five algorithms were tested in order to evaluate their performance. The tests are related with fronthaul distance, percentage of connected RRHs in distance intervals, maximum and minimum capacity that the BBU Pools need to have and multiplexing gain. In this way, the selected algorithm to analyse the performance parameters is the Capacity Load Balance algorithm because although it has a parallel performance as the Flatness algorithm, the maximum traffic per BBU Pool in the network is forced to balance in the selected algorithm.

Analysing the reference scenario with the Capacity Load Balance algorithms, an approach in the maximum and minimum capacity per BBU Pool shows that the algorithm equilibrates the traffic both in GB/h and in GOPS. The traffic is well balanced between all the BBU Pools, having the majority values of traffic the same order of magnitude. In the GOPS study, it is illustrated that having digital operations that do not depend on the traffic, the BBU Pools minimums reaches values closer to the maximums.

Evaluating the costs associated with the reference scenario, there is 14% of CAPEX savings by comparing the C-RAN with local architecture. One should notice that is assumed that the operator owns 85% of the haul (backhaul in local and fronthaul in C-RAN) infrastructure. In this way, the investment is 8.6 and 7.4 million € in local and C-RAN, respectively. The most representative component in both architectures is the haul, approximately 73% and 84% of the total CAPEX, respectively of local and C-RAN. This majority is justified by the expensive cost of fibre links. The component that has the high percentage of cost savings is the sites construction, having 59%. The annual OPEX has a reduction of

13% considering the C-RAN architecture. This reduction is represented for an OPEX of 669 and 584 thousand € per year in local and C-RAN, respectively. As similar to the CAPEX, the component has a higher percentage of the total OPEX is the haul. The haul represents 59% and 65% of the total OPEX respectively in local and C-RAN. The component that contributes to a higher percentage of the savings, around 37%, is the renting. In what concerns to the fronthaul connections, the outcomes illustrate that a microwave link is not cost effective comparing with fibre.

Considering the Minho scenario, the outputs were also evaluated varying the maximum fronthaul distance. The first analysis takes into consideration the BBU Pool to RRH connections. As the maximum fronthaul distance increases from 2 km to 40 km, the percentage of connected RRHs also increases from 40% to 100%. Considering the classifications made in terms of RRH geographical area, as the constraint increases, the percentage of dense urban RRHs decreases, reaching its maximum value at 2km. The same analysis was made, but based on the traffic profile of the RRHs. This classification affects directly not only the total multiplexing gain but also the multiplexing gain in the BBU Pools classified based on the higher percentage of a different geographical area of RRHs. The maximum overall multiplexing gain is obtained at 4 km, where the residential and commercial RRHs have a majority and the residential ones reach its maximum value. In this way, by having complementary curves, the gain is maximised to 1.15. The dense urban BBU Pools have a maximum multiplexing gain of 1.29 at 4km but, if the fronthaul distance increases, the percentage of commercial RRHs will decrease and the mixed one will increase. In [ChHC14], the maximum multiplexing gain achievable is 1.6. In fact, only two types of traffic profiles, namely commercial and residential for every RRHs, are considered to connect just one BBU Pool. This shows that with a real case scenario, a vast diversity of traffic profiles and more BBU Pools, the multiplexing gain achievable decreases. In this way, the mixed cells, resulting from rural areas, is a drawback for the multiplexing gain. Nevertheless, in smaller scenarios, the multiplexing gain should be higher due to the diversity of traffic profiles.

Still considering the latency impact in the Minho scenario and using the Capacity Load Balance algorithm, the average fronthaul distance of the connected RRHs is approximately half of the maximum established. Using the Minimise Delay algorithm, one can conclude that the percentage of microwave fronthaul links is always above the reference algorithm, which is around 9% and 24% greater at 2km and 40km, respectively. Both algorithms present a decreasing trend as the fronthaul distance increases. Testing the Minimise Number of BBU Pools algorithm, as the fronthaul distance increases, the number of required BBU Pools decreases. Justified by the overlapping of BBU Pools coverage areas, the scenario never uses all the 42 BBU Pools available, using only 31 and 9 BBU Pools, respectively at 2 km and 40 km of maximum fronthaul distance. This usage of less BBU Pools increases the maximum traffic of the most loaded BBU Pool as the fronthaul distance increases even though it exists some declines supportable by the coinciding coverage areas. The Capacity Load Balance algorithm behaves with an almost constant maximum traffic of the most loaded BBU Pool. Although the processed traffic of the entire network increases, the algorithm target remains coherent.

Thanks to the maximum fronthaul distance constraint, the CAPEX and OPEX, behaves with a potential increasing trend. This trend occurs both in local and C-RAN architecture. As far as the maximum

fronthaul distance increases, although the CAPEX increases, the savings between the two architectures decreases 9%. This decreasing trend is justified by the swap of the most significant component as the constraint increases. As similar to the CAPEX analysis, the OPEX has a growth trend as the maximum fronthaul distance increases but its saving margin behaves in the opposite tendency, having a reduction of 8%. The main factor responsible for this reduction is the haul.

Considering the Minho scenario, with the maximum fronthaul distance at 40 km, varying the maximum capacity per BBU Pool, the outputs were assessed. First of all, 98% of the RRHs have a peak of traffic between 0 and 3 GB/h. Using the Capacity Load Balance algorithm, the minimum capacity that one BBU Pool should have to deal with the traffic of 100% of the RRHs is 50 GB/h. Using the Minimise Number of BBU Pools algorithm, the percentage of BBU Pools that needs to handle the traffic of the connected RRHs decreases almost 80%, meaning that 33 BBU Pools are unnecessary considering 40 km of fronthaul. In fact, the maximum capacity needed per BBU Pool to connect 100% of the RRHs increases approximately 360% comparing with the Capacity Load Balance algorithm, reaching 180 GB/h.

It is expected that the traffic in 2021 will be 7.59 times higher comparing with 2016. Therefore, it is expected that in Minho scenario, using the Capacity Load Balance algorithm, the maximum capacity of the most loaded BBU Pool behaves proportionally to the growth rate, reaching a maximum of 350 GB/h in 2021. This traffic growth among the years suggests a capacity margin when designing a C-RAN network. This margin should be a percentage of the planned consumption, allowing BBU Pools to deal with higher traffic peaks if they occur and to account for forecasted traffic growth.

The costs, both CAPEX and OPEX, also changes while studying different values of maximum capacity per BBU Pool. On the one hand, the CAPEX behaves with a potential trend. But on the other hand, the OPEX performs with a logarithmic tendency. Not only the total CAPEX, but also the CAPEX saving increases. This saving, reaching 14% at 50 GB/h, is correspondent to 8% growth. The OPEX savings have a constant percentage of 13% as the constraint varies.

Portugal scenario, that comparing with Minho scenario towards the number of RRHs and area is respectively 7 and 8 times greater, was analysed. Considering the number of possible BBU Pools location, this number only duplicate with the scenario growth. Due to its dimension, the latency is a key aspect in the RRH to BBU Pool connection. Using the Capacity Load Balance and with no capacity limits per BBU Pool, the outputs were evaluated varying the fronthaul distance. As the maximum fronthaul distance increases, the percentage of connected RRHs also increases. At the maximum value of distance, 40 km, it is not possible to connect all the RRHs with the BBU Poll locations available in this scenario. From the around 3.4% of unconnected RRHs in a C-RAN architecture, considering the type of area, 100% of them are in rural. Considering the RRH traffic profile classification, 53% are residential and 47% are mixed. Taking into consideration the type of RRH correspondent to the different areas, due to the characteristics of the country, the percentage of rural RRHs is higher than the sum of dense urban and urban RRHs from 24 km of maximum fronthaul distance. The peak of dense urban RRHs is reached in 4 km due to the highly deployed RRHs in this area. This peak does not occur at 2 km of fronthaul distance because the metropolitan areas are not fully covered. Considering the different type of RRHs based on the traffic profile, and knowing that this characterisation is extrapolated from the Minho

scenario, the residential RRHs always present a higher dominance comparing with the sum of commercial and mixed RRHs for any value of maximum fronthaul distance. Using the Minimise Number of BBU Pools algorithm without capacity limits, the number of BBU Pools used for different values of maximum fronthaul distance was evaluated. The minimum number of BBU Pools needed for Portugal are 44, almost 5 times more than in Minho. This number only allow the connection of 96.6% of the total RRHs.

Finally, considering the Portugal scenario in reference conditions, the costs impact were assessed both in CAPEX and OPEX. One should remember that is assumed that the operator owns 85% the haul (backhaul in local and fronthaul in C-RAN) infrastructure. The first insight taken from the CAPEX is the 13% of cost savings using C-RAN. Thus, the investment is 66.2 and 76.5 million € in local and C-RAN, respectively. As well as the cost savings percentage is higher comparing with Minho, the amount of money saved is also greater, being almost 9 times superior. The amount of money saved in Portugal assures the development of Minho scenario, and there is still money left. The component with higher relevance, approximately 78% and 90% of the total CAPEX in local and C-RAN, respectively, is the haul. The most responsible factor for the savings is the sites construction, representing 69%. The baseband component has 4% of savings introduced by the multiplexing gain. This low multiplexing gain is justified by the fact that in this scenario only three curves of traffic, based on Minho average, are considered. The OPEX presents 10% of cost savings. In local, the annual investment is around 5.6 million €. Considering the C-RAN architecture, the investment is approximately 4.9 million €. Although the percentage of savings decreases comparing with Minho, justified by the decrease of the multiplexing gain, the amount of money that is saved is around 8 times greater comparing both scenarios. The component that introduces a high percentage of savings, about 38%, is the renting.

Regarding the future work, the present model studies the best solution taking into consideration all the BBU Pools available, but it does not guarantee that it is optimal. So it would be interesting to add optimisation techniques to the model. Hence, not only the minimisation of the number of useful BBU Pools will increase, but also the traffic distribution between them should be well balanced.

The algorithm proposed to develop this thesis just take into consideration a burst of traffic information correspondent to one day. The traffic variation in weekdays and weekend days are different for the same locations, as well as in different seasons of the year. It would be interesting to improve the model in order to analyse these variations to take the better use of the BBU Pool capacities in all days. Thus, it should be possible to turn off some BBU Pools in some regions due to these dissimilarities.

Some approximations were made regarding the lengths of the fronthaul links. In order to obtain accurate values, it would be interesting to have a map of the optical and microwave links already deployed in the scenario. Thus, it is possible to obtain the real fronthaul distance.

Regarding the costs considered in the model, it would be interesting to evaluate the cost taking into consideration the model proposed in [ATPH15] due to its complexity and specific technical factors considered.

Annex A

User's Manual

This Annex gives detailed instructions on how to configure the parameters and run a simulation.

To run the model simulator, one must start by configuring the Input_File.xlsx, which is divided in three reconfigurable main sheets:

- Parameters – responsible for the network configuration parameters.
- Flags – responsible for preferences parameters.
- Costs – responsible for costs parameters.

The parameters sheet is related to the network configurations, allowing the user to change not only the parameters, but also the paths of the files. Figure A.1 illustrates the outlook with an example of how this excel sheet can be filled. The first column is associated to the name of the parameter and the second illustrate the units of the parameter.

Path_Input	/.../Input_Files/
Path_Ouput	/.../Output_Files/
Path_Network_Info	/.../Network_Info/
Path_Matlab_Files	/.../Matlab_Files/
Configuration_File	.xlsx
Propagation_Fiber	[km/ms]
Propagation_MicroWave	[km/ms]
Radius_for_MicroWave	[km]
Radius_for_Density	[km]
Maximum_Radius	[km]
Maximum_Capacity	[GB or GOPS]
Flatness_Timestamps	[h]
Years_for_Opex	[years]
Year_to_Forecast	[year]
Traffic_Growth	[%/year]

Figure A.1. Network configuration parameters layout in the input file.

The performance parameters sheet, which the layout is depicted in Figure A.2, are related to the algorithms. The first column is associated to the name of the parameter and the second illustrate the possible values to configure the network.

Flag_UL(0)/DL(1)	UL (0) / DL (1)
Flag_Minimize_Delay	
Flag_RRH_Balance	
Flag_Minimize_BBUs	Choose just one algorithm (1)
Flag_Flatness	
Flag_Capacity_Balance	
Flag_GOPS	GB/h (0) / GOPS (1)
Flag_NOS_local_Costs	Compute local costs (1)
Flag_NOS_CRAN_Costs	Compute C-RAN costs (1)

Figure A.2. Preferences parameters layout in the input file.

The costs sheet is associated to the value of costs to be computed in the model. Figure A.3 shows an appearance of this sheet in where in the first column is the name of the costs parameter, the second has units of the cost related parameters.

Cabinet	[€]
BBU_10	[€]
BBU_20	[€]
Site	[€]
Fibre	[€/km]
Microwave	[€/link]
Renting_DU	[€/(m^2)]
Renting_U	[€/(m^2)]
Renting_R	[€/(m^2)]

Figure A.3. Costs parameters layout in the input file.

Before run the simulator, all the .m files must be in the Matlab_Files folder. After that, to run the simulator, the one must run the main.m file.

When the simulator finish, the output file will be in the Output_Files folder with the performance parameters information.

Annex B

Processing Power Complexity Tables

Auxiliary values for the calculation of the Processing Power per RRH are shown in this appendix.

As explained in section 3.2.3, the computation of the processing power depends on the reference complexity of the digital components, whether it is UL or DL, and on the scaling exponents for each sub-component. The following tables show the different values of complexity associated with each function.

Table B.1. Reference Complexity of Digital Components.

Subcomponent	Downlink [GOPS]	Uplink [GOPS]
Predistortion	10.7	0
Filtering	6.7	6.7
Up/Down-sampling	2	2
TD non-ideal. est./comp.	1.3	6.7
FFT/IFFT, FD non-ideal	4	4
MIMO precoding	1.3	0
Synchronisation	0	2
Channel est. & interp.	0	3.3
Equaliser computation	0	3.3
Equalisation	0	2
OFDM Mod./Demod.	1.3	2.7
Mapping/Demapping	1.3	2.7
Channel coding	1.3	8
Control	2.7	1
Network	8	5.3

Table B.2. Scaling Exponents for Digital Sub-Components.

Subcomponent	BW	S. E.	Ant.	Load	Streams	Q
Predistortion	1	0	1	0	0	1.2
Filtering	1	0	1	0	0	1.2
Up/Down-sampling	1	0	1	0	0	1.2
TD non-ideal. est./comp.	1	0	1	0	0	1.2
FFT/IFFT, FD non-ideal	1.2	0	1	0	0	1.2
MIMO precoding	1	0	1	1	1	1.2
Synchronisation	0	0	1	0	0	1.2
Channel est. & interp.	1	0	1	0.5	1	1.2
Equaliser computation	1	0	3	1	0	1.2
Equalisation	1	0	2	1	0	1.2
OFDM Mod./Demod.	1	0	1	0.5	0	1.2
Mapping/Demapping	1	1.5	0	1	1	1.2
Channel coding	1	1	0	1	1	1.2
Control	0	0	0.5	0	0.2	0.2
Network	1	1	0	1	0	0

Annex C

Microwave licencing costs

Auxiliary values for the calculation of the microwave licencing are shown in this appendix.

As explained in section 3.2.4, the computation of the microwave licences costs depends on the frequency, the distance and the constant based on the bandwidth. The following tables show the different reference values for each combination of parameters.

Table C.1. Reference values for microwave licencing costs.

Frequency Band [GHz]	d_{min}[km]	$k_1[€/MHz/\sqrt{km}]$
[1,3]	-	44
[4,11]	10	52
[12,15]	5	27.5
[18,24]	2	14
[25,28]	-	11.5
[47,59]	-	8
[61,71]	-	4
[72,∞]	-	0.75

Annex D

Confidential Information

This Annex presents some confidential information related with this thesis, namely the location of the RRHs.

References

[3GPP14] 3GPP, Technical Specification Group Services and System Aspects, *Quality of Service (QoS) Concept and Architecture (Release 12)*, Report TS 23.107, V12.0.0, Sep. 2014 (http://www.3gpp.org/ftp/Specs/html-info/23107.htm).

[ACHC15] R. Al-obaidi, A. Checko, H. Holm and H. Christiansen, "Optimizing Cloud-RAN Deployments in Real-Life Scenarios Using Microwave Radio", in *Proc. of EuCNC'15 – 24th European Conference on Networks and Communications*, Paris, France, June 2015 (http://ieeexplore.ieee.org/stamp/stamp.jsp?tp=&arnumber=7194060).

[ANAC12] ANACOM, *Information on multi-band spectrum auction (3)*, Public Consultation, Lisbon, Portugal, Dec. 2012 (http://www.anacom.pt/render.jsp?contentId=1106646&languageId =1).

[ANAC15] ANACOM, *Unidirectional point to point microwave links in frequency intervals above 1 GHz* (in Portuguese), Public Consultation, Lisbon, Portugal, June 2015, (http://www.anacom.pt/render.jsp?categoryId=336153#.V8g75pMrLfY).

[ArSR15] M. Arslan, K. Sundaresan and S. Rangarajan, (2015). "Software-Defined Networking in Cellular Radio Access Networks: Potential and Challenges", *IEEE Commun. Mag.*, Vol. 53, No. 1, Jan. 2015, pp.150-156 (http://ieeexplore.ieee.org/stamp/stamp.jsp?tp=&arnumber =7010528).

[ATPH15] M. Andrade, M. Tornatore, A. Pattavina, A. Hamidian and K. Grobe, "Cost Models for Baseband Unit (BBU) Hotelling: from Local to Cloud", in *Proc. of CloudNet, IEEE 4th International Conference on Cloud Networking,* Niagara Falls, ON, Canada, Oct. 2015 (http://ieeexplore.ieee.org/stamp/stamp.jsp?arnumber=7335306).

[BrMe14] W. Braun and M. Menth, "Software-Defined Networking Using OpenFlow: Protocols, Applications and Architectural Design Choices", *Future Internet*, No. 6, May 2014, pp. 302-336 (http://www.mdpi.com/1999-5903/6/2/302).

[CCYS14] A. Checko, H.L. Christiansen, Y. Yan, L. Scolari, G. Kardaras, M.S. Berger and L. Dittmann, "Cloud RAN for Mobile Networks—A Technology Overview", *IEEE Communications Surveys & Tutorials*, Vol. 17, No. 1, Sep. 2014, pp. 405-426 (http://ieeexplore.ieee.org/ stamp/stamp.jsp?tp=&arnumber=6897914).

[ChCB13] A. Checko, H. Christiansen and M. Berger, "Evaluation of energy and cost savings in mobile Cloud Ran", in *Proc. of OPNETWORK – OPNET Conference*, Washington, D.C., USA, Aug.2013.

[ChHC14]   A. Checko, H. Holm and H. Christiansen, "Optimizing Small Cell Deployment by the Use of C-RANs", in *Proc. of 20th European Wireless Conference - European Wireless,* Barcelona, Spain, May 2014 (http://ieeexplore.ieee.org/stamp/stamp.jsp?arnumber=6843207).

[CHLS15]   J. Chen, Z. He, Y. Li, T. Swahn and H. Zirath,"A Data-Rate Adaptable Modem Solution for Millimeter-Wave Wireless Fronthaul Networks", in *Proc. of ICCW - IEEE International Conference Communication Workshop,* London, UK, June 2015 (http://ieeexplore.ieee.org/stamp/stamp.jsp?tp=&arnumber=7247066).

[CJCB15]   A. Checko, A.C. Juul, H.L. Christiansen and M.S. Berger, "Synchronization Challenges in Packet-Based Cloud-RAN Fronthaul for Mobile Networks", in *Proc. of ICCW - IEEE International Conference Communication Workshop*, London, UK, June 2015 (http://ieeexplore.ieee.org/stamp/stamp.jsp?tp=&arnumber=7247590).

[CLZW15]   L. Cheng, C. Liu, M. Zhu, J. Wang and G.K. Chang, "Optical CoMP Transmission in Millimeter-Wave Small Cells for Mobile Fronthaul", in *Proc. of OFC - Optical Fiber Communications Conference*, San Francisco, CA, USA, Mar. 2014 (http://ieeexplore.ieee.org/stamp/stamp.jsp?arnumber=6887075).

[Corr15]   L.M. Correia, *Mobile Communication Systems – Lecture Notes*, Instituto Superior Técnico, Lisbon, Portugal, 2015.

[CPLR13]   P. Chanclou, A. Pizzinat, F. Le Clech, T.L. Reedeker, Y. Lagadec, F. Saliou, B. Le Guyader, L. Guillo, Q. Deniel, S. Gosselin, S. Le, T. Diallo, R. Brenot, F. Lelarge, L. Marazzi, P. Parolari, M. Martinelli, S. O'dull, S.A. Gebrewold, D. Hillerkuss, J. Leuthold, G. Gavioli and P. Galli, "Optical fiber solution for mobile fronthaul to achieve cloud radio access network", in *Proc. of FutureNetworkSummit - Future Network and Mobile Summit* , Lisbon, Portugal, July 2013 (http://ieeexplore.ieee.org/stamp/stamp.jsp?arnumber=6633565).

[DeDL15]   B. Debaillie, C. Desset and F. Louagie, "A Flexible and Future-Proof Power Model for Cellular Base Stations", in *Proc. of VTC Spring - 81st IEEE Vehicular Technology Conference,* Glasgow, Scotland, July. 2015 (http://ieeexplore.ieee.org/stamp/stamp.jsp?arnumber=7145603).

[DKYK15]   P. Dat, A. Kanno, N. Yamamoto and T. Kawanishi, "Full-Duplex Transmission of LTE-A Carrier Aggregation Signal over a Bidirectional Seamless Fiber-Millimeter-Wave System", *J. Lightwave Technol.,* Vol. 34, No. 2, Jan 2015, pp 691-700 (http://ieeexplore.ieee.org/stamp/stamp.jsp?tp=&arnumber=7182740).

[Eric15]   Ericsson, Ericsson Mobility Report, Public Consultation, Lisbon, Portugal, June 2015, (http://www.ericsson.com/mobility-report)

[ERSE16]   ERSE, *Final electricity tariffs in Portugal* (in Portuguese), Public Consultation, Lisbon, Portugal, June 2016, (http://www.edpsu.pt/pt/particulares/EDP%20Documents/Tarifas%20Transit%C3%B3rias%20janeiro%202016.pdf).

[ETSI12]   M. Chiosi, D. Clarke, P. Willis, A. Reid, J. Feger, M. Bugenhagen and P. Sen, "Network functions virtualisation: An introduction, benefits, enablers, challenges and call for action", *SDN and OpenFlow World Congress*, pp. 22-24, Oct. 2012 (https://portal.etsi.org/NFV/NFV_White_Paper.pdf).

[HCAC15]   H. Holm, A. Checko, R. Al-obaidi and H. Christiansen, "Optimal Assignment of Cells in C-RAN Deployments with Multiple BBU Pools", in *Proc. of EuCNC'15 – 24th European Conference on Networks and Communications*, Paris, France, June 2015. (http://ieeexplore.ieee.org/stamp/stamp.jsp?arnumber=7194069)

[HDDM13]   M. Hadzialic, B. Dosenovic, M. Dzaferagic and J. Musovic, "Cloud-RAN: Innovative Radio Access Network Architecture", *ELMAR,* in *Proc. of 55th International Symposium*, Zadar, Croatia, Sep 2013 (http://ieeexplore.ieee.org/stamp/stamp.jsp?tp=&arnumber=6658331).

[HGJL14]   B. Han, V. Gopalakrishnan, L. Ji and S. Lee, "Network Function Virtualization: Challenges and Opportunities for Innovations", *Commun. Mag.*, Vol. 53, No. 2, Feb. 2015, pp. 90-97 (http://ieeexplore.ieee.org/stamp/stamp.jsp?tp=&arnumber=7045396).

[HoTo11]   H. Holma and A. Toskala, *LTE for UMTS: Evolution to LTE Advanced (2nd Edition)*, John Wiley & Sons, Chichester, UK, 2011.

[HSMA14]   H. Hawilo, A. Shami, M. Mirahmadi and R. Asal "NFV: state of the art, challenges, and implementation in next generation mobile networks (vEPC)", *IEEE Network*, Vol. 28, No. 6, Dec. 2014, pp. 18-26 (http://ieeexplore.ieee.org/stamp/stamp.jsp?tp=&arnumber=6963 800).

[HUAW12]   Huawai, BBU3900 Description, Public Consultation, Lisbon, Portugal, July 2012, (http://e.huawei.com/en/marketing-material/onLineView?MaterialID={B53F8D57-018E-415D-AE33-F17B4E483D15}).

[Imov16]   Imovirtual, http://www.imovirtual.com/estatisticas/mercado-imobiliario/, June 2016.

[JSSA14]   M. Jammal, T. Singh, A. Shami, R. Asal, and Y. Li, "Software defined networking: State of the art and research challenges", *Elsevier's Journal of Computer Networks*, Vol. 72, June 2014, pp. 74-98 (http://arxiv.org/pdf/1406.0124.pdf).

[JZHT14]   M. Jarschel, T. Zinner, T. Hossfeld, P. Tran-Gia and W. Kellerer, "Interfaces, attributes, and use cases: A compass for SDN", *IEEE Commun. Mag.*, Vol. 52, No. 6, June 2014, pp. 210-217 (http://ieeexplore.ieee.org/stamp/stamp.jsp?tp=&arnumber=6829966).

[LiMR12]   L.E. Li, Z.M. Mao, and J. Rexford, "Toward Software-Defined Cellular Networks", in *Proc. of EWSDN - European Workshop on Software Defined Networking,* Darmstadt, Germany, Oct. 2012 (http://ieeexplore.ieee.org/stamp/stamp.jsp?tp=&arnumber=6385040).

[MBCT15]   F. Musumeci, C. Bellanzon, N. Carapellese, M. Tornatore, A. Pattavina and S. Gosselin, "Optimal BBU Placement for 5G C-RAN Deployment Over WDM Aggregation Networks", *Journal of Lightwave Technology*, Vol. 34, No. 8, Apr. 2015, pp. 1963-1970 (http://ieeexplore.ieee.org/stamp/stamp.jsp?arnumber=7368094).

[MHLW15]   Y. Ma, X. Huo, J. Li, X. Mu and J. Wen, "Optical Solutions for Fronthaul Application (invited)", in *Proc. of ICOCN - 14th International Conference on Optical Communications and Networks,* Nanjing, China, July 2015 (http://ieeexplore.ieee.org/stamp/stamp.jsp?tp=&arnumber=7203716).

[Mont16]   T. Monteiro, *Implementation Analysis of Cloud Radio Access Network Architectures in Small Cells*, M.Sc. Thesis, IST*,* Technical University of Lisbon, Lisbon, Portugal, 2016.

[ONFo12]   Open Networking Foundation, *Software-Defined Networking: The New Norm for Networks*, White Paper, 2012 (https://www.opennetworking.org/images/stories/downloads/sdn-resources/white-papers/wp-sdn-newnorm.pdf).

[PCSD15]   A. Pizzinat, P. Chanclou, F. Saliou and T. Diallo, "Things you Should Know About Fronthaul", *Journal of Lightwave Technology*, Vol. 33, No. 5, Jan. 2015, pp. 1077-1083 (http://ieeexplore.ieee.org/stamp/stamp.jsp?tp=&arnumber=7009970).

[Pent11]   J.T. Penttinen, *The LTE/SAE Deployment Handbook*. John Wiley & Sons, Chichester, UK, 2011.

[PWLP15]   M. Peng, C. Wang, V. Lau, and H.V. Poor, "Fronthaul-Constrained Cloud Radio Access Networks: Insights and Challenges", *IEEE Wireless Commun.*, Vol. 22, No. 2, Apr. 2015, pp. 152-160 (http://ieeexplore.ieee.org/stamp/stamp.jsp?tp=&arnumber=7096298).

[RaWW15]   C. Ran, S. Wang and C. Wang "Optimal Load Balancing in Cloud Radio Access Networks", in *Proc. of WCNC - IEEE Wireless Communications and Networking Conference,* Istanbul, Turkey, Mar. 2015 (http://ieeexplore.ieee.org/stamp/stamp.jsp?arnumber=7127607).

[SARS15]   K. Sundaresan, M.Y. Arslan, S. Singh, S. Rangarajan and S.V. Krishnamurthy, "FluidNet: a flexible cloud-based radio access network for small cells" *IEEE/ACM Transactions on Networking*, Vol. 23, No. 2, Apr. 2015, pp 915-928 (http://ieeexplore.ieee.org/stamp/stamp.jsp?tp=&arnumber=7089323).

[Saut10]   M. Sauter, *From GSM to LTE: an introduction to mobile networks and mobile broadband.* John Wiley & Sons, Chichester, UK, 2010.

[SeTB11]   S. Sesia, I. Toufik and I. Baker, *LTE - The UMTS Long Term Evolution: From Theory to Practice (2nd Edition)*, John Wiley & Sons, Chichester, UK, 2011.

[WeGP13]   T. Werthmann, H. Grob-Lipski and M. Proebster, "Multiplexing Gains Achieved in Pools of Baseband Computation Units in 4G Cellular Networks", in *Proc. of PIMRC, 24th IEEE International Symposium,* London, United Kingdom, Sep. 2013 (http://ieeexplore.ieee.org/stamp/stamp.jsp?arnumber=6666722).

[WZHW15]   J. Wu, Z. Zhang, Y. Hong, and Y. Wen, "Cloud radio access network (C-RAN): a primer". *IEEE Network*, Vol. 29, No. 1, Jan. 2015, pp. 35-41 (http://ieeexplore.ieee.org/stamp/stamp.jsp?tp=&arnumber=7018201).